Extreme precipitation in Iceland: Climate projections and historical changes in precipitation type

Andréa-Giorgio R. Massad
Guðrún Nína Petersen
Halldór Björnsson
Matthew J. Roberts
Tinna Þórarinsdóttir

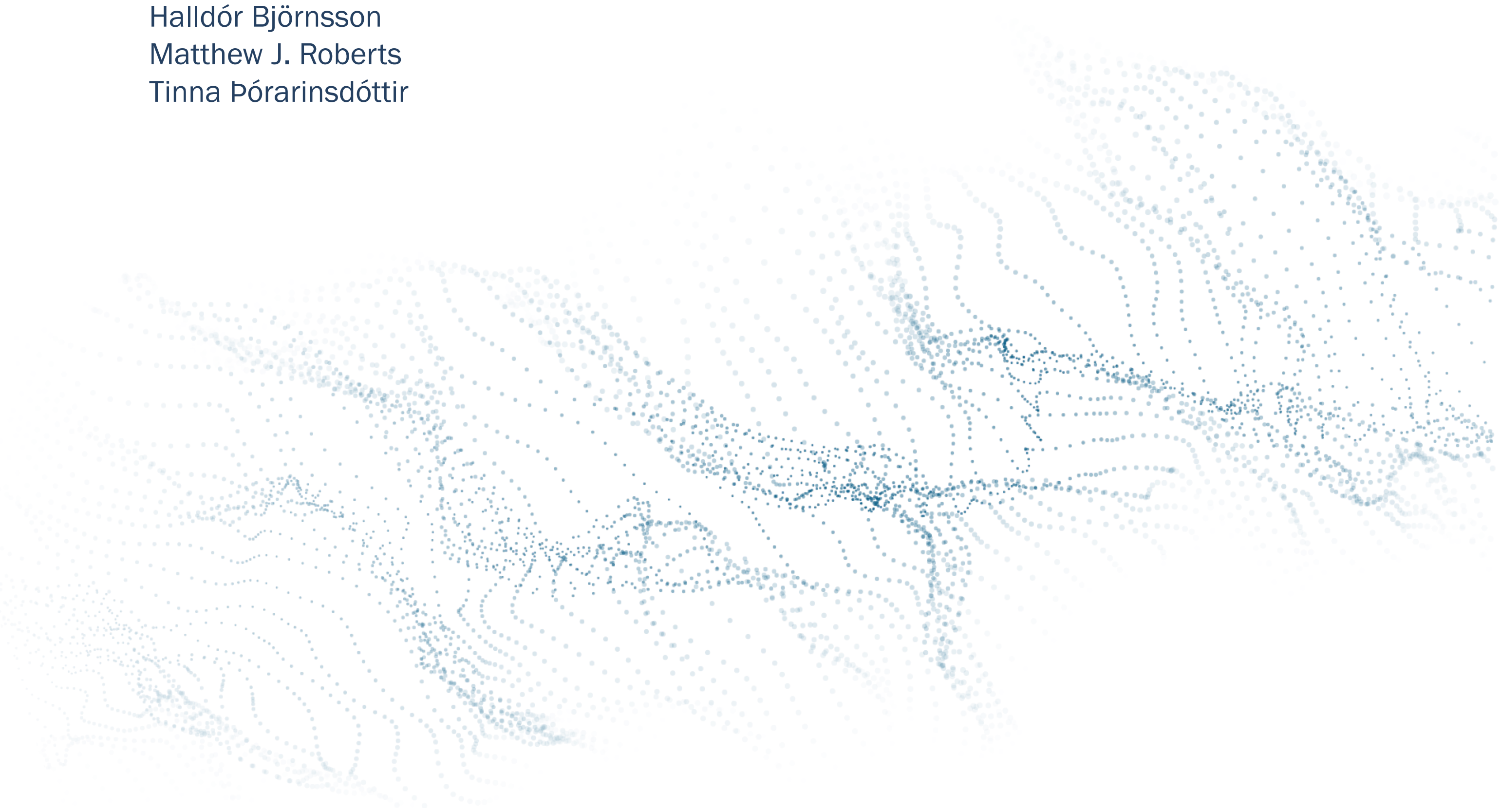

Skýrsla

VÍ 2022-006

Veðurstofa Íslands

Extreme precipitation in Iceland: Climate projections and historical changes in precipitation type

Andréa-Giorgio R. Massad
Guðrún Nína Petersen
Halldór Björnsson
Matthew J. Roberts
Tinna Þórarinsdóttir

Skýrsla

Veðurstofa Íslands
Bústaðarvegur 7–9
108 Reykjavík

+354 522 6000
vedur@vedur.is

VÍ 2022-006

Veðurstofa Íslands

LYKILSÍÐA

Skýrsla nr.	Dags.	ISSN	Dreifing: Opin ☒ Lokuð ☐
VI-2022-006	September 2022	1670-8261	**Skilmálar:**
Heiti skýrslu: Extreme precipitation in Iceland: Climate projections and historical changes in precipitation type			**Upplag:** Rafræn útgáfa **Fjöldi síðna:** 99 **Framkvæmdastjóri sviðs:** Jórunn Harðardóttir
Höfundar: Andréa-Giorgio R. Massad, Guðrún Nína Petersen, Halldór Björnsson, Matthew J. Roberts, Tinna Þórarinsdóttir			**Verkefnisstjóri:** Matthew J. Roberts **Verknúmer:** 4314-0-0001
Gerð skýrslu/verkstig:			**Málsnúmer:** 2021-0044
Unnið fyrir: Orkurannsóknasjóð Landsvirkjunar			
Samvinnuaðilar:			

Útdráttur:

In Iceland, periods of intense rainfall have caused localised damage on numerous occasions. Estimates of precipitation extremes are important for assessing the spatial and temporal variability of precipitation. This research addressed two questions: Firstly, are systematic changes in the seasonality of precipitation observed already in the ICRA reanalysis data covering 39 years in eleven hydropower watersheds operated by Landsvirkjun? Secondly, how are climate projections expected to affect the return levels of precipitation in Iceland, and specifically in the eleven hydropower catchments? Overall, the results show that systematic changes can be observed in the seasonality of precipitation in the ICRA dataset for most of the catchments. Using climate projections from the CMIP5, results show that precipitation return levels will have increased by the end of the century. The mean increase in the precipitation return levels within the hydropower catchments ranges from 3.2 to 5.7%, depending on the greenhouse gas concentration trajectory.

Lykilorð:	Undirskrift framkvæmdastjóra sviðs:
Extreme precipitation, climate projections, historical changes in precipitation type, reanalysis, ICRA	Undirskrift verkefnisstjóra:
	Yfirfarið af: SG, ÞÞ, KBÓ

Contents

1 INTRODUCTION....4
2 STUDY AREA....7
3 DATA....9
3.1 The ICRA dataset....9
3.2 The ERA-20c dataset....9
3.3 The CMIP5 projections....9
4 HISTORICAL CHANGES IN PRECIPITATION SEASONALITY....11
4.1 Melt season analysis....11
4.1.2 Methodology....11
4.1.2 Results....15
4.2 Change in precipitation type....18
4.2.1 Total snow-fraction change over the winter months....18
4.2.2 Monthly snow-fraction changes....21
5 CATCHMENT-SCALE EXTREME PRECIPITATION ANALYSIS AND CLIMATE PROJECTIONS....24
5.1 Return levels for the hydropower catchments....24
5.1.1 Return level tables....24
5.1.2 1M5 maps....24
5.2 Return levels for the hydropower catchments in relation to CMIP5 climate scenarios....27
5.2.1 Presentation of the climate datasets....27
5.2.2 Incorporation of the climate projections to the ICRA dataset....28
5.2.3 New 1M5 maps including climate projections....31
5.2.4 New return levels for the hydropower catchments....36
6 CONCLUSIONS....41
BIBLIOGRAPHY....42
APPENDIX I. MELT SEASON ANALYSIS....43
APPENDIX II. TEMPORAL CHANGES IN SNOW-FRACTION....49
APPENDIX III. PRECIPITATION RETURN LEVELS....66

1 Introduction

In Iceland, periods of intense rainfall have caused localised damage on numerous occasions. Recent examples include a flash flood in Siglufjörður in August 2015, widespread flooding in southeast Iceland in September 2017, as well as the recent landslides in Seyðisfjörður in December 2020, caused by record-breaking rainfall amounting to almost 570 mm over five days.

Estimates of precipitation extremes are important for assessing the spatial and temporal variability of precipitation. Extreme Value Analysis (EVA) is a statistical discipline used to predict the occurrence of rare events by assessing their frequency from the most extreme values of a dataset. In the case of precipitation, these extremes are in the right tail of the distribution. It allows for the calculation of return levels associated with periods that can be longer than the length of the timeseries available for the analysis. These calculations can then be used as the basis for flood warnings and in the design of the built environment. A newly published Icelandic study by Massad *et al*. (2020) reassessed precipitation return levels in Iceland, resulting in a new national map of 24-hour precipitation thresholds for a 5-year event, see Figure 1, in agreement with the general precipitation pattern in Iceland, shown in Figure 2 and documented in Björnsson *et al*. (2018) and Crochet *et al.* (2007). The study, based on the previous research of Jónas Elíasson (Elíasson, 2000; Elíasson *et al*., 2009) also presented intensity-duration-frequency curves for over 40 locations in Iceland. These curves describe the relationship between rainfall intensity, duration, and return periods, making them useful for flood warnings and the design of hydrological infrastructure, including dams, bridges, and spillways (Hlodversdottir *et al.*, 2015).

The impact of rapid climate change is a major ongoing concern, and weather-driven effects are evident in recent decades (IPCC, 2021, see Chapter 11.4: Heavy precipitation). As Arctic and subarctic regions warm rapidly, precipitation extremes are expected to increase in the coming decades (Bintanja, 2018). In terms of projections, there are large uncertainties regarding the future of precipitation in Iceland. Indications of an increase in precipitation intensity have been found (Björnsson *et al.*, 2018), but there is need for further research. Another aspect is the effect of global warming on precipitation type, and how the seasonal ratio of snowfall and rainfall is affected by a warming climate (Li *et al.*, 2020; Feng and Hu, 2017).

The aim of this project is twofold: Firstly, to use the existing reanalysis of atmospheric conditions in Iceland (ICRA), 1979 – 2017, to investigate temporal changes in precipitation type, focussing on the melt season and the evolution of the snow-fraction in eleven hydropower catchments operated by the National Power Company of Iceland, Landsvirkjun. Secondly, apply two climate projection scenarios of precipitation changes from the fifth phase of the Coupled Model Intercomparison Project (CMIP5) to the ICRA dataset, and then the EVA methodology developed in Massad *et al.* (2020) to calculate new return levels, both for Iceland and for the aforementioned catchments. By comparing the precipitation return levels at catchment-scale, with and without projections, the results will give insights into hydrological trends, helping in the future design of critical infrastructure.

This research was funded in 2021 by Landsvirkjun, under the Orkurannsóknasjóður grant.

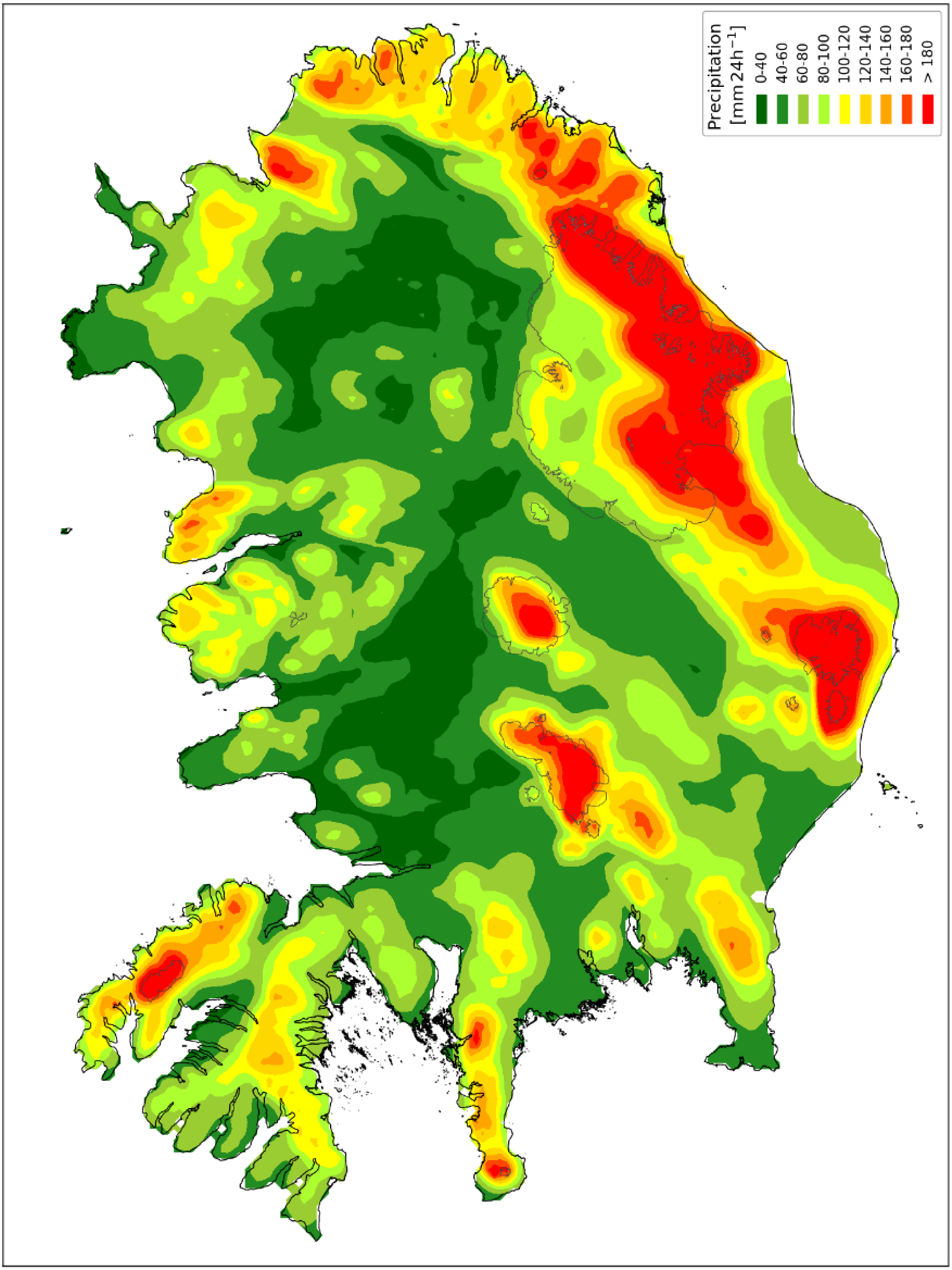

Figure 1 – 1M5 map based on 24-hour accumulated precipitation, obtained from the entire ICRA dataset using the Peak-over-Threshold method with Maximum Likelihood Estimation. From Massad et al., 2020.

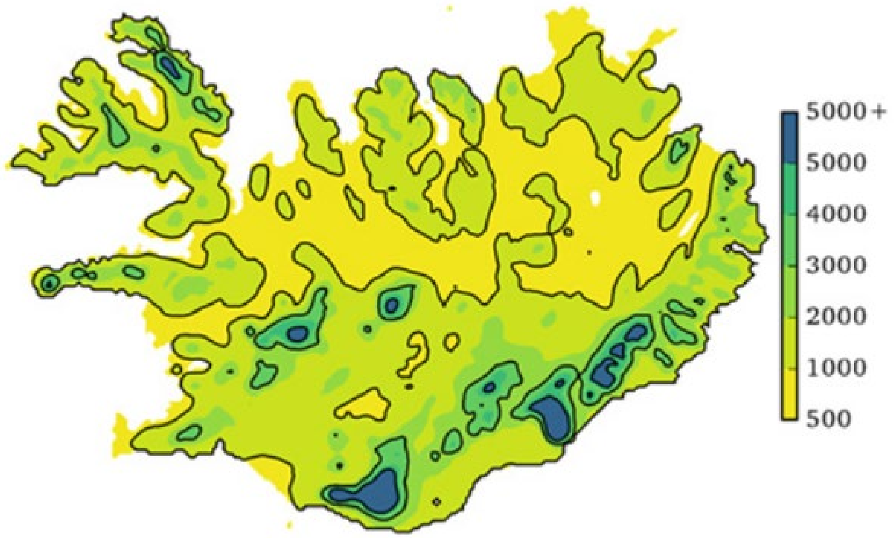

Figure 2 – Distribution of annual rainfall (mm year^{-1}) in Iceland for the period 1981 – 2010. Solid lines show the 1000, 3000, and 5000 mm year^{-1} values. Results based on the ICRA dataset. From Björnsson et al., 2018.

2 Study area

Eleven hydropower catchments operated by Landsvirkjun were selected for this study. Figure 3 shows the locations of the catchments, and Table 1 outlines the overall area, mean elevation, and the percentage of glacier cover for each catchment. The values in Table 1 were calculated using the ICRA dataset (presented in the next section) and they are thus grid based. The discrepancy between the actual catchments and the gridded version can be seen on the map, in Figure 3, as gridded nature of the ICRA dataset does not match exactly with catchment boundaries.

Out of the eleven catchments, only Þingvallavatn, with a mean altitude below 500 m a.s.l., is not completely in the highland region. Six catchments are located between the Hofsjökull and Vatnajökull ice-caps and they share common borders: Búðarháls, Hágöngulón, Kvíslaveita, Sultartangi, Þórisvatn, and Tungnaá. Three watersheds are clustered together on the north-eastern flank of Vatnajökull: Hálslón, Ufsarlón, and Hraunaveita, while Blönduvirkjun extends between Langjökull and Hofsjökull.

The hydropower catchments vary in size, ranging from about 130 km^2 (Hraunaveita) to almost 1,800 km^2 (Hálslón), and two of them have a mean elevation above 1,000 meters (Hágöngulón and Hálslón). Only Búðarháls has no direct glacial influence within its catchment. The glacial cover varies greatly between the catchments, reaching 74% for Hálslón, the only one with a glacial coverage above 50%. Three other catchments have glaciers occupying more than 10% of their surface: Hágöngulón, Sultartangi, and Ufsarlón.

Table 1 – Properties of the eleven hydropower catchments. Note that the values are derived from the ICRA dataset.

Catchment	**Area** *km²*	**Mean elevation** *m a.s.l.*	**Glacier cover** *%*
Blönduvirkjun	1,508	761	8.8
Búðarháls	312	540	0.0
Hágöngulón	612	1,208	42.7
Hálslón	1,785	1,141	73.9
Hraunaveita	131	805	2.5
Kvíslaveita	1,260	843	6.3
Sultartangi	1,696	728	12.7
Þingvallavatn	1,167	471	4.6
Þórisvatn	806	774	6.6
Tungnaá	1,481	738	6.2
Ufsarlón	304	975	35.2

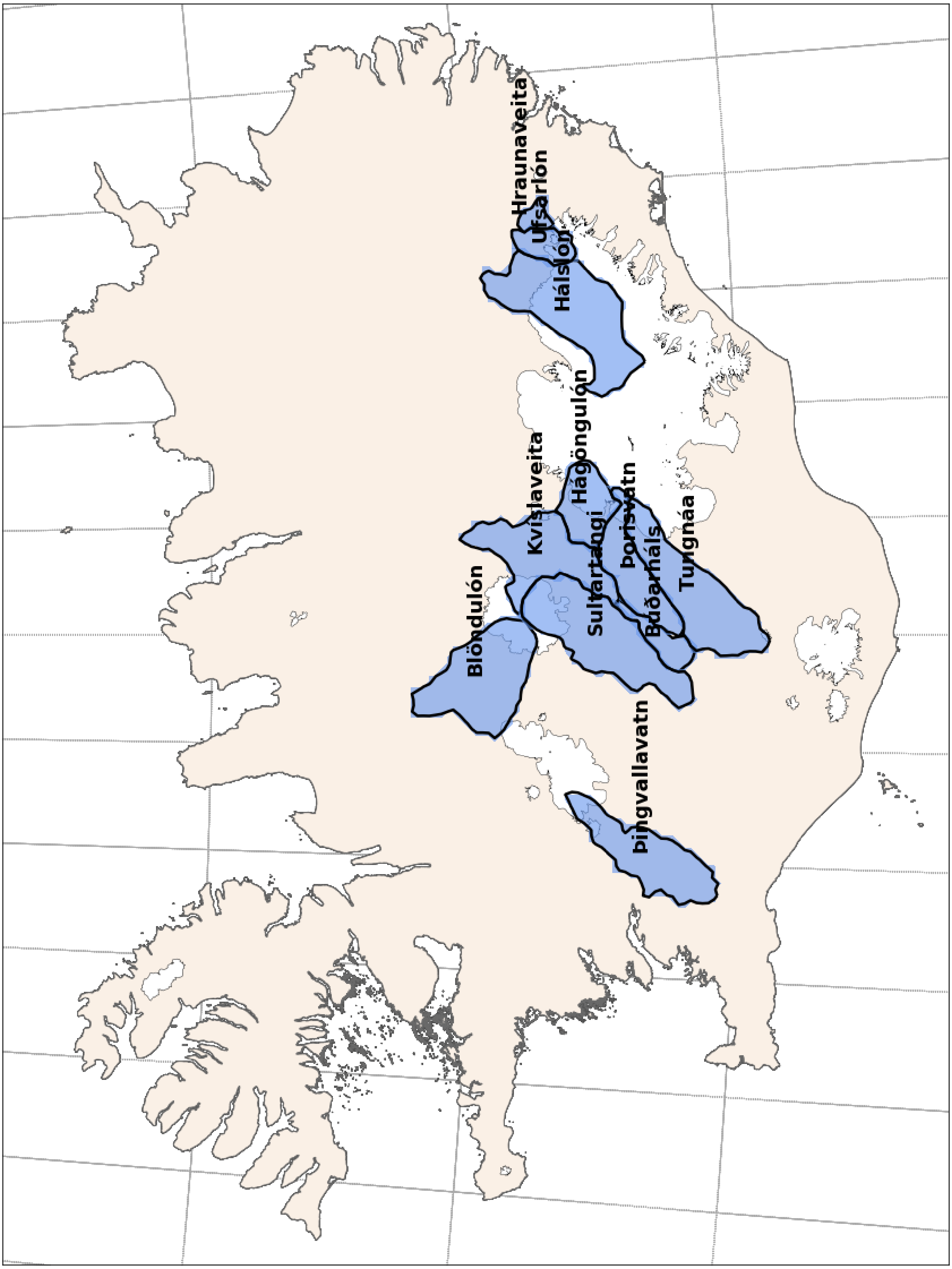

Figure 3 – Location of the eleven hydropower catchments. Black lines show the catchments boundaries, and shaded areas within catchments represent the grid.

3 Data

3.1 The ICRA dataset

The operational numerical weather prediction (NWP) system used by the Icelandic Meteorological Office (IMO) is the non-hydrostatic HARMONIE–AROME model, with a horizontal resolution of 2.5 km and 65 vertical levels (Bengtsson *et al.*, 2017). The fine-scale gridding gives 66,181 terrestrial points over Iceland. The model has been used to reanalyse atmospheric conditions in Iceland at hourly time-steps between September 1979 and August 2017, resulting in the Icelandic Reanalysis (ICRA) dataset (Nawri *et al.*, 2017). From the range of simulated variables, seven were selected for this study:

- ***T2m***, the temperature at 2 meters above sea level
- ***rf***, the rainfall rate
- ***sf***, the snowfall rate
- ***gr***, the rate of fall of graupel
- ***swe***, the snow water equivalent -
- ***evap***, the evaporation rate
- ***subl***, the sublimation rate

From those variables, three additional variables were calculated:

- ***tpr***, the total precipitation *(tpr = rf + sf + gr)*
- ***mlt***, the snow meltwater amount *(mlt = gr + sf – subl – δswe*, with *δswe,* the snow water equivalent difference between two timesteps)
- ***ro***, the runoff *(ro = rf – evap + mlt)*

Based on the 2.5 km horizontal resolution of the dataset, timeseries were extracted for the hydropower watersheds by taking the mean value from all grid-points within the catchment outlines.

3.2 The ERA-20c dataset

The ERA-20c dataset is an atmospheric reanalysis produced by the European Centre for Medium-Range Weather Forecasts (ECMWF) for the time-period 1900 – 2010. The reanalysis assimilated observations of surface pressure and surface marine winds and produced variables that describe the spatio-temporal evolution of the atmosphere, the land-surface and the ocean waves with a horizontal resolution of 125 km. The reanalysis is single member and was run ten times to get an estimate of uncertainties. Further details can be found in Poli *et al.* (2016).

Data from the ten realizations were retrieved for temperature, total precipitation and snow-fraction for a box around Iceland, extending between latitudes 58 to 72°N and longitudes -5 to -30°W. Data were available from the ECMWF archive at hourly resolution, but for this project, only monthly summed variables were used.

Because the ERA-20c dataset has a much coarser resolution than the ICRA dataset, for each catchment a mean latitude and longitude was calculated and this point value used to retrieve a timeseries based on the weighted-average among the four nearest grid-points. These timeseries were then used to complement the results from the ICRA.

3.3 The CMIP5 projections

The Coupled Model Intercomparison Project (CMIP) is a large framework that collects the output from global coupled ocean-atmosphere general circulation models (GCMs) to project future climatic changes due to anthropogenic activity. For this project, results from the fifth phase of the project (referred to as CMIP5; for details, see Taylor *et al.*, 2012) are used based on two different greenhouse gas concentration trajectories (Representative Concentration Pathway, RCP) adopted by the Intergovernmental Panel on Climate Change (IPCC). The first projection is the RCP 2.6, a mild-warming scenario, which requires carbon dioxide emissions to start declining in 2020 and reach zero by 2100. This scenario is likely to keep global temperature rise under 2°C by the end of the century. The second projection is the RCP 8.5, in which greenhouse gas concentrations will continue to rise. This scenario is often used as the worst-case scenario, if nothing is done to reduce the emissions.

A subset for both scenarios is archived at the IMO and is available for a large domain around Iceland, extending between latitudes 60.5 and 69.5°N and longitudes 10 and 30°W, with a horizontal resolution of 1°. Subsequently, the domain was cropped so that only grid-points between latitudes 62.5 and 66.5°N and 13 and 25°W were kept. In the end, data from 65 grid-points were used, instead of 130 before cropping the domain.

Projections are given for two periods: 2040 – 2060 and 2080 – 2100, and for an ensemble of 33 climate models. For each one of them, two types of data are available: monthly precipitation and monthly-averaged precipitation ratio changes for both intervals. In this investigation, the focus is on the precipitation ratio change.

Because of the coarse horizontal resolution, precipitation changes were seasonally averaged over the whole domain. This is because the noise from the ensemble climate models is too large to use the results at a grid-point level. To assess the variability of the results from all members of the ensemble, the 10^{th} and 90^{th} percentiles were used in addition to the median values. This is expected to give the magnitude of the uncertainties within the 33 models.

4 Historical changes in precipitation seasonality

4.1 Melt season analysis

In this part of the study, the goal is to investigate if a trend concerning the onset date of the melt season is apparent over the period covered by the ICRA dataset. Firstly, three experimental methods are outlined for automatically determining the onset of the melt season. Following the methodological descriptions, the results for the eleven catchments are presented and discussed.

4.1.2 Methodology

In total, the ICRA dataset covers 39 complete hydrological years. As explained in the previous section, for each catchment and variable a single timeseries was extracted from the dataset. The melt parameter is not a direct output from the model and was therefore calculated from the rate of rainfall, sleet fall, evaporation and the snow water-equivalent difference. In total, 419 dates representing the onset of the melt season need to be retrieved from the data (39 years in 11 catchments). To select those dates automatically, several filtering methods were tested. Three of them are presented in the following paragraphs.

4.1.2.1 First filtering method: positive temperature for more than 10 consecutive days

The first method sets the start date of the melt season as the first day preceding a period of 10 consecutive days of positive temperatures. Results were plotted for every hydrological year and catchment on graphs as shown in Figure 4. They show the accumulated snowpack (solid black line) for the hydrological year considered, along with the accumulated melting (dashed blue line) and daily runoff (grey bars). Vertical red lines indicate the date considered as the beginning of the melt season, as defined by the filter.

In the case of Þingvallavatn for the hydrological year 1980 – 1981 (Figure 4, top), the method works well. The date retrieved corresponds exactly to the moment the snowpack starts decreasing continuously, and a steep increase in the melting line can be noted, indicating the onset of the melt season. However, this filter does not work in all cases, as shown for Hágöngulón for the years 1986 – 1987 (Figure 4, bottom). In that case, the filter gives a result that is about a month too late (June 11), as shown by the vertical red line. The snowpack began to recede earlier than the criteria was fulfilled with a corresponding increase in cumulative melt and daily runoff.

4.1.2.2 Second filter: snowpack decreases for more than 10 consecutive days

A second filter was tested, this time focusing only on the snowpack: the first day preceding a period of 10 days of decreasing snowpack is selected as the beginning of the melt season. Two examples are shown on Figure 5. The top panel shows the same case for Hágöngulón as in the previous section. This time the filter selects the expected date. Nevertheless, this method does not always prove successful, especially in the case of mild winters when the snow cover fluctuates, or in the case of an early winter, when the snowpack has time to melt before the next snowfall. This can be seen in Figure 5 (bottom) for the same catchment, for the hydrological year 1984 – 1985. In that case, the melting date is set about a month too early when the snowpack remains mostly stable, but decreased slightly. This decrease did not convert into melting, and the peak in snowpack was reached a month and a half later. Despite that, the fact that the snowpack decreased for more than 10 days, even though slightly, was enough for the filter to select this date.

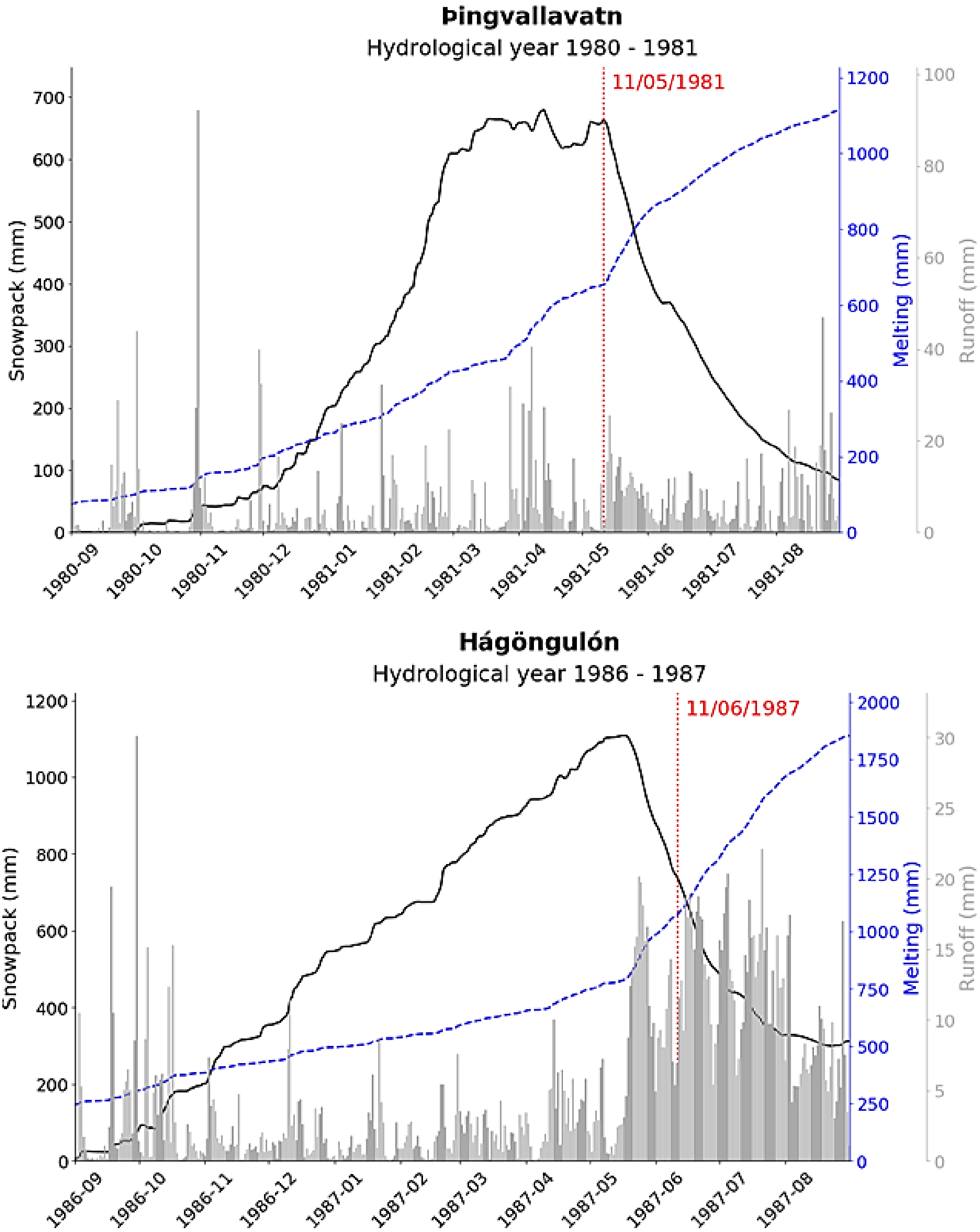

Figure 4 – Evolution of the snowpack (black line), accumulated melting (dashed blue line), and daily runoff (grey bars) for catchment Þingvallavatn (year 1980 – 1981, top) and catchment Hágöngulón (year 1986 – 1987, bottom). The vertical red lines indicate the start date of the melt season as retrieved by the first filtering method.

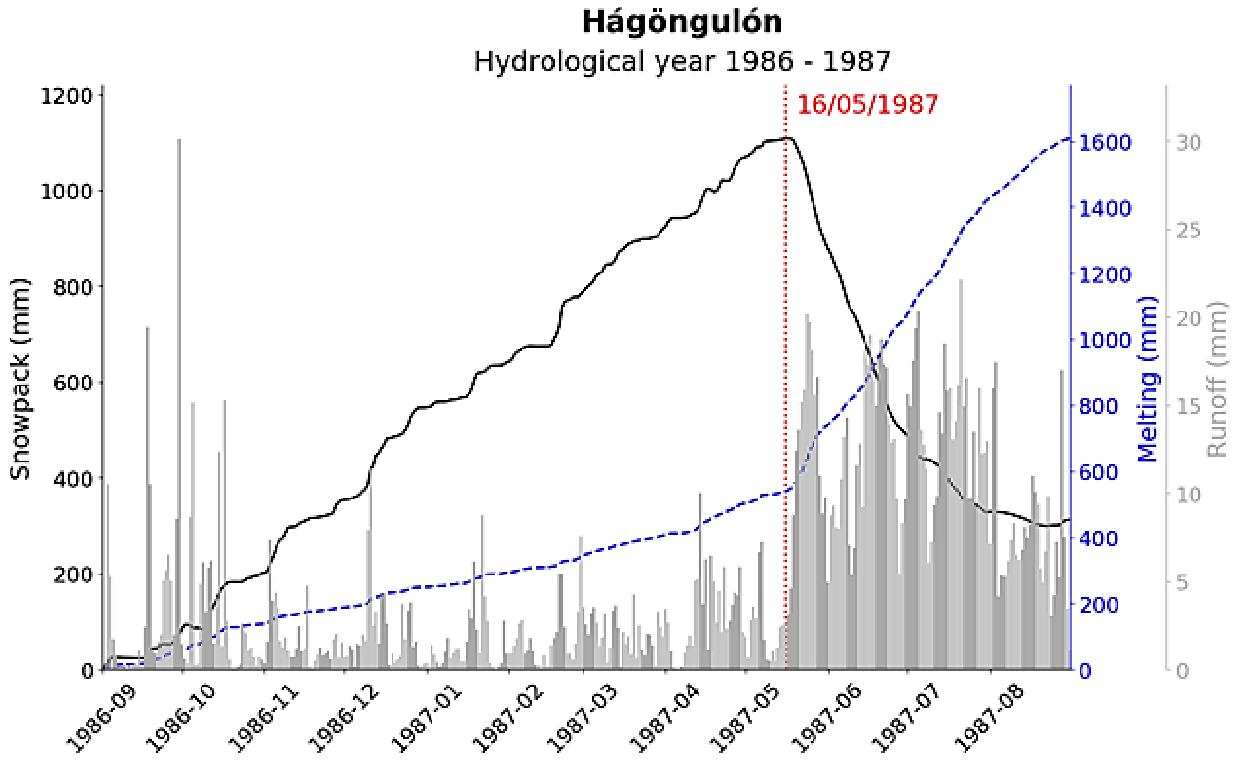

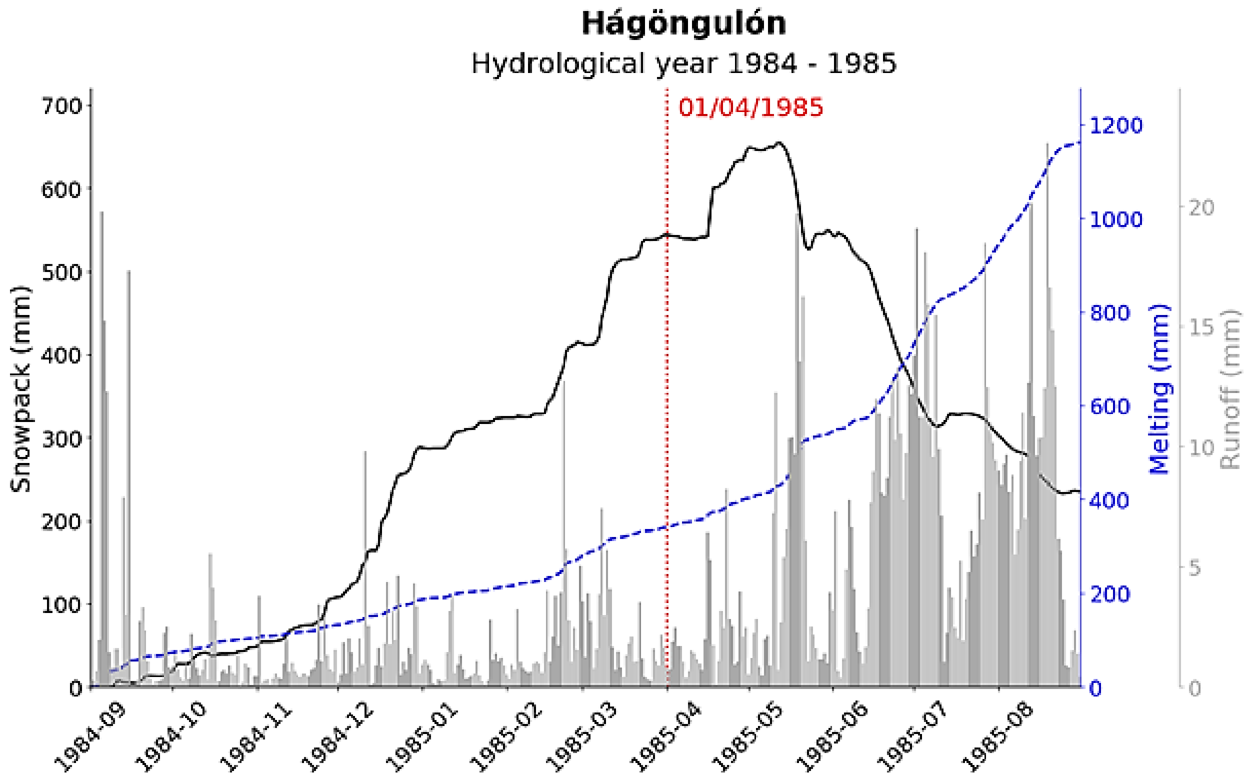

Figure 5 – Evolution of the snowpack (black line), cumulative melting (dashed blue line), and daily runoff (grey bars) for Hágöngulón (year 1986 – 1987, top; year 1984 – 1985, bottom). The vertical red lines indicate the start date of the melt season as retrieved by the second filtering method.

4.1.2.3 Third filter: Conditions on snowpack, temperature and melting

A few other methods of filtering were tested with a filter combining a few meteorological parameters showing more success than the previous approaches. Firstly, a condition is set that the onset date of the melt season can only occur between 1st March and 31st July. Then, during this interval, the maximum snowpack is located. Hence, the beginning of the melt season can only start after this peak is reached. In some cases, as seen for catchment Búðarháls in Figure 6, the snowpack maximum happens very early in the year (mid-February), followed by a sharp decrease until a new high is reached, although not as high as the first maximum. Here, the assumption that the melt season cannot begin before March prevents untimely detection. Once the maximum is found, the first 10-day period with accumulated melting exceeding 20 mm and a median temperature above 0°C is identified and the first day of this period selected as the onset date. In the case of Búðarháls in Figure 6, the filter picked 06/04 correctly as the beginning of the melt season.

The third filter is better than its predecessors, although it did not produce entirely accurate results. In the case of Búðarháls, the melting threshold had to be lowered to 10 mm, otherwise the results were unconvincing. Overall, this filtering method worked well for some catchments such as Hágöngulón, Sultartangi, and Kvíslaveita. For others, like Hraunaveita or Hálslón, in a few cases the onset dates selected did not fit the data very well, and results from previous filters were chosen instead. However, note that this applied to less than 10 cases out of the 401.

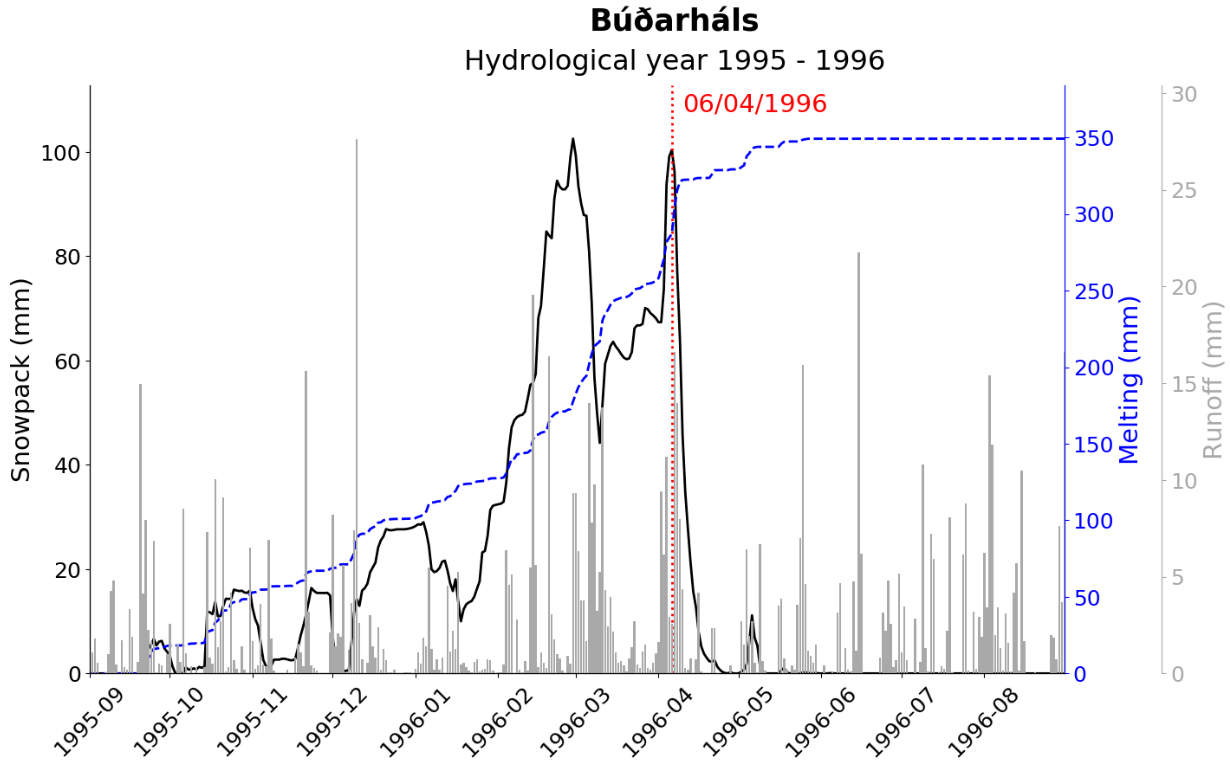

Figure 6 – Evolution of the snowpack (black line), accumulated melting (dashed blue line), and daily runoff (grey bars) for catchment Búðarháls and hydrological year 1995 – 1996. The vertical red line indicates the start date of the melt season as retrieved by the third filtering method.

4.1.2 Results

For each catchment, all the dates retrieved by the last filter were stored in a table. These dates were then plotted together, as shown for four catchments in Figure 7. Results for the other catchments are included in Appendix I (Figures I.1 – 11). On each plot, the x-axis shows the 39 years used for the study, and the y-axis the dates between March and July. For every year, the melt season starting date is plotted (blue dots), and a blue line connects the dates for all the years. A regression line fitting those values (orange line) is shown, and the difference in days between the beginning and the end of the period, as calculated from the regression line, is indicated at the top of the plot.

In 9 cases out of 11, the trend line indicates an onset of the melt season earlier in the year. For those catchments, the decrease ranges from 5 days (Hágöngulón), to 29 days (Tungnaá, see Figure 7, top panel). It should be noted that those values need careful evaluation, as the results show a great variability from one year to the other. In the case of Tungnaá, it appears that before 1995, the melt season never started before late April, while in the years after 1995 it would start early-to-mid April. In the case of Hálslón (Figure 7, bottom left), the regression line is flat, indicating no trend for this period, although for the interval 1996 – 2017, except for 2011, the melting started in late May at the latest, whereas previously it could occur as late as early June. The most surprising result is for Ufsarlón, with a positive trend of 8 days (Figure 7, bottom right).

Table 2 lists the mean starting dates of the melt season, as well as the overall differences in onset, over the span of the ICRA dataset. Additionally, the same results are shown in map form in Figure 8, with differences expressed in colours. The colour scheme is as follows: orange if the difference is null or positive; yellow for a decrease between 0 and 7 days; light blue between 7 and 14 days and dark blue for a decrease exceeding two weeks. Catchments located in the southwest of Iceland show a larger recession in the onset of the melt season, with a value around -20 days in four of them: Búðarháls, Þingvallavatn, Tungnaá, and Þórisvatn. Both catchments with a null or positive trend (Hálslón and Ufsarlón) are in the northern part of Vatnajökull, and it can be seen from Table 2 that those catchments have a mean starting date later in the year (respectively 22/05 and 18/05) than the catchments in southwest-Iceland.

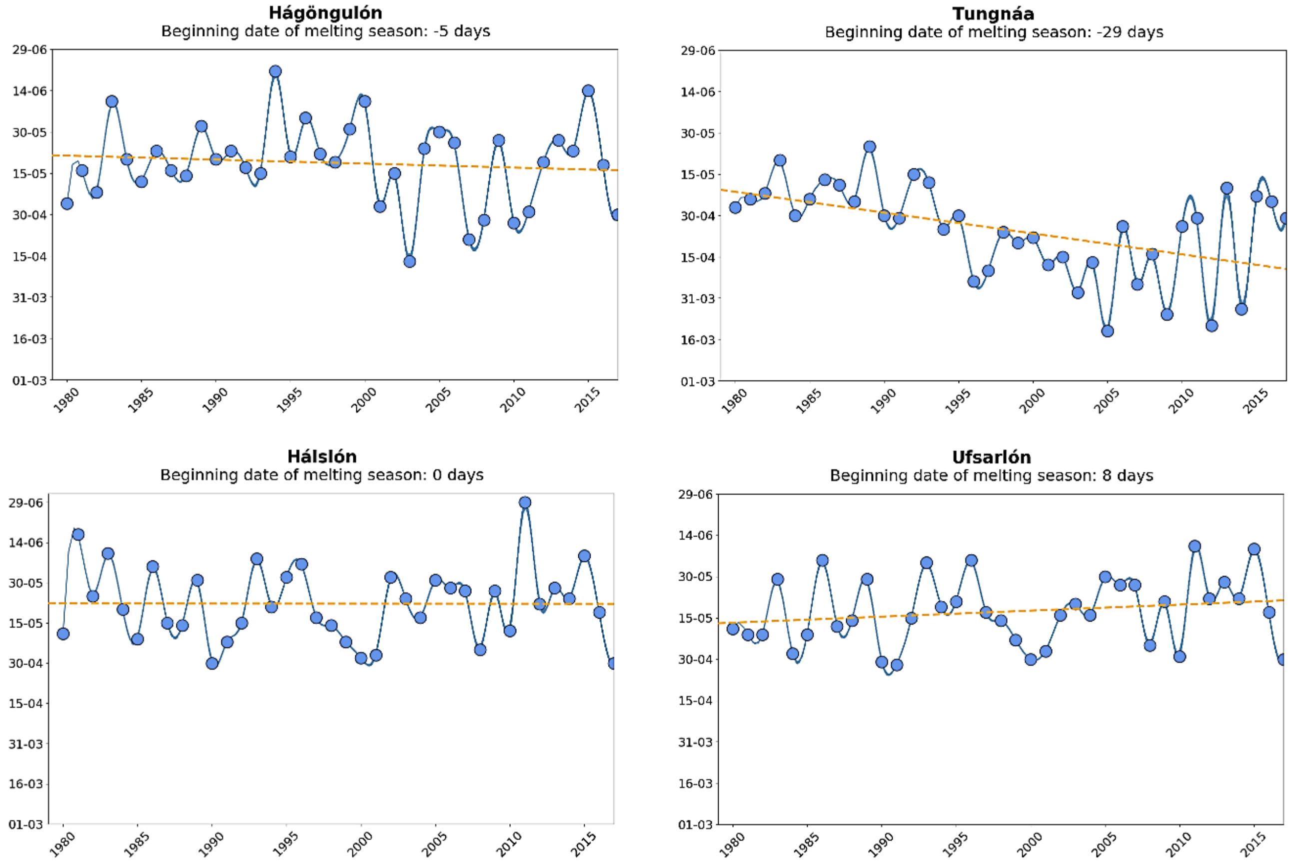

Figure 7 – Evolution of the beginning date of the melt season in four catchments for the period 1979 – 2017. Results were obtained using an automatic filter on the snowpack, temperature and melting timeseries extracted from the ICRA dataset.

Table 2. Difference in the beginning of the melt season (in days) for all catchments over the timespan 1979 – 2017.

Catchment	Difference in beginning of the melt season *days*	Mean date
Blönduvirkjun	-9	01/05
Búðarháls	-21	04/04
Hágöngulón	-5	19/05
Hálslón	0	22/05
Hraunaveita	-11	08/05
Kvíslaveita	-12	05/05
Sultartangi	-12	01/05
Þingvallavatn	-19	22/04
Þórisvatn	-27	25/04
Tungnaá	-29	25/04
Ufsarlón	8	18/05

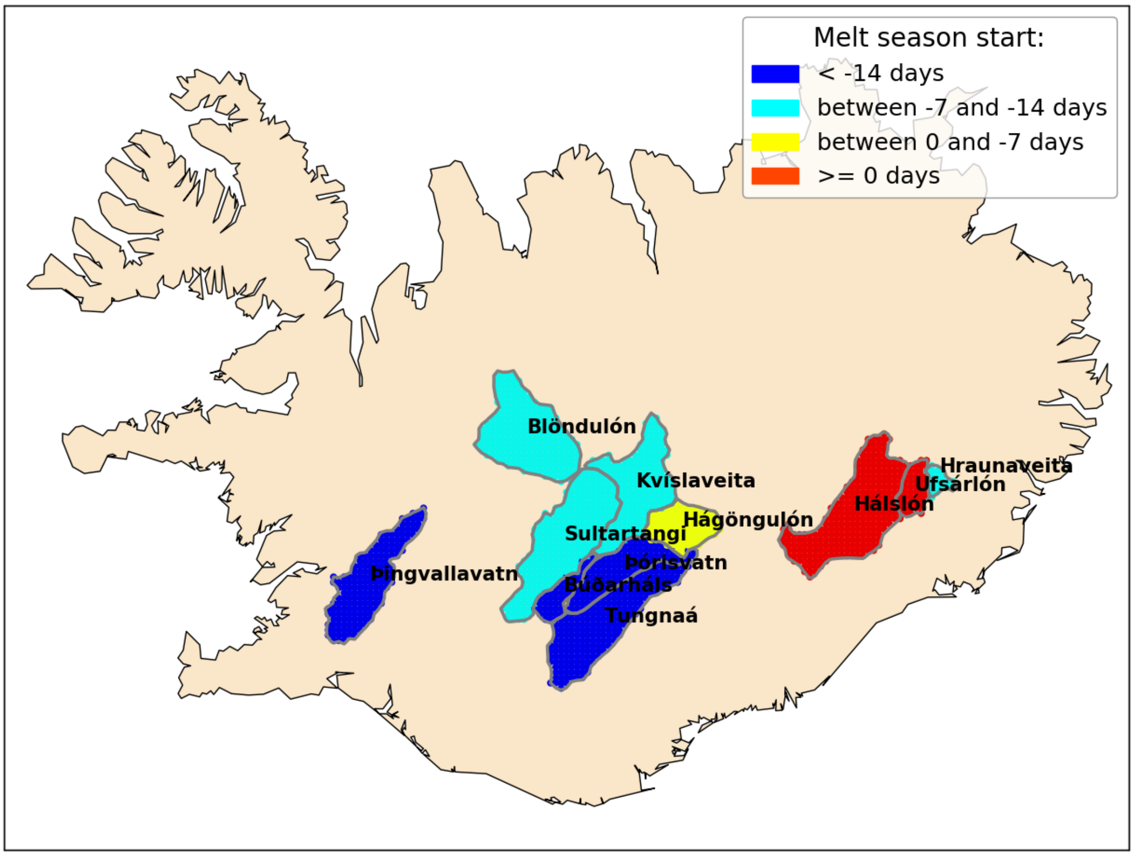

Figure 8 – Change in the beginning of the melt season (in days) based on the ICRA dataset. Catchments are coloured according to the magnitude of the change (for details, see main text).

4.2 Change in precipitation type

In this part of the study, the ICRA dataset is used to assess if precipitation type has already been affected by increasing surface temperatures, over the period 1979 – 2017. The precipitation can be divided into two categories: liquid (only rainfall), or solid (sleet and snowfall). Total precipitation is defined as the sum of those three variables (rainfall, sleet and snowfall) and snow-fraction as the sum of solid precipitation divided by the total precipitation:

$$Snowfraction = \frac{(rgr + sf)}{(rn + rgr + sf)}$$

The focus in this section is on the changes of snow-fraction during the winter months, defined here as the period extending from the beginning of November to the end of April. Although most of the hydropower catchments are in the highlands where snow can fall in summertime, as a first attempt to study the change of snowfall fraction in the dataset, summer months between May and October were discarded.

4.2.1 Total snow-fraction change over the winter months

Firstly, solid precipitation was summed for each catchment over all the winter months and compared to the total precipitation summed over the same period. Results for four catchments are shown in Figure 9; all the others are available in Appendix II (Figures II.1 – 11). In each plot, the solid blue line shows the evolution of the total snow-fraction over the study period, while the dashed blue line shows the regression that fits the data best. At the top of each plot, a percentage change over the 39 years is indicated, calculated as the difference between the snow-fraction of the first and last year of reanalysis as given by the regression line.

In all the catchments, the trend lines give decreasing snow-fraction, from -1.5% (Hálslón) to -14.6% (Búðarháls). Two trends can be observed in the plot for catchment Búðarháls: one for the period 1979 – 2000, with a mean value around 75%, and one after 2000, with a mean value in the high 60%. Overall, the snow-fraction in that catchment never exceeds 90%, which can be explained by the comparatively low mean elevation (540 m, see Table 1). Hálslón on the other hand, shows a completely different pattern, and has the lowest snow-fraction change of all the catchments. The snow-fraction does not vary a lot from one year to the other, staying around 98% for the period 1979 – 2000, slightly lower but always above 95% for the later years. This can be explained by the high elevation of the catchment and the fact that most of it is glaciated. Catchments Hraunaveita and Þingvallavatn present similar patterns with large fluctuations from one year to the other. In the case of Hraunaveita, the snow-fractions range between 65 and 97%, with only five years under 75%. For catchment Þingvallavatn, being in the lowlands, the snow-fraction never exceeds 80%.

Percentage changes, as calculated from the regression line between the beginning and the end of the ICRA time-period, are given for all the catchments. Those results are also shown with a color code on a map (see Figure 10). Overall, the catchments oriented on the southern parts of the glaciers (Sultartangi, Þórisvatn, Tungnaá), and catchments at lower altitudes (Búðarháls, Þingvallavatn) are showing snow-fraction decreases superior to 10% over the 39 years of reanalysis. Smaller changes are found in the catchments facing northward (Blöndulón, Hálslón, Ufsarlón, Kvíslaveita, Hágöngulón), except for Hraunaveita.

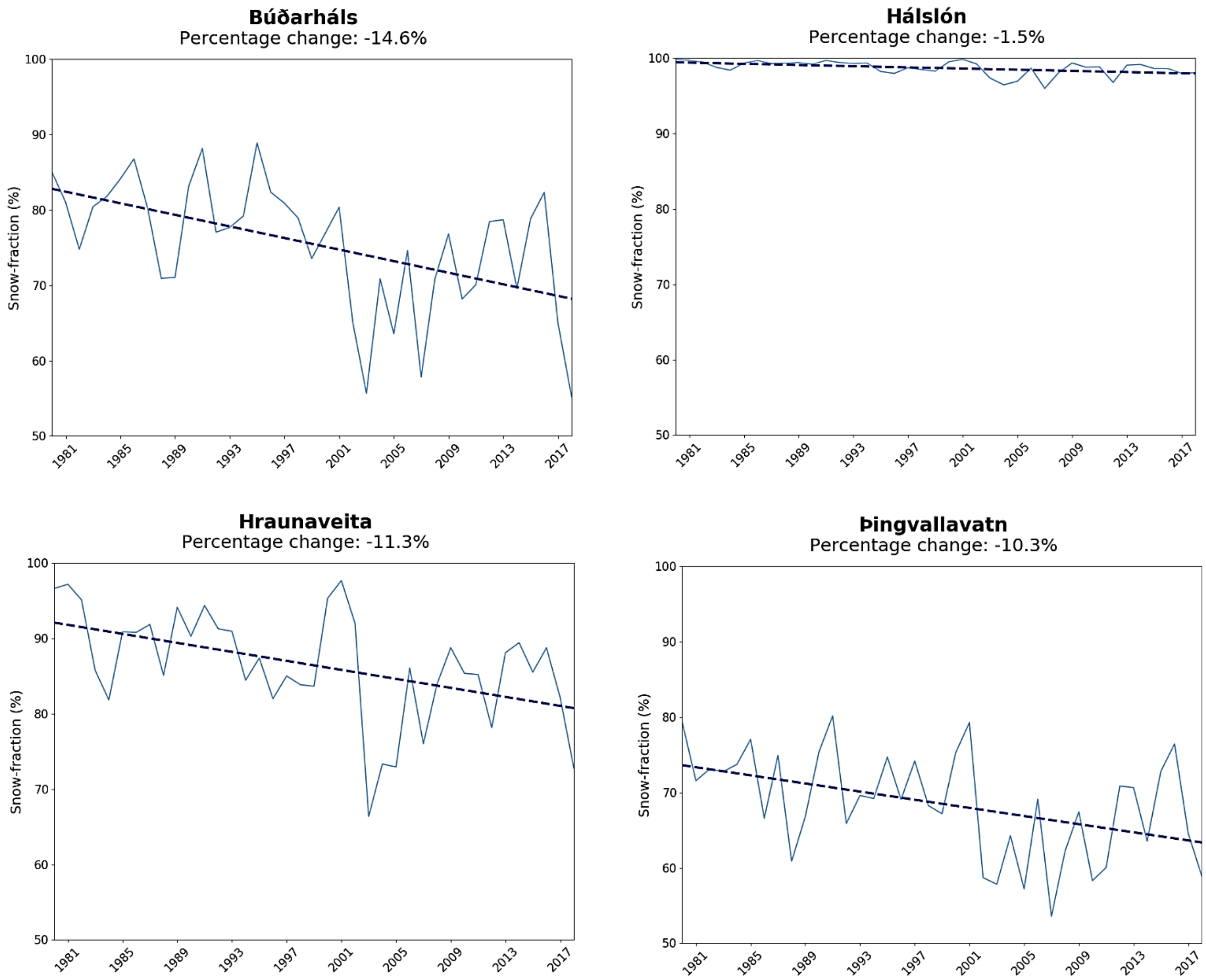

Figure 9. Total snow-fraction evolution (%) for catchments Búðarháls, Hálslón, Hraunaveita and Þingvallavatn, based on the ICRA dataset for the period 1979 – 2017. Solid blue lines show the yearly change of snow-fraction, and the trend lines in dashed blue. Percentage changes as calculated from the regression line are also given.

Table 3. Total snow-fraction change (%) for all the hydropower catchments of the study based on the ICRA dataset for the period 1979 – 2017.

Catchment	Total snow-fraction difference %
Blönduvirkjun	-4.7
Búðarháls	-14.6
Hágöngulón	-1.6
Hálslón	-1.5
Hraunaveita	-11.3
Kvíslaveita	-4.2
Sultartangi	-6.9
Þingvallavatn	-10.3
Þórisvatn	-9.0
Tungnaá	-12.3
Ufsarlón	-5.1

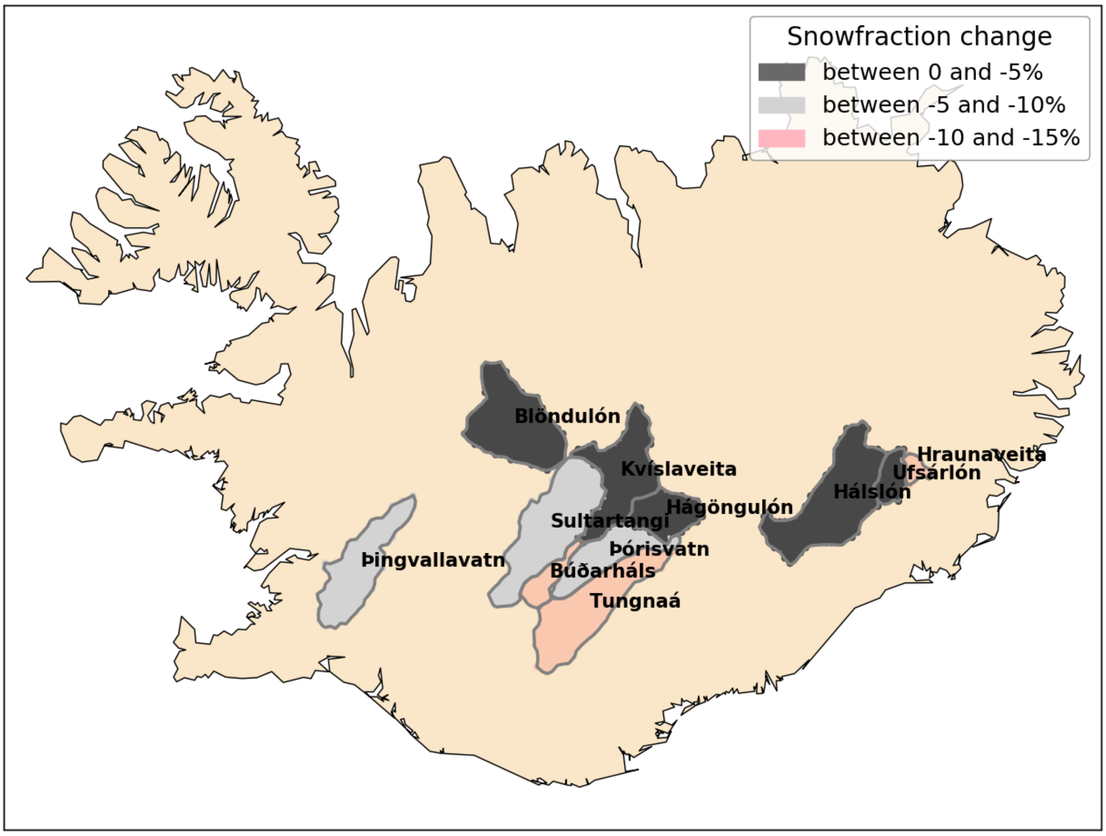

Figure 10 – Total snow-fraction percentage decrease based on the ICRA dataset for the time-period 1979 – 2010. Catchments are coloured according to the magnitude of the change.

4.2.2 Monthly snow-fraction changes

Secondly, snow-fractions were studied on a monthly basis for all the winter months. For each month and each catchment, the solid precipitation proportion of the total precipitation was calculated.

An example is shown in Figure 11 for catchment Hraunaveita; results for the other catchments are available in Appendix II (Figures II.12 – 22). Results from the ICRA dataset are shown in blue. The solid blue line shows the monthly snow-fraction evolution over the years, while the dashed-blue line indicates the regression fit. To complement those results, the snow-fraction from the ERA-20c reanalysis was added. Data are available for all 10 realizations of this reanalysis; therefore, the figure shows the minimum-maximum snow-fraction interval (in orange), with the mean values represented by the solid orange line. The dashed red line indicates the regression fit based on the mean snow-fraction values from the ERA-20c.

As seen in Figure 11, the trend lines give clear decreasing results for all the winter months. When comparing the percentage differences obtained by the ICRA and the ERA-20c, they are within the same 10% range, and show the same decreasing trends. Snow-fractions from the ERA-20c are lower than from the ICRA, for all the catchments. This can be justified by the very coarse horizontal resolution of the model, with the mountainous terrain mixed with lowland within the grid-cells, therefore leading to less snow.

Monthly percentage changes were compiled in Table 4 for all catchments. In 9 cases out of 11, November is the month with the largest snow-fraction decrease. It is also the month with the largest mean percentage change with -11.2%, and by a strong margin (the second month is December with -5.9%). This indicates that over the period considered, snow tends to come later, presumably indicating a later start of the winter. Another reason could be that early snow is melted by milder weather. This is further illustrated by Table 5, where monthly temperature changes were calculated for each catchment based on the ICRA. January is the month with the largest increase (around 3°C in all the catchments), although this is also the month with the highest amount of snow, thus the snow-fraction decrease is less significant than for November.

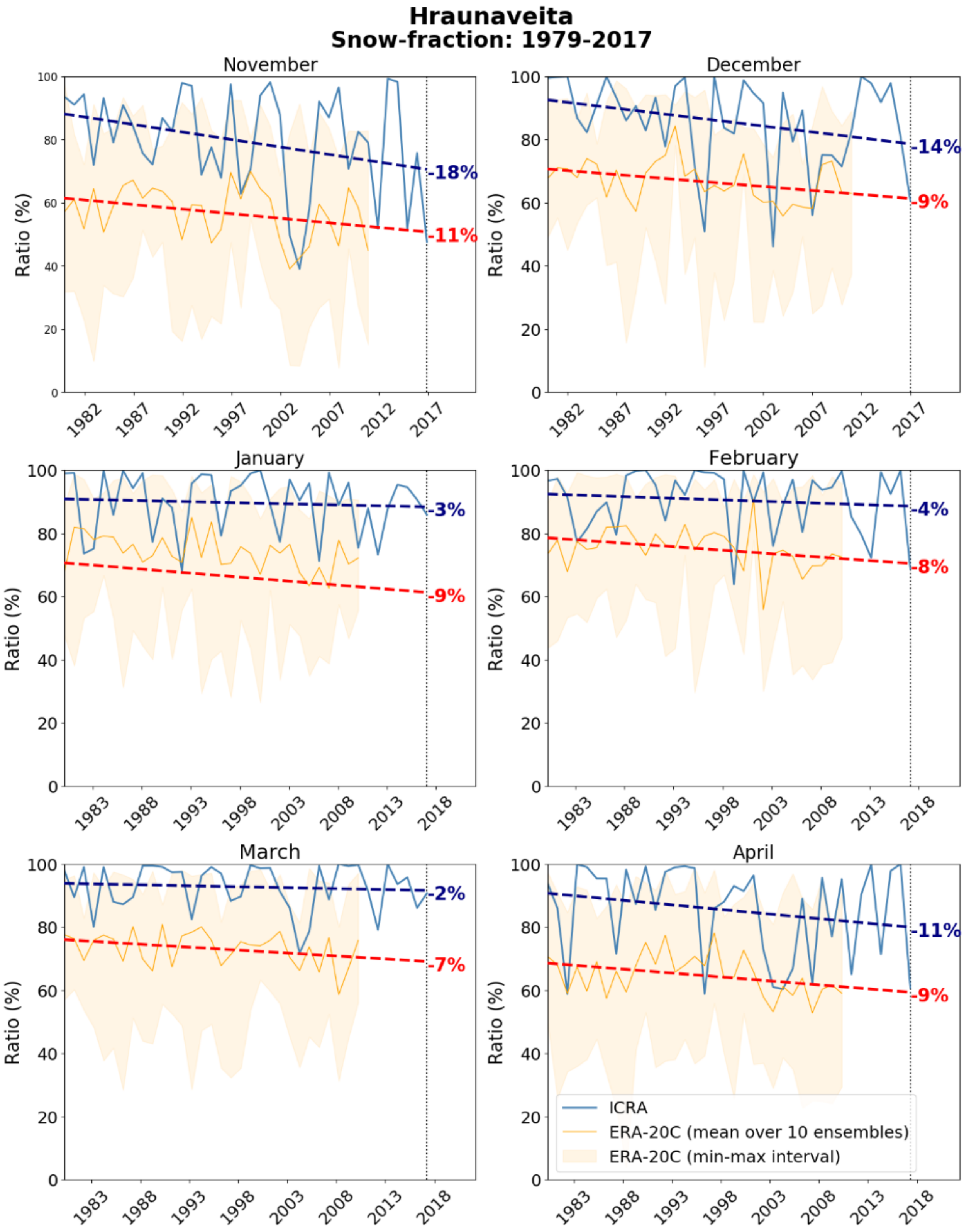

Figure 11 – Monthly snow-fraction evolution (%) for catchment Hraunaveita for the months November – April. Results are based on the ICRA and ERA-20c datasets. Regression lines are shown for both datasets results.

Table 4 – Monthly snow-fraction difference (%) for all the catchments for the winter months. Results were calculated from the ICRA dataset over the period 1979 – 2017.

Catchment	**Snow-fraction difference %**					
	Nov.	**Dec.**	**Jan.**	**Feb.**	**Mar.**	**Apr.**
Blönduvirkjun	-6	-3	-4	-6	-4	-2
Búðarháls	-20	-8	-9	-12	-16	-8
Hágöngulón	-4	-2	0	-5	-2	-1
Hálslón	-4	-1	-1	0	0	-2
Hraunaveita	-18	-14	-3	-4	-2	-11
Kvíslaveita	-5	-1	0	-9	-6	-1
Sultartangi	-9	-4	-4	-9	-7	-3
Þingvallavatn	-13	-8	-9	-3	-9	-5
Þórisvatn	-15	-4	-3	-9	-9	-5
Tungnaá	-18	-14	-7	-2	-4	-15
Ufsarlón	-11	-6	-1	-1	0	-7
Mean	***-11.2***	***-5.9***	***-3.7***	***-5.5***	***-5.4***	***-5.5***

Table 5 – Monthly temperature increase (°C) for all the catchments for the winter months. Results were calculated from the ICRA dataset over the period 1979 – 2017.

Catchment	**Temperature change °C**					
	Nov.	**Dec.**	**Jan.**	**Feb.**	**Mar.**	**Apr.**
Blönduvirkjun	2.2	2.0	3.2	0.8	1.9	1.7
Búðarháls	2.3	1.9	3.2	1.2	2.3	2.1
Hágöngulón	2.0	1.6	3.4	1.1	1.7	1.0
Hálslón	2.3	1.8	2.8	1.2	1.6	0.9
Hraunaveita	2.0	1.7	3.0	1.1	1.5	0.8
Kvíslaveita	2.1	1.9	2.7	1.1	1.8	1.2
Sultartangi	2.2	1.8	3.1	1.2	1.9	1.5
Þingvallavatn	1.9	1.6	3.2	1.1	2.1	1.7
Þórisvatn	2.2	1.7	3.2	1.1	2.0	1.6
Tungnaá	2.4	1.7	3.1	0.9	2.0	1.7
Ufsarlón	2.1	1.7	2.8	1.0	1.5	0.7
Mean	***2.2***	***1.8***	***3.1***	***1.1***	***1.8***	***1.4***

5 Catchment-scale extreme precipitation analysis and climate projections

5.1 Return levels for the hydropower catchments

In this section, the return levels for all the hydropower catchments selected for this study are presented in tables and on 1M5 maps of 24-hour precipitation thresholds for a 5-year event.

5.1.1 Return level tables

In Section 2, a methodology for extracting ICRA timeseries for the hydropower catchments was detailed. Before performing the EVA, the first step was to resample the hourly precipitation to produce new timeseries with 3-, 6-, 12-, 24-, and 48-hour accumulated precipitation using a rolling window. Within each time-step, maximum values were selected, and the Peak-over-Threshold method with MLE was thereafter applied to obtain results with a 2-, 5-, 10-, 25-, 50- and 100-year return period. Details about the selection of the EVA and the statistics behind the Peak-over-Threshold method can be found in Massad *et al.* (2020), Chapters 3 and 5.2, and were derived from Coles (2001).

Results are shown in Table 6 for two catchments: Hálslón and Þingvallavatn. Return levels for the other watersheds are in Appendix III (Tables III.1 – 11). The return values are larger for Þingvallavatn than Hálslón. Þingvallavatn catchment extends northward over the southern part of Langjökull, which is a wet region. Hálslón catchment, on the other hand, is located on and just north of Vatnajökull, on the leeside, in a region with relatively low precipitation poor region (Crochet *et al.*, 2007). These results are in accordance with Figure 2, which depicts precipitation patterns, with larger precipitation values typically on the southern flanks of the ice caps.

Results presented in the tables are based on average precipitation timeseries, i.e., hourly precipitation for each grid-point within the catchment was averaged over the grid-points to give a single timeseries for the watershed. Some of the watersheds cover large areas and the landscape variation within the catchments. Thus, these results should be used carefully as the ICRA dataset may not be able to represent the complexity of the terrain, due to its horizontal resolution of 2.5 km.

5.1.2 1M5 maps

One of the main results presented in Massad *et al.* (2020) was a new map showing 24-hour precipitation return levels with a 5-year return period (Figure 1). A similar product can be made for the eleven hydropower catchments considered here.

Results for catchments Hálslón and Þingvallavatn are shown in Figures 12 and 13, with other maps to be found in Appendix III (Figures III.1 – 11). Median values are shown on the maps. Overall, as expected values are higher for catchment Þingvallavatn than for Hálslón, with no part of the catchment with an 1M5 value lower than 60 mm. For catchment Hálslón, there is a very strong south-to-north gradient with the highest values seen in the southern part of the catchment (red), and the lowest values (dark green) in the highlands, in the precipitation shadow of Vatnajökull. This strong gradient shows the horizontal variability of the 1M5 results, as Hálslón is geographically located less than 100 km to the north-northeast of Kvísker, the wettest location in Iceland.

In Figures 12 and 13, the median 1M5 values shown differ from the 24-hour return level with a 5-year return period from the tables. As discussed earlier, this outcome is expected as the values were calculated differently. Indeed, on the maps, the median values are extracted after performing the Peak-over-Threshold method on all the timeseries included within the catchment; whereas in the tables, a single average timeseries was extracted before the EVA method was applied. This can lead to significant differences, especially for the largest catchments that are covered partly by glacial ice but are also partly in lowland regions, such as Hálslón.

Table 6 – ***Return levels (mm) for catchment Hálslón (top) and Þingvallavatn (bottom)****. Values are given for 3-, 6-, 12-, 24- and 48-hour return levels with a 2-, 5-, 10-, 25-, 50- and 100-year return period, based on the complete ICRA dataset. Timeseries were extracted using the average value of all the grid-points within the catchment. 1M5 value is shown in red.*

Hálslón

	2 years	**5 years**	**10 years**	**25 years**	**50 years**	**100 years**
3 hours	8	11	13	15	18	20
6 hours	18	23	27	31	36	39
12 hours	35	43	49	54	62	67
24 hours	60	**70**	78	85	94	101
48 hours	91	105	115	125	137	147

Þingvallavatn

	2 years	**5 years**	**10 years**	**25 years**	**50 years**	**100 years**
3 hours	12	15	18	19	21	23
6 hours	26	31	35	38	41	44
12 hours	48	56	62	67	73	77
24 hours	78	**90**	99	107	117	124
48 hours	113	128	138	148	159	168

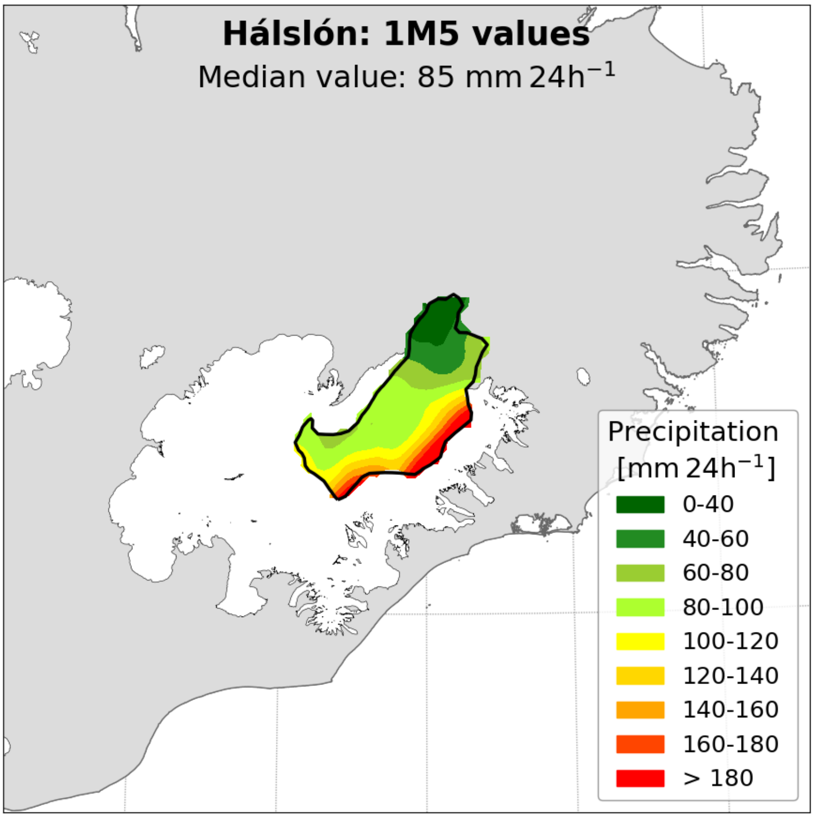

Figure 12 – 1M5 map for catchment Hálslón based on the complete ICRA dataset.

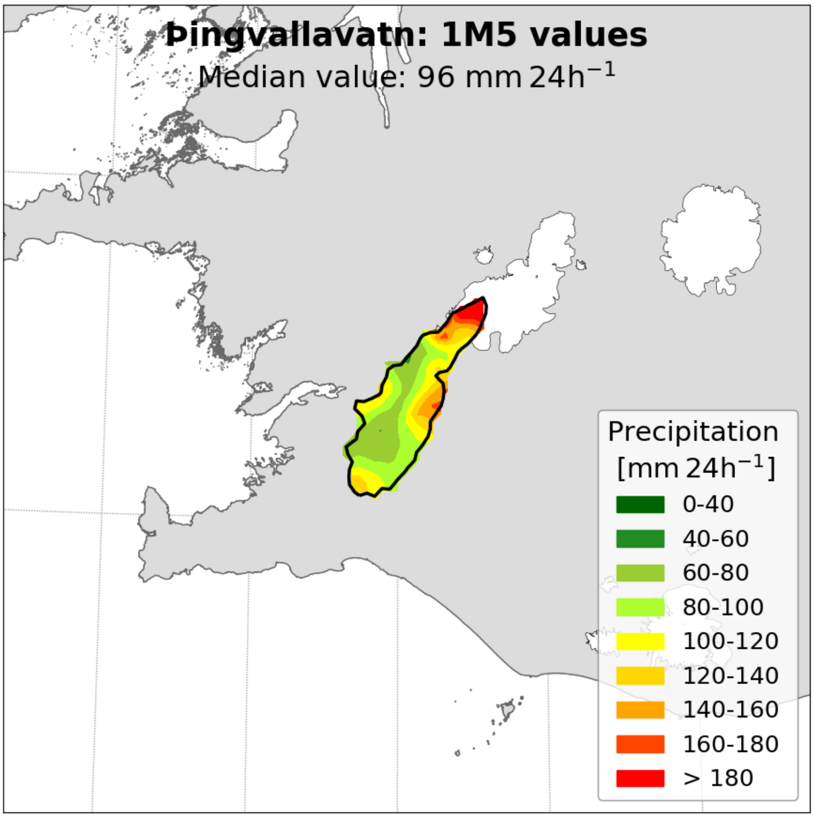

Figure 13 – 1M5 map for catchment Þingvallavatn based on the complete ICRA dataset.

5.2 Return levels for the hydropower catchments in relation to CMIP5 climate scenarios

5.2.1 Presentation of the climate datasets

The CMIP5 projections were briefly presented in Section 2. For this project, two types of simulations were used: the mild-warming scenario RCP 2.6, and the high-warming scenario RCP 8.5, each covering two periods: 2040 – 2060 and 2080 – 2100. Projections are given for an ensemble of 33 climate models.

For all the climate models and periods, monthly-averaged precipitation ratio changes are available. Because of the coarse horizontal resolution, those precipitation changes were averaged seasonally and for the whole country. To assess the variability of the results from the ensemble, the 10^{th} and 90^{th} percentiles were used in addition to the median values. This is expected to give the magnitude of the uncertainties within the 33 models.

Results for the seasonal precipitation changes averaged over the whole country are shown in Table 7 for scenarios RCP 2.6 and RCP 8.5. For each scenario, values are given for the two periods and based on the 10^{th}, 50^{th} and 90^{th} percentiles.

Results are comparable to those from Björnsson *et al.* (2018), based on monthly data and for a larger domain. As expected, changes are more significant when projecting into the later part of the century (period 2080 – 2100). From the tables, for RCP 2.6, a mild-warming scenario, the difference between the two periods is small. This was expected as those projections are calculated considering a more controlled carbon emission scenario, not impacting the climate in the long term as much as the other scenario. Perhaps more unexpectedly, for both cases the 10^{th} percentile of the ensemble climate dataset leads to a decrease of over 10% in all cases. However, the results for the 90^{th} percentile show an increase in excess of 20% in both scenarios and for the two timespans, i.e., the distribution of the results is right-skewed. Thus, the results show the variability within the climate model ensemble, with precipitation in some models expected to decrease.

Table 7 – Seasonal precipitation changes (%) for scenario RCP 2.6 (top) and RCP 8.5 (bottom) for the whole country. Results are shown for time periods 2040 – 2060 and 2080 – 2100 and using the 10th, 50th and 90th percentile of the climate data ensemble. Note that calendar months are abbreviated to first letters.

	RCP 2.6 *Percentage change (%)*					
	2040 - 2060			**2080 – 2100**		
	10th	**50th**	**90th**	**10th**	**50th**	**90th**
DJF	-12	1	17	-14	2	20
MAM	-12	4	23	-13	3	22
JJA	-12	3	21	-13	4	24
SON	-9	4	21	-9	5	21
Annual	*-11.3*	*3*	*20.5*	*-12.3*	*3.5*	*21.8*

	RCP 8.5 *Percentage change (%)*					
	2040 - 2060			**2080 – 2100**		
	10th	**50th**	**90th**	**10th**	**50th**	**90th**
DJF	-11	2	21	-15	3	27
MAM	-13	3	21	-15	5	23
JJA	-11	3	22	-10	6	28
SON	-9	5	20	-7	10	30
Annual	*-11*	*3.3*	*21*	*-11.8*	*6*	*27*

5.2.2 Incorporation of the climate projections to the ICRA dataset

The inclusion of the two RCP scenarios into the reanalysis was done following several steps. Firstly, the complete ICRA dataset was detrended to remove any bias related to climate change within the period 1979 – 2017. Consequently, the dataset was flattened out, preventing the future analysis to only focus on the later years of the dataset when precipitation extremes are possibly more frequent (as seen in Section 4.2 as well as in Björnsson *et al.* (2018)). Then, the average values for each grid-point were added back to the detrended timeseries, and because precipitation cannot be negative, all negative values were set back to zero.

An example can be seen in Figure 14. The figure shows the regression lines associated with the timeseries extracted for grid-point [100,100], arbitrarily chosen, based on the original dataset (blue line) and after detrending (red line). The difference between the first time step and the last one for the original timeseries is 0.1154 mm, while for the detrended timeseries the value is 0.040 mm. Note that, the detrended timeseries would have had a net difference of zero if the negative values had not been set back to zero. This shows that over the 39 years of data, there was a slight precipitation increase for this grid-point. This trend has been removed, resulting in a detrended, almost flat dataset.

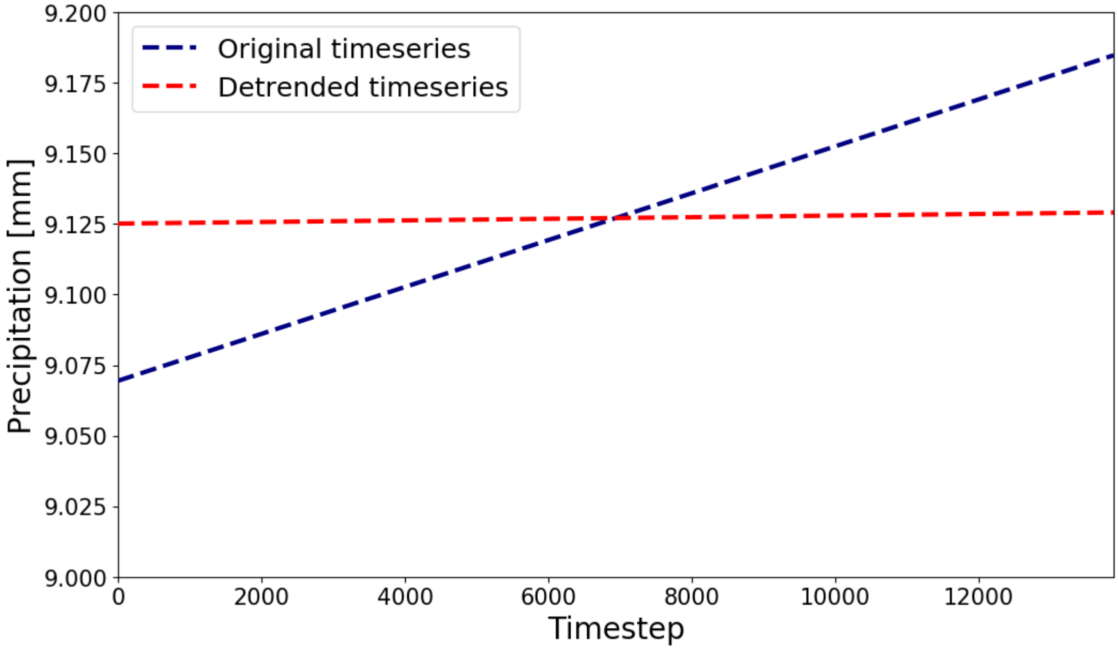

Figure 14. Regression lines for hourly precipitation timeseries of grid-point [100, 100] from the ICRA dataset, before (blue line) and after (red line) detrending.

Subsequently, the seasonal percentage changes presented in Table 7 were applied to the whole dataset. Because of the different scenario presented (RCP 2.6 or 8.5), the period considered (2040 – 2060 or 2080 – 2100), and the type of data used (10^{th}, 50^{th} or 90^{th} percentile), a total of 12 new datasets were generated. The same percentage changes were also applied to the catchment timeseries.

Density plots for catchment Þingvallavatn are found in Figure 15, showing how the overall precipitation distribution is affected by the different scenarios. For more clarity, the density plots are shown according to the various percentiles. Overall, the results are not drastically changed. This is especially notable for the middle figure where density plots are shown for the original precipitation timeseries, modified by the median climate data projections. For the 10^{th} percentile projections (top figure), the new timeseries peaks higher and for a slightly lower precipitation intensity, and consequently there are not as many occurrences of higher precipitation intensities (above 20 mm). Therefore, when looking at the 10^{th} percentile results, the projections lead to a narrower range of precipitation intensities. However, for the 90^{th} percentile, the opposite trend is observed: the peak in the low precipitation intensity is not as high as for the original dataset, but more occurrences of high precipitation can be seen. The scenario RCP 8.5 for the period 2080 – 2100 shows more extreme results, which was expected from the percentage changes displayed in Table 7. Note that for the 50^{th} and 90^{th} percentiles there is a significant decrease in low precipitation intensity from the first period to the second, indicating a shift towards higher precipitation intensity with time.

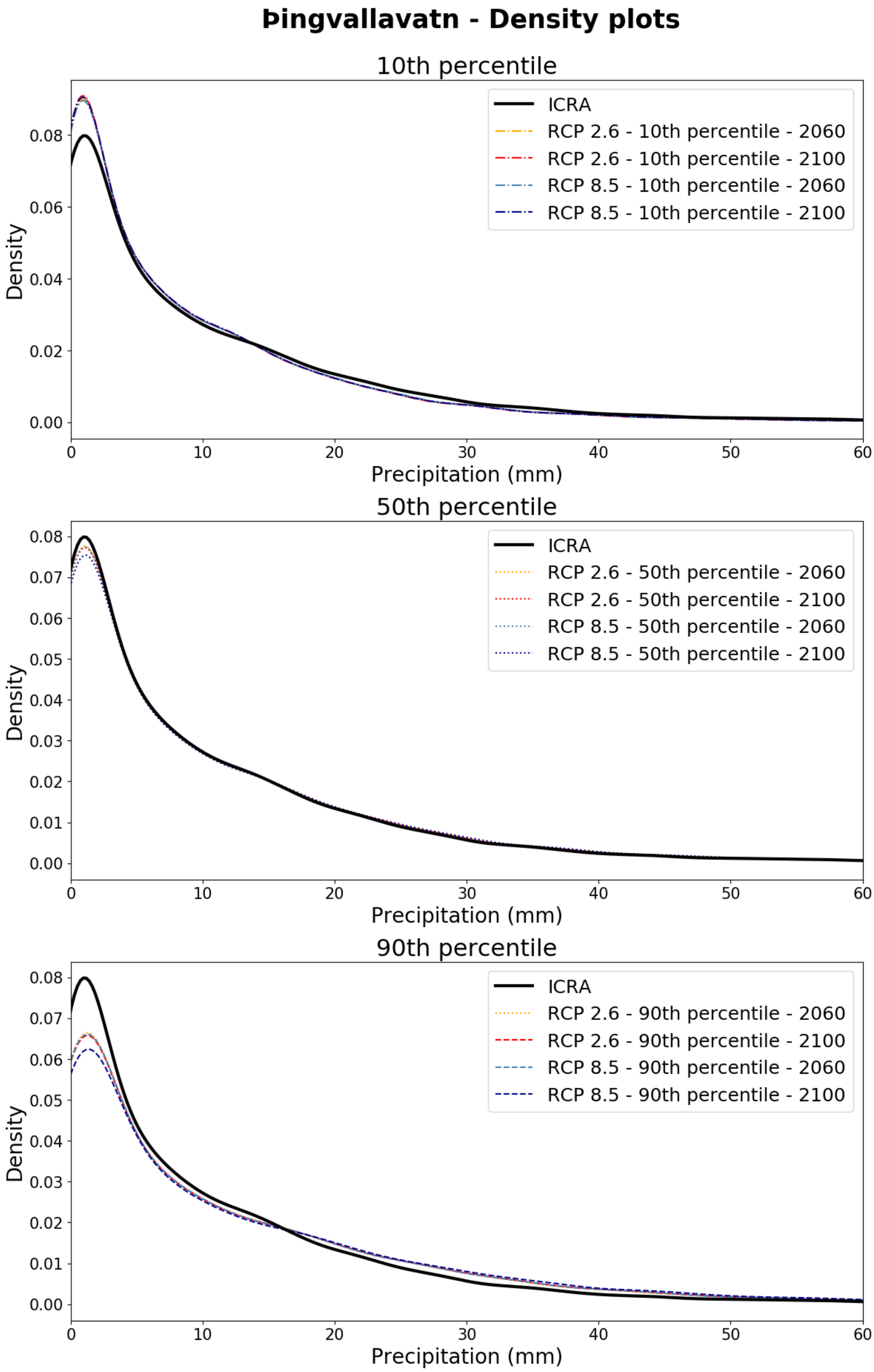

Figure 15 – Density plots for catchment Þingvallavatn. Precipitation distributions are shown in the original dataset (solid black line), along with the different projections while looking at the 10th (top), 50th (middle), and 90th (bottom) percentiles of the ensemble climate dataset.

5.2.3 New 1M5 maps including climate projections

5.2.3.1 1M5 results for the whole country

Eventually, an EVA was performed using the Peak-over-Threshold method with Maximum Likelihood Estimation on all the datasets, resulting in twelve new 1M5 maps. From now on, results will only be shown for the period 2080 – 2100, as projections for the end of the century are of more interest for this study. Some results for the period 2040 – 2060 are included in Appendix III (Figures III.1 – 11).

Three maps are presented in this report: the 1M5 map with median percentage changes from the ensemble climate models with RCP 8.5 projections (Figure 16), the 1M5 map with 10th percentile percentage changes with RCP 2.6 projections (Figure 17), and the 1M5 map with 90th percentile percentage changes with RCP 8.5 projections (Figure 18). According to the tables, it is expected that Figure 16 gives the lowest 1M5 results and Figure 18 the highest. They are included here to assess the variability of the results, with all the other results falling somewhere in between those two maps.

Upon initial inspection, these maps do not differ greatly from the original 1M5 map (Figure 1). In the original map, higher values are found over icecaps (most notably on Vatnajökull, Mýrdalsjökull and Langjökull). The highest 1M5 values are calculated for a grid-point on the southern part of the Vatnajökull icecap. In general, except for Snæfellsjökull and Drangajökull, higher values are found on the southern sides of the icecaps while lower values are in drier lowland areas. The northern lowlands are generally drier as indicated by a large dark green area on the map. Lowlands in the southern half of the country typically have values ranging between 40 and 60 mm day^{-1} and in a few places under 40 mm day^{-1}. Regions of complex orography such as the East- and Westfjords are associated with higher 5-year return levels than the lowlands, with values ranging from 80 to 180 mm day^{-1} in the East and values between 60 and 140 mm day–1 in the Westfjords. Locally, higher values are also reached in other mountainous regions such as Bláfjöll, Tröllaskagi or Flateyjarskagi. The median value over Iceland is 72 mm 24-h^{-1} and the maximum is 470 mm 24-h^{-1}.

Overall, the same geographical patterns can be observed on the new maps and the differences lie in the details. Figure 16 shows the new values obtained with the RCP 8.5 projections using the median percentage changes from the climate model ensemble. Under this scenario, the median value for the whole country is 76 mm 24-h^{-1} and the maximum is 502 mm 24h^{-1}. The red areas in the East- and Westfjord regions, corresponding to values above 180 mm 24-h^{-1}, are slightly wider while the dark green region, with low values, over the lowland is narrowed. This is further visible for the RCP 2.6 projections with the 10th percentile values (Figure 17) with a median value of 63 mm 24-h^{-1} and the highest value of 416 mm 24-h^{-1}. On the 1M5 map presenting the results with the RCP 8.5 projections based on the 90th percentile precipitation changes (Figure 18), the dark green area has almost disappeared, indicating very few instances of values under 40 mm 24-h^{-1}. A red area extends almost continuously from Mýrdalsjökull northeastward to the northern part of the Eastfjords, values above 180 mm 24-h^{-1}. The same can be seen for Tröllaskagi, Snæfellsness and Hornstrandir, where the regions are almost completely covered with 1M5 values above 180 mm 24-h^{-1}. Under these projections, the median value for the whole country is 92 mm 24-h^{-1} and the maximum value is 602 mm 24-h^{-1} and can be found a few kilometres south of Hvannadalshnjúkur.

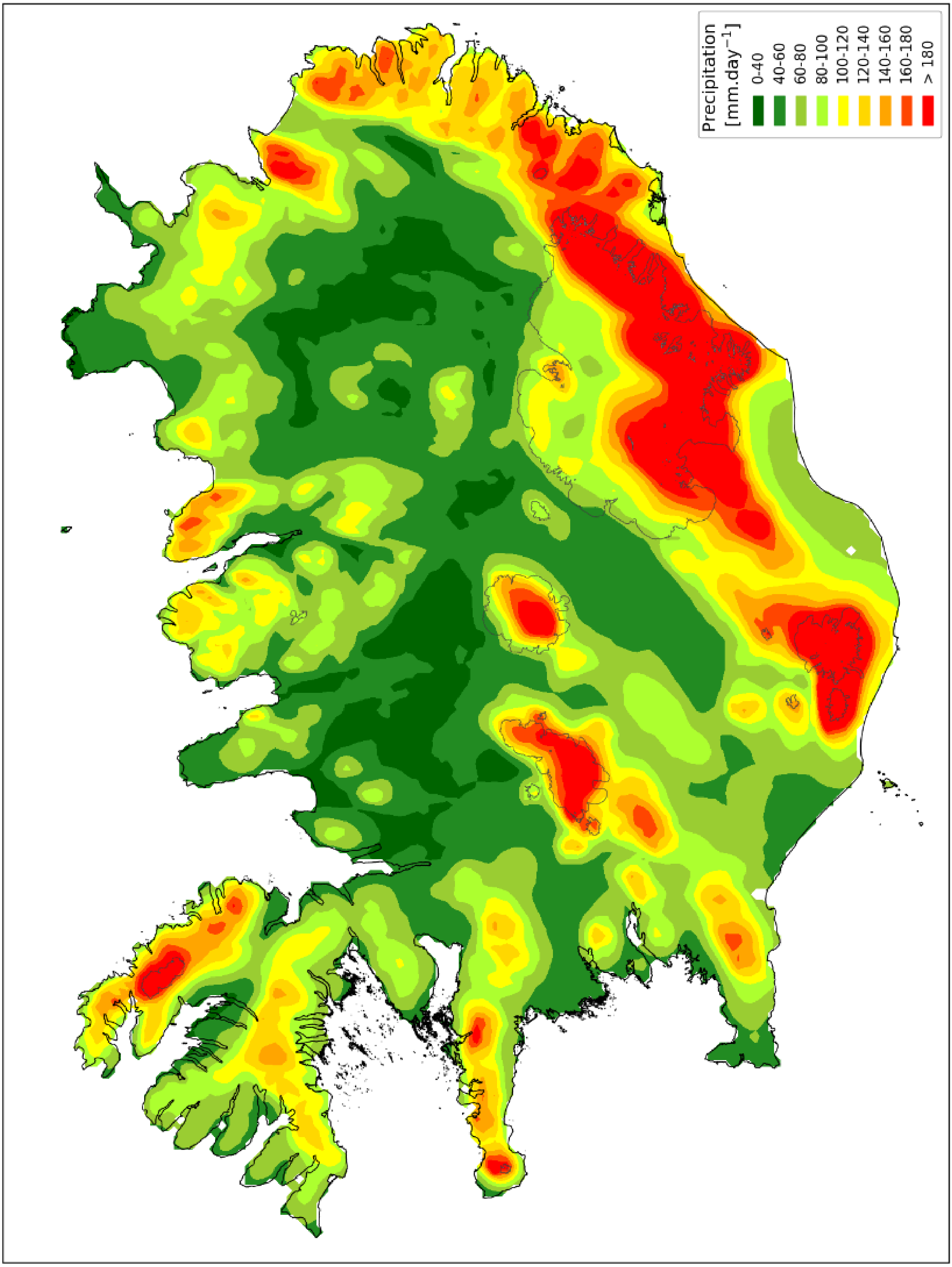

Figure 16 – 1M5 map based on 24-hour accumulated precipitation, with projections from the RCP 8.5 for the interval 2080 – 2100, using the 50th percentile from the climate model ensemble. Results obtained using the Peak-over-Threshold method with MLE.

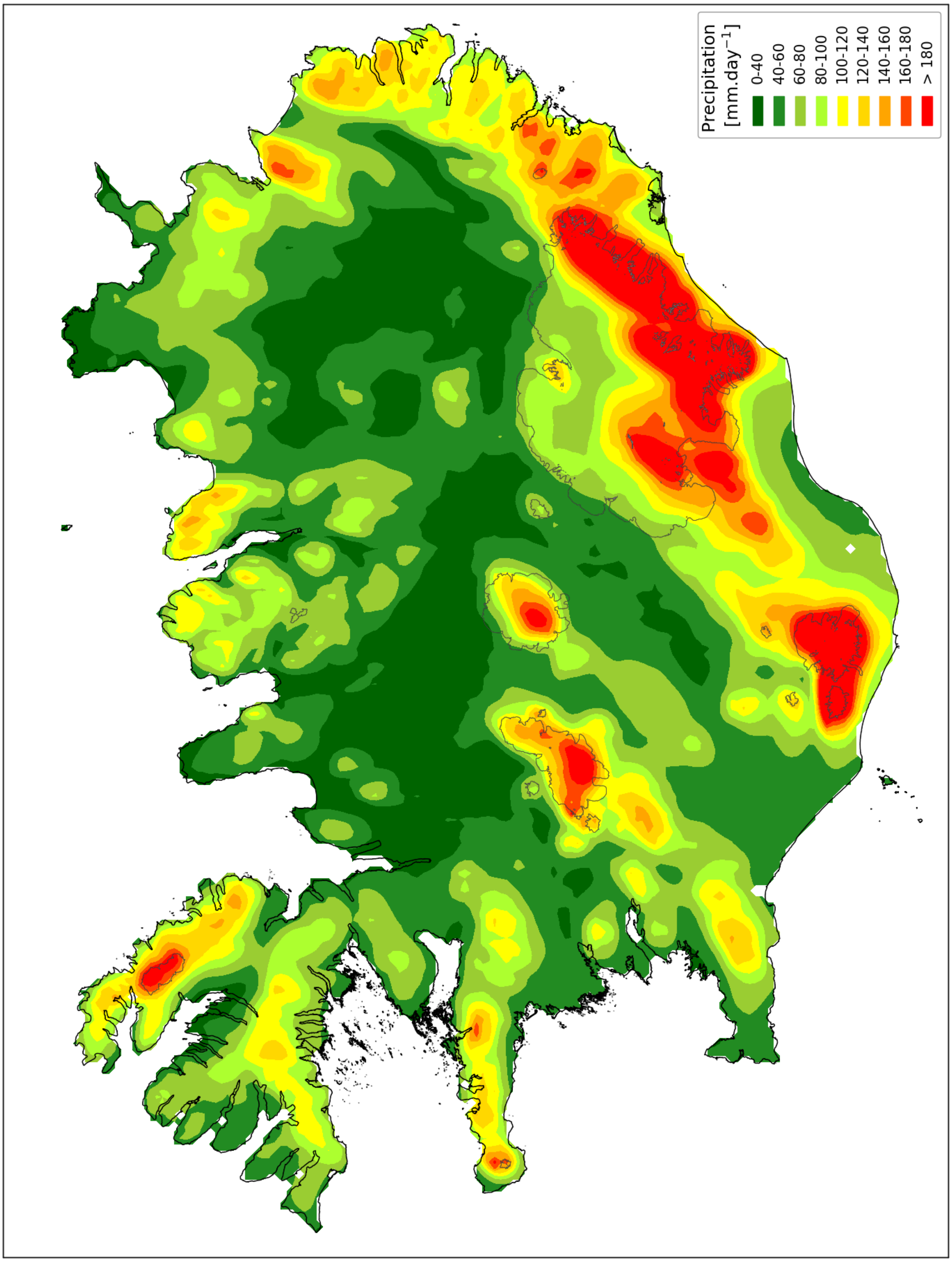

Figure 17 – 1M5 map based on 24-hour accumulated precipitation, with projections from the RCP 2.6 for the time-period 2080 – 2100, using the 10th percentile from the climate model ensemble. Results obtained using the Peak-over-Threshold method with MLE.

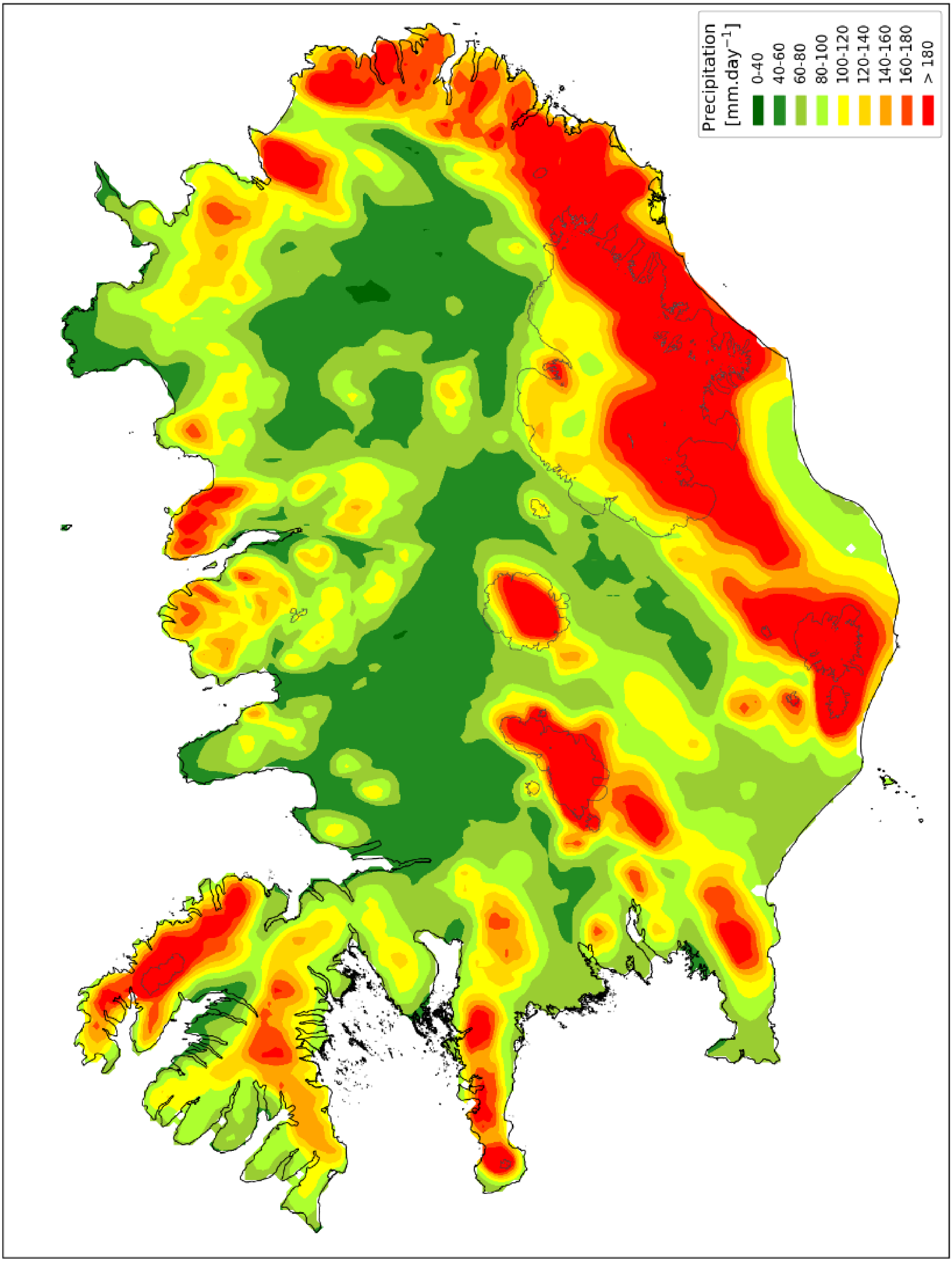

Figure 18 – 1M5 map based on 24-hour accumulated precipitation, with projections from the RCP 8.5 for the interval 2080 – 2100, using the 90th percentile from the climate model ensemble. Results obtained using the Peak-over-Threshold method with MLE.

5.2.3.2 1M5 results for the hydropower catchments

Table 8 shows the median 1M5 results for all the catchments with the two projections and for the period 2080 – 2100. For comparison, original values are shown in the first column. Overall, changes are more significant with the RCP 8.5 scenarios, with higher values reached by using the 90th percentile percentage changes. Results are shown in map format on Figure 19 for catchment Hálslón. Even though the increase is minimal while using median percentage change from the RCP 8.5 projections (top right), it can be noted that almost no values under 40 mm 24-h^{-1} (dark green area) are left compared to the original map without projection (top left). Most changes can be seen on the map that includes the RCP 8.5 projections with the 90th percentile percentage changes (bottom right), with values above 100 mm 24-h^{-1} (yellow, orange and red areas) spreading towards the northern part of Vatnajökull.

Table 8 – Median 1M5 values (mm 24-h^{-1}) for eleven hydropower catchments with and without climate projections for the period 2080 – 2100.

Catchment	**1M5 median value** ***mm 24-h^{-1}***						
	Original	**RCP 2.6**			**RCP 8.5**		
		10%	**50%**	**90%**	**10%**	**50%**	**90%**
Blönduvirkjun	**48**	41	49	58	42	50	61
Búðarháls	**46**	40	47	56	40	48	59
Hágöngulón	**63**	55	65	76	55	66	81
Hálslón	**85**	75	88	104	77	91	109
Hraunaveita	**132**	116	136	159	117	140	169
Kvíslaveita	**48**	42	49	58	42	51	61
Sultartangi	**66**	57	68	80	58	69	84
Þingvallavatn	**96**	84	99	117	85	102	123
Þórisvatn	**47**	41	49	57	42	50	60
Tungnaá	**76**	67	79	92	67	80	98
Ufsarlón	**104**	92	108	126	93	112	134

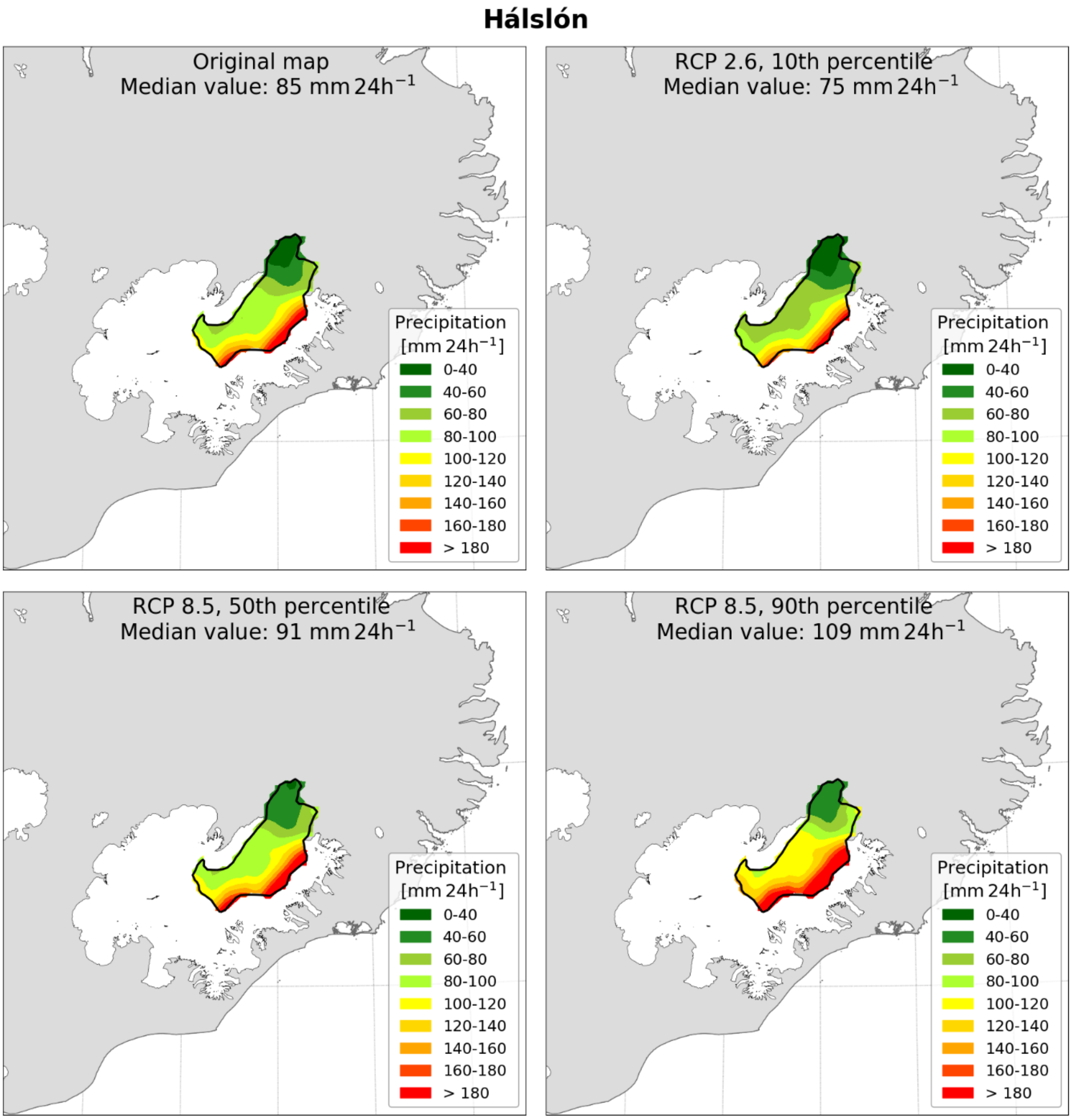

Figure 19 – 1M5 maps for catchment Hálslón based on the ICRA dataset without projection (top left), with RCP 2.6 and 10th percentile percentage changes (top right), with RCP 8.5 and median percentage changes (bottom left) and with RCP 8.5 and 90th percentile percentage changes (bottom right). Projections were calculated for the time-period 2080 – 2100 and come from the CMIP5.

5.2.4 New return levels for the hydropower catchments

Lastly, the climate projections were added to the catchment timeseries to calculate new return levels for various time durations and return periods. Both RCP scenarios were investigated for the period 2080 – 2100. Here, only the 50th percentile changes (corresponding to the median values) from the climate ensemble models are used.

Results for catchments Hálslón and Þingvallavatn are shown in Tables 9 and 10, without and with projections to facilitate the comparison. Results for the other catchments are in Appendix III (Tables III.1 – 11). With the RCP 2.6 scenario, return levels increase on average by 3.3% for catchment Hálslón and 3.1% for catchment Þingvallavatn. As expected, changes are higher under the RCP 8.5 scenario with an increase of 5.8 % and 5.9%, respectively. Results for all the catchments fall within the same range, with a mean increase of 3.2% with the RCP 2.6 scenario, and 5.7% with the RCP 8.5 scenario. Note that those averaged increases were calculated from precise return levels, and not from rounded values as shown in the tables. Those averages are comparable to the annual percentage changes for those scenarios shown in Table 7: 3.5% with RCP 2.6 and 6% with RCP 8.5.

Another way of looking at those results is to show them graphically, as Intensity-Duration-Frequency graphs (known as IDF curves). Those graphs are used to represent the relationship between the precipitation intensity, duration, and frequency. This type of data presentation allows users to visualise and compare return period thresholds from different locations. Contrary to the 1M5 values, given in mm day^{-1}, precipitation intensity in IDF curves is to be read in mm h^{-1} on the y-axis. Results are shown for all catchments in Appendix III (Figures III.12 – 22), and for catchments Hálslón and Þingvallavatn on Figure 20, with and without the RCP scenarios. On the IDF curves, values are ranked according to the projection used: precipitation intensities without projections are lower than with RCP 2.6, which are lower than with RCP 8.5. As expected, the amount of precipitation over a given interval increases with the duration of the event. However, in some cases (e.g., see 2-year return period line for catchment Þingvallavatn), when converted to mm h^{-1} and shown graphically, precipitation intensities sometimes increase with the duration, creating a bump in the usually decreasing IDF curves. Those values are attributed to the fact that the Peak-over-Threshold method was applied independently on timeseries for each duration. Comparing both sets of IDF curves, return levels are higher for catchment Þingvallavatn, and values are less spread, with some curves even overlapping (see 50- and 100-year return periods lines).

*Table 9 – **Return levels (mm) for catchment Hálslón.** Results are based on the ICRA dataset without projections (top), with RCP 2.6 scenario (middle) and with RCP 8.5 scenario (bottom). Values are given for 3-, 6-, 12-, 24- and 48-hour return levels with a 2-, 5-, 10-, 25-, 50- and 100-year return period. Timeseries were extracted using the average value of all the grid-points within the catchment. The 1M5 value is shown in red.*

	2 years	**5 years**	**10 years**	**25 years**	**50 years**	**100 years**
3 hours	8	11	13	15	18	20
6 hours	18	23	27	31	36	39
12 hours	35	43	49	54	62	67
24 hours	60	**70**	78	85	94	101
48 hours	91	105	115	125	137	147

	2 years	**5 years**	**10 years**	**25 years**	**50 years**	**100 years**
3 hours	8	11	13	16	19	21
6 hours	18	24	28	32	37	41
12 hours	36	44	50	56	64	69
24 hours	62	**72**	80	88	97	104
48 hours	94	108	119	129	142	152

	2 years	**5 years**	**10 years**	**25 years**	**50 years**	**100 years**
3 hours	8	11	14	16	19	22
6 hours	19	24	29	33	38	42
12 hours	37	46	52	58	65	71
24 hours	63	**74**	82	90	100	107
48 hours	97	111	121	131	143	152

*Table 10 – **Return levels (mm) for catchment Þingvallavatn.** Results are based on the ICRA dataset without projections (top), with RCP 2.6 scenario (middle) and with RCP 8.5 scenario (bottom). Values are given for 3-, 6-, 12-, 24- and 48-hour return levels with a 2-, 5-, 10-, 25-, 50- and 100-year return period. Timeseries were extracted using the average value of all the grid-points within the catchment. 1M5 value is underlined in red.*

	2 years	**5 years**	**10 years**	**25 years**	**50 years**	**100 years**
3 hours	12	15	18	19	21	23
6 hours	26	31	35	38	41	44
12 hours	48	56	62	67	73	77
24 hours	78	**90**	99	107	117	124
48 hours	113	128	138	148	159	168

	2 years	**5 years**	**10 years**	**25 years**	**50 years**	**100 years**
3 hours	12	16	18	20	22	23
6 hours	26	32	36	39	43	45
12 hours	49	58	64	69	76	80
24 hours	80	**93**	102	110	120	128
48 hours	117	132	142	151	163	172

	2 years	**5 years**	**10 years**	**25 years**	**50 years**	**100 years**
3 hours	13	16	19	21	23	24
6 hours	27	33	37	40	44	46
12 hours	50	59	66	71	78	83
24 hours	82	**95**	104	112	123	130
48 hours	120	135	146	156	168	177

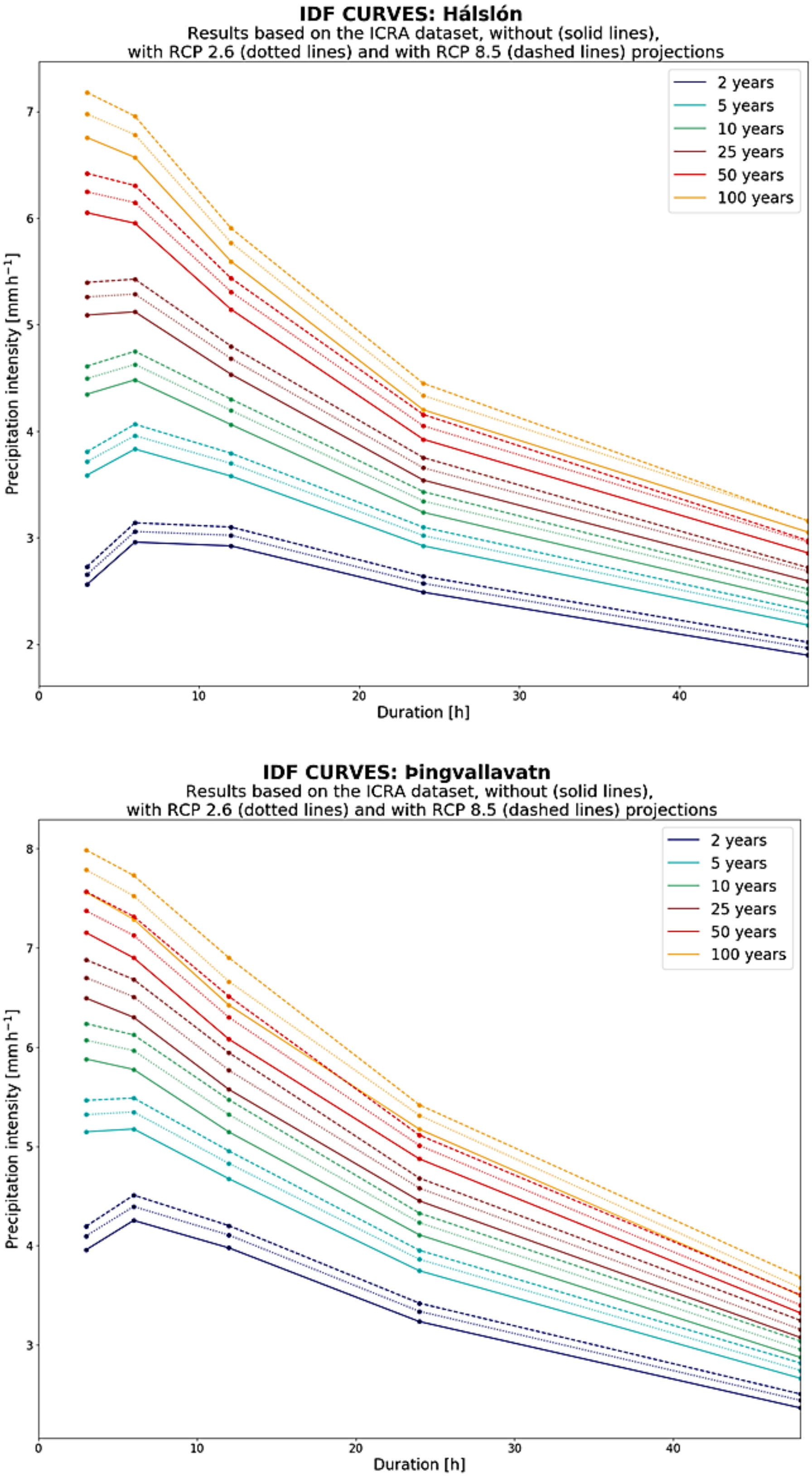

Figure 20 – IDF curves for catchment Hálslón (top) and Þingvallavatn (bottom) based on the ICRA dataset, without projections (solid lines), with RCP 2.6 projections (dotted lines) and with RCP 8.5 projections (dashed lines). Solid points give return levels for 3-, 6-, 12-, 24- and 48-hour duration with a 2-, 5-, 10-, 25-, 50- and 100-year return period. Each coloured line corresponds to a different return period as stated by the legend.

6 Conclusions

This research addressed two questions: Firstly, are systematic changes in the seasonality of precipitation observed already in the ICRA reanalysis data covering 39 years, in particular in the eleven hydropower watersheds operated by Landsvirkjun? Secondly, how are climate projections expected to affect the return levels of precipitation in Iceland, and specifically in the eleven hydropower catchments?

Firstly, the change in the onset of the melt season was investigated using the ICRA dataset. In most catchments, a shift in the onset date of the melt season is apparent over the 39 years of reanalysis. Even though great year to year variability was observed, in 9 catchments out of 11, the melt season advanced by 5 to 29 days. Catchments located in the south-west of Iceland (Búðarháls, Þingvallavatn, Tungnaá and Þórisvatn) showed a larger recession in the beginning date of the melt season. In two instances (Hálslón and Ufsarlón), the linear regression led to no shift or a delay.

Secondly, the temporal variability of the snow-fraction was then studied. In all cases, the total snow-fraction decreased over the period between 1.5 and 14.6%. The largest changes (exceeding 10%) were observed for catchments at lower altitudes (Búðarháls, Þingvallavatn), or located on the southern parts of the ice-caps (Sultartangi, Þórisvatn, Tungnaá). Snow-fraction was also assessed monthly, and in most cases, November was the month with the largest percentage change, indicating a delay in the start of the snow season throughout the period 1979 – 2017.

Finally, the return levels in the hydropower catchments were calculated using the Peak-over-Threshold method. First, the EVA was applied to the ICRA dataset, and return levels for the eleven catchments were presented in tables and maps. Then, two CMIP5 projections were investigated: the mild-warming scenario RCP 2.6, and the high-warming scenario RCP 8.5. New 1M5 maps for Iceland including projections were produced using projections for the period 2080 – 2100. Results shared the same geographical patterns as the original 1M5 map. The most significant changes were found within the 1M5 map with RCP 8.5 projections based on the 90th percentile precipitation increases. On this map, very few instances of values under 40 mm 24-h^{-1} remain. An area with values above 180 mm 24-h^{-1} extends almost continuously from Mýrdalsjökull to the northern part of the Eastfjords. The same trend can be seen for Tröllaskagi, Snæfellsness and Hornstrandir, where 1M5 values exceed 180 mm 24-h^{-1} in most cases. Under these projections, the median value for the whole country is 92 mm 24-h^{-1} and the maximum value is 602 mm 24-h^{-1}, against 72 mm 24-h^{-1} and 470 mm 24-h^{-1} in the original 1M5 map. Return levels with median projections from the two RCP scenarios were then calculated for the eleven hydropower catchments and results presented in maps, tables and on IDF curves.

Overall, these results show that systematic changes can be observed in the seasonality of precipitation in the ICRA dataset for most of the catchments. With ongoing global warming, precipitation return levels will have increased by the end of the century, with a mean increase in the hydropower catchments ranging from 3.2 to 5.7%, depending on the greenhouse gas concentration trajectory. These results will assist Landsvirkjun with long-term assessments of runoff potential for the hydropower catchments featured in this research.

Bibliography

Bengtsson, L., Andrae, U., Aspelien, T., Batrak, Y., Calvo, J., de Rooy, W. & Køltzow, M.Ø. (2017). The HARMONIE-AROME model configuration in the ALADIN-HIRLAM NWP system. *Mon. Wea. Rev*, 145, 1919–1935

Bintanja, R. (2018) The impact of Arctic warming on increased rainfall. *Scientific Reports*, 8, 16001. https://doi.org/10.1038/s41598-018-34450-3.

Björnsson, H., Sigurðsson, B. D., Davíðsdóttir, B., Ólafsson, J., Ástþórssson, Ó. S., Ólafsdóttir, S., Baldursson, T. & Jónsson, T. (2018). Loftslagsbreytingar og áhrif þeirra á Íslandi – Skýrsla vísindanefndar um loftslagsbreytingar 2018. *Veðurstofa Íslands*. 238 pp.

Coles, S. (2001). An Introduction to Statistical Modeling of Extreme Values. London; *Springer*.

Crochet P., Johannesson T., Jonsson T., Sigurdsson O., Bjornsson H., Palsson F. & Barstad I. (2007). Estimating the spatial distribution of precipitation in Iceland using a linear model of orographic precipitation. *Journal of Hydrometeorology* 8, 1285–1306.

Elíasson, J. (2000). Design values for precipitation and floods from M5 values; *Nordic Hydrology*, 31 (4/5), 357–372.

Elíasson, J., Rögnvaldsson, Ó. & Jónsson, T. (2009). Extracting statistical parameters of extreme precipitation from a NWP model. *Hydrology & Earth System Sciences* 13, 11, 2233–2240

Feng, S. & Hu, Q. (2007), Changes in winter snowfall/precipitation ratio in the contiguous United States, *J. Geophys. Res*., 112, D15109, doi:10.1029/2007JD008397.

Hlodversdottir, Á.Ó., Björnsson, B., Andradottir, H., Elíasson, J. & Crochet, P. (2015). Impacts of climate change on combined sewer systems in Reykjavik. *Water Science and Technology*, 71(10), 1471–1477. doi: 10.2166/wst.2015.119.

IPCC (2021). Climate Change 2021: The Physical Science Basis. Contribution of Working Group I to the Sixth Assessment Report of the Intergovernmental Panel on Climate Change [Masson-Delmotte, V., P. Zhai, A. Pirani, S.L. Connors, C. Péan, S. Berger, N. Caud, Y. Chen, L. Goldfarb, M.I. Gomis, M. Huang, K. Leitzell, E. Lonnoy, J.B.R. Matthews, T.K. Maycock, T. Waterfield, O. Yelekçi, R. Yu, and B. Zhou (eds.)]. *Cambridge University Press.* In Press.

Li, Z., Chen, Y. & Li, Y. (2020). Declining snowfall fraction in the alpine regions, Central Asia. *Sci Rep* **10,** 3476.

Massad, A.-G. R., Petersen, G. N., Þórarinsdóttir, T., Roberts, M. J. (2020). Reassessment of return levels in Iceland. *Veðurstofa Íslands*. VÍ 2020-008. 140 pp.

Nawri, N., Pálmason, B., Petersen, G. N., Björnsson, H. & Þorsteinsson, S. (2017). The ICRA atmospheric reanalysis project for Iceland. *Veðurstofa Íslands*. VÍ 2017-005. 39 pp.

Poli, P., Hersbach, H., Dee, D.P., Berrisford, P., Simmons, A.J., Vitart, F., Laloyaux, P., Tan, D.G.H., Peubey, C., Thépaut J.-N., Trémolet, Y., Hólm, E.V., Bonavita, M., Isaksen, L. & Fisher, M. (2016). ERA-20C: an atmospheric reanalysis of the twentieth century**.** *J Clim*, 29 (11), pp. 4083-4097.

Taylor, K.E., Stouffer R.J. & Meehl, G. A., 2012. A summary of the CMIP5 experiment design. *Bull. Am. Meteorol.* Soc. 93, 485–498.

Appendix I. Melt season analysis

In this appendix, figures similar to Figure 7 in Section 4.1 are presented.

Figures I.1 – I.11 show the starting date of the melt season for each catchment, for the time-period 1979 – 2017. On each plot, the x-axis shows the 39 years used for the study, and the y-axis the start date of the melt season, between March and July. For every year, the melt season starting date is plotted with a blue dot, and a blue line connects the dates for all the years. A regression line fitting those values (light orange line) is shown. The difference in days between the beginning and the end of the period, as calculated from the regression line, is indicated at the top of the plot.

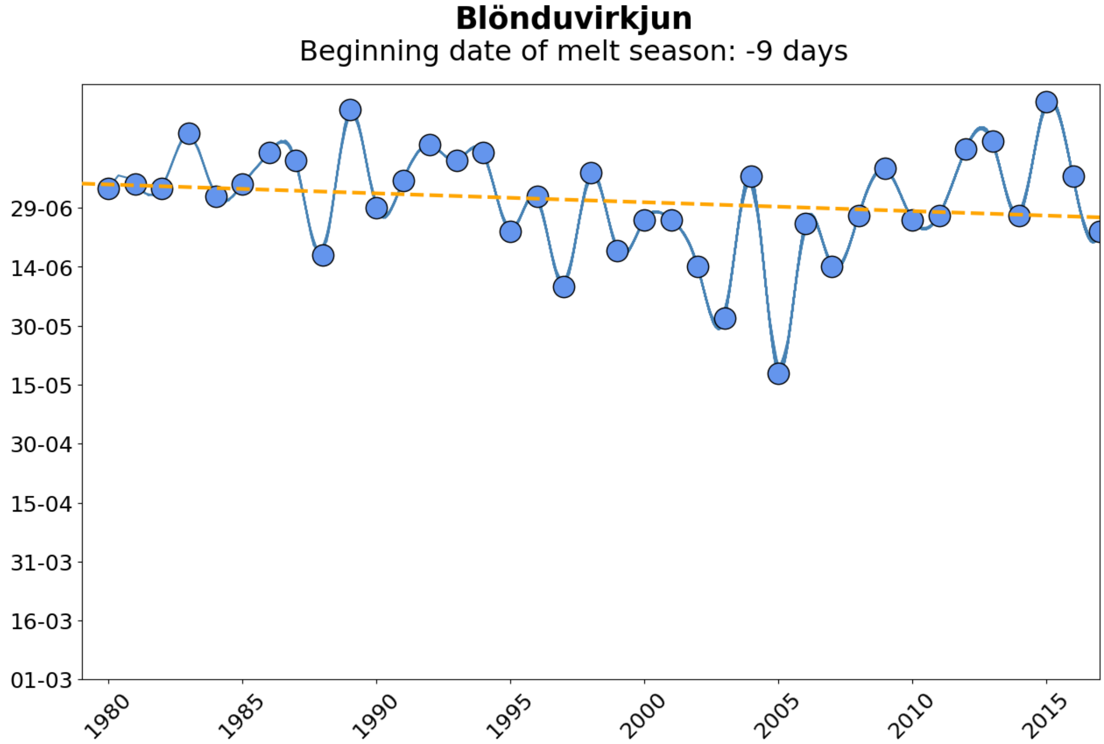

Figure I.1 – Evolution of the beginning date of the melt season for catchment Blönduvirkjun for the period 1979 – 2017. Results were obtained using an automatic filter on the snowpack, temperature and melting timeseries extracted from the ICRA.

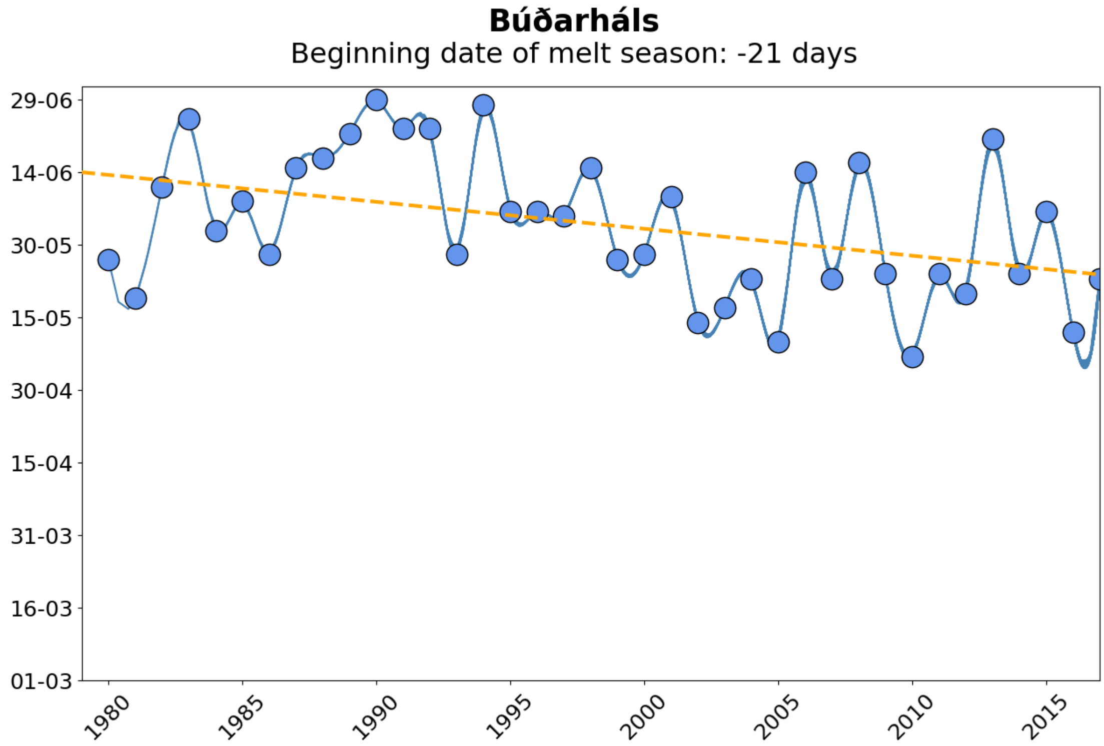

Figure I.2 – Evolution of the beginning date of the melt season for catchment Búðarháls for the period 1979 – 2017. Results were obtained using an automatic filter on the snowpack, temperature and melting timeseries extracted from the ICRA.

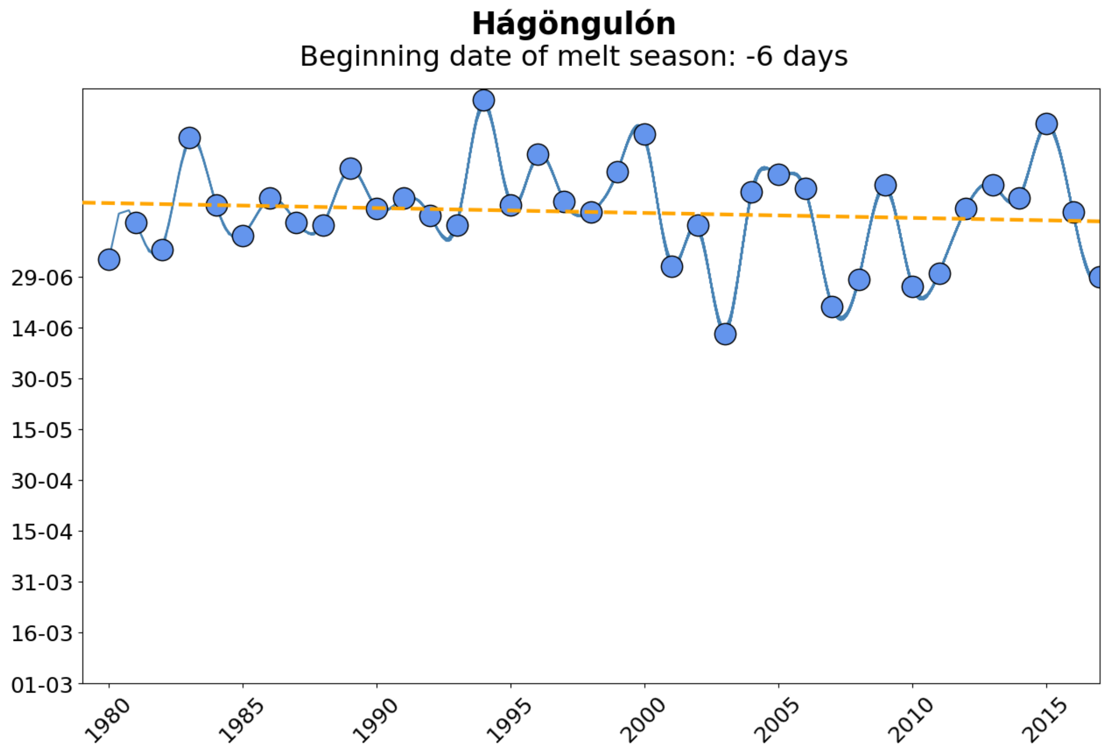

Figure I.3 – Evolution of the beginning date of the melt season for catchment Hágöngulón for the period 1979 – 2017. Results were obtained using an automatic filter on the snowpack, temperature and melting timeseries extracted from the ICRA

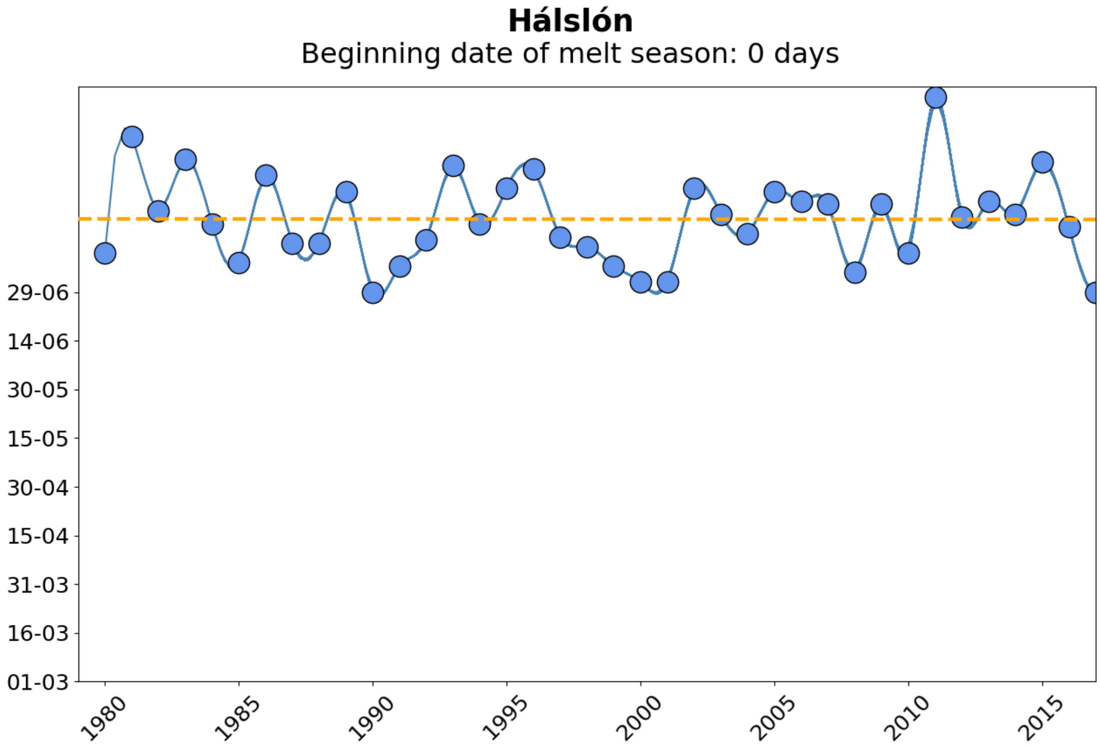

Figure I.4 – Evolution of the beginning date of the melt season for catchment Hálslón for the period 1979 – 2017. Results were obtained using an automatic filter on the snowpack, temperature and melting timeseries extracted from the ICRA.

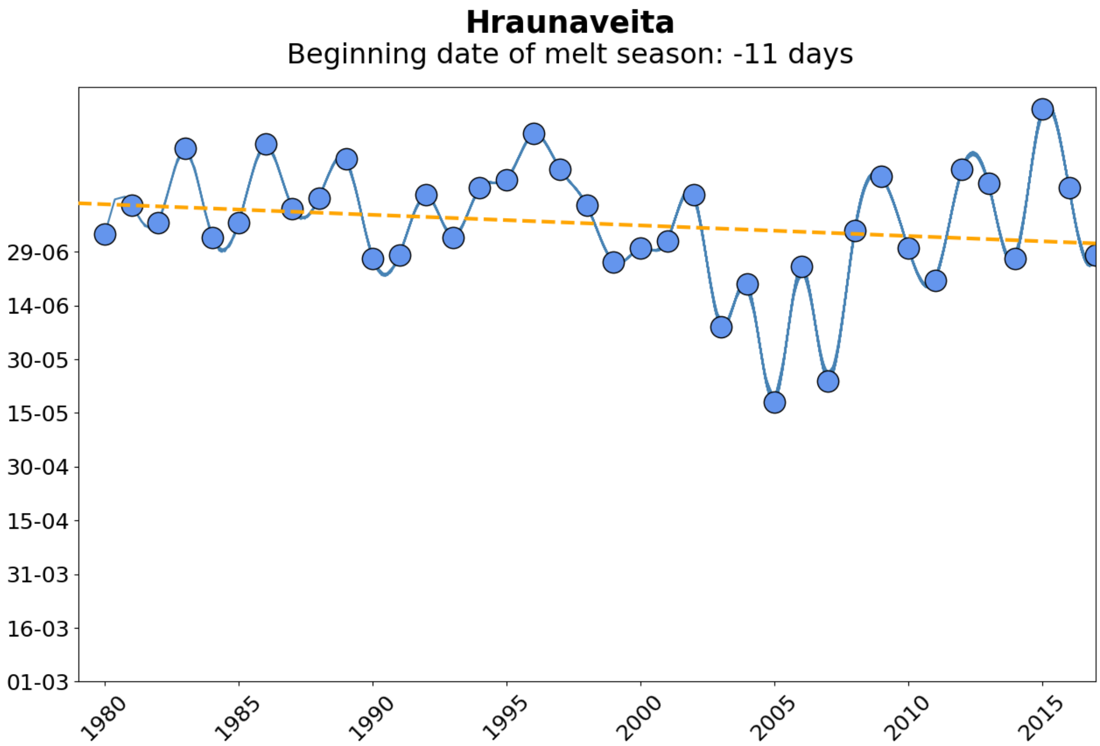

Figure I.5 – Evolution of the beginning date of the melt season for catchment Hraunaveita for the period 1979 – 2017. Results were obtained using an automatic filter on the snowpack, temperature and melting timeseries extracted from the ICRA.

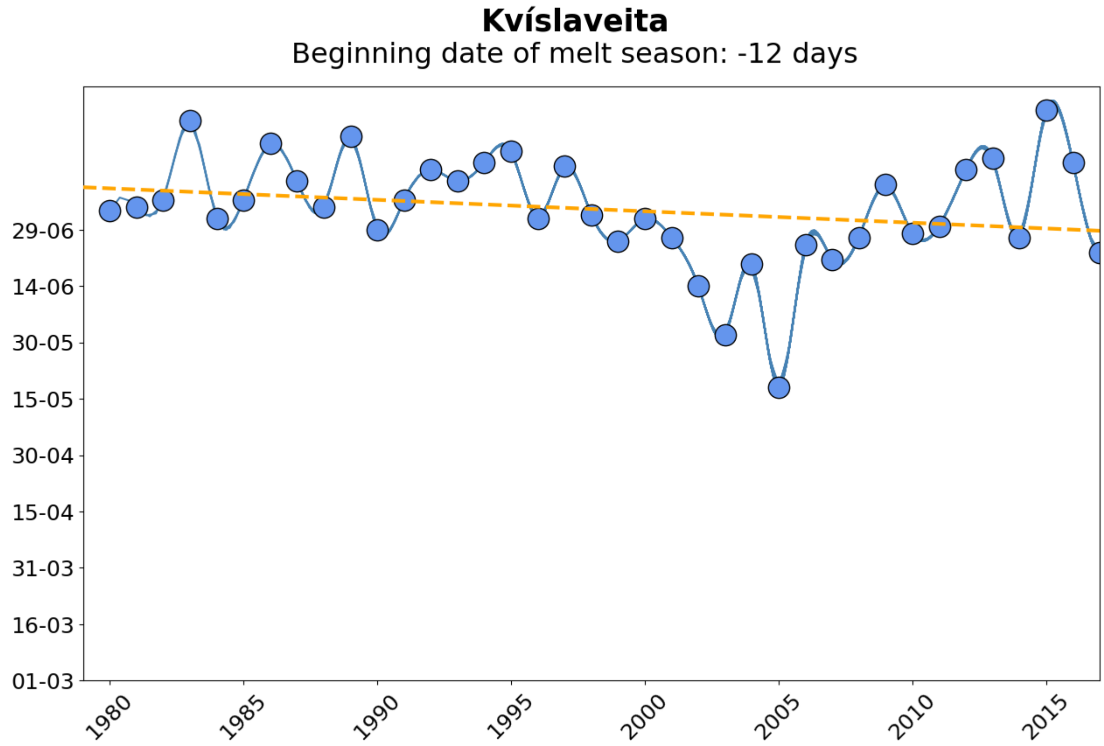

Figure I.6 – Evolution of the beginning date of the melt season for catchment Kvíslaveita for the period 1979 – 2017. Results were obtained using an automatic filter on the snowpack, temperature and melting timeseries extracted from the ICRA.

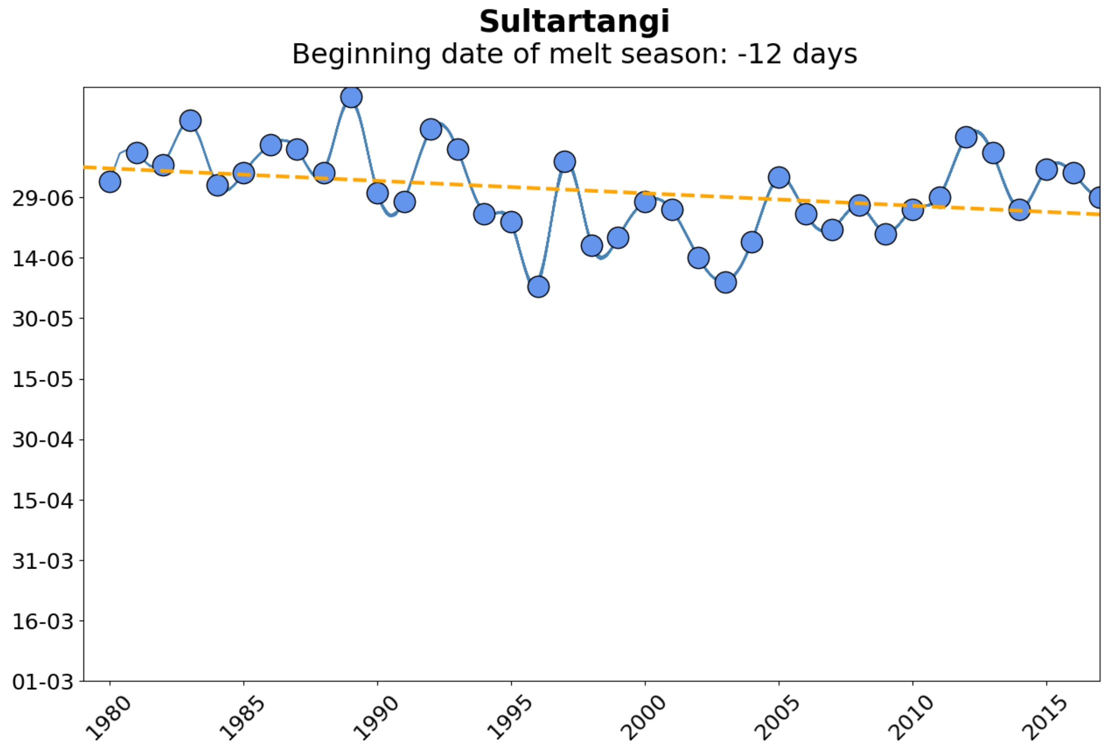

Figure I.7 – Evolution of the beginning date of the melt season for catchment Sultartangi for the period 1979 – 2017. Results were obtained using an automatic filter on the snowpack, temperature and melting timeseries extracted from the ICRA.

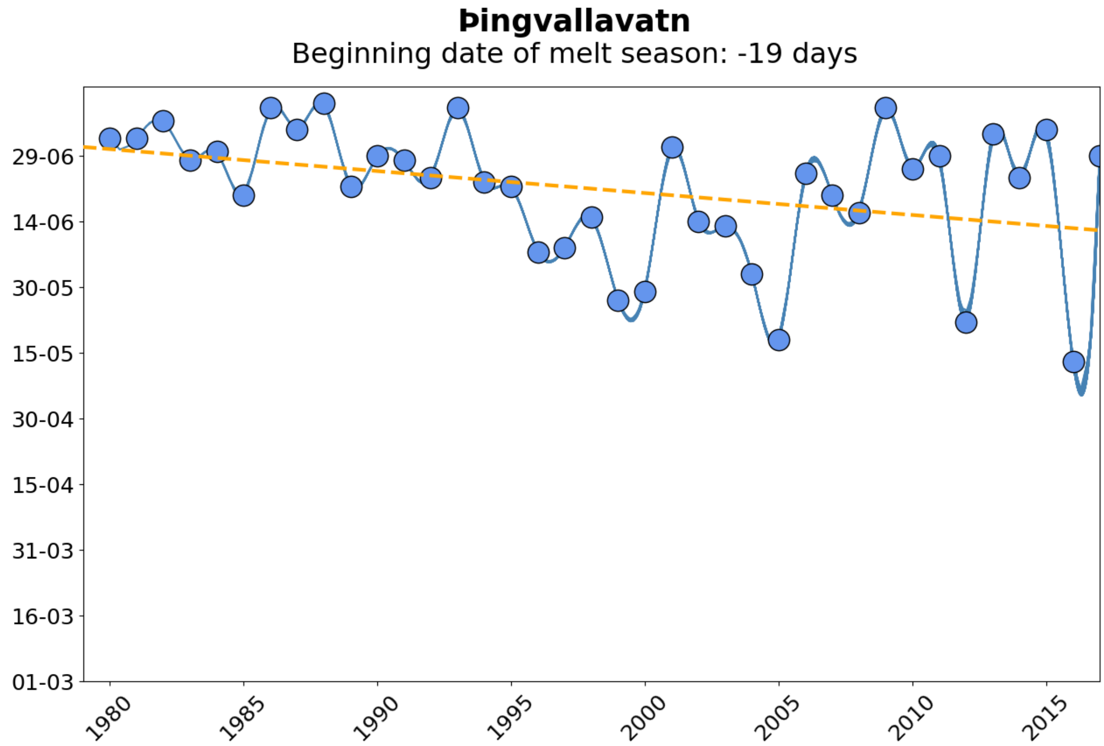

Figure I.8 – Evolution of the beginning date of the melt season for catchment Þingvallavatn for the period 1979 – 2017. Results were obtained using an automatic filter on the snowpack, temperature and melting timeseries extracted from the ICRA.

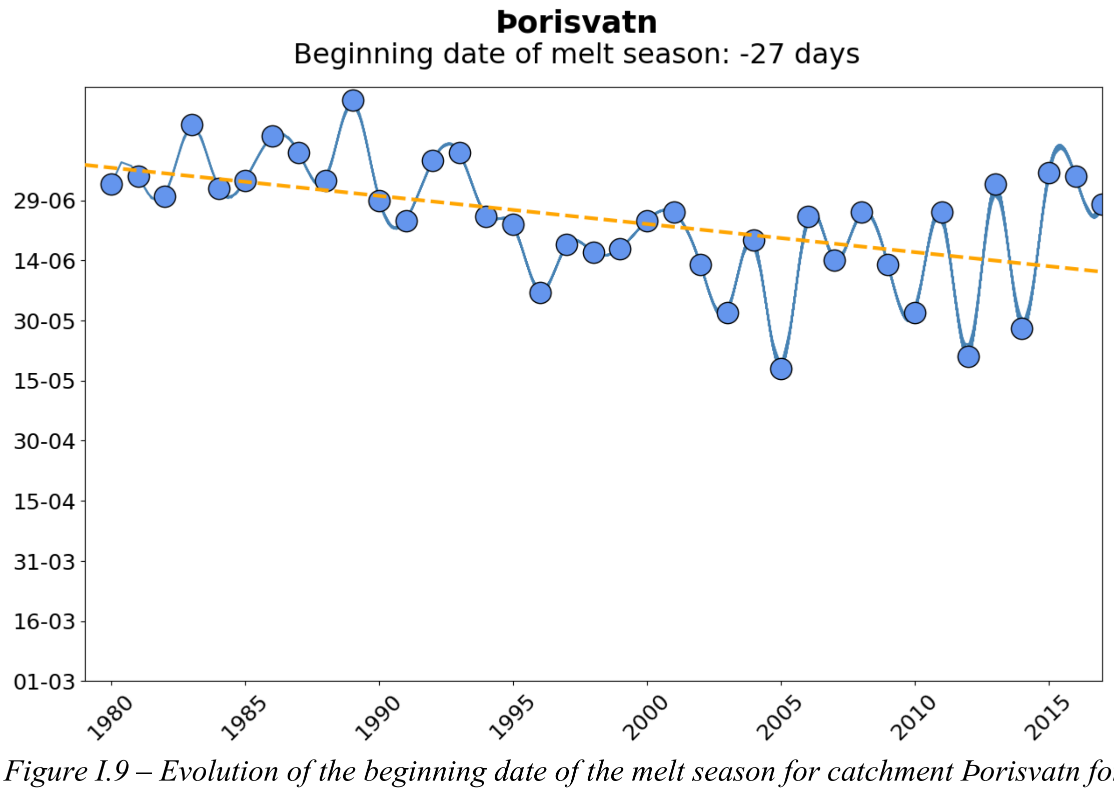

Figure I.9 – Evolution of the beginning date of the melt season for catchment Þorisvatn for the period 1979 – 2017. Results were obtained using an automatic filter on the snowpack, temperature and melting timeseries extracted from the ICRA.

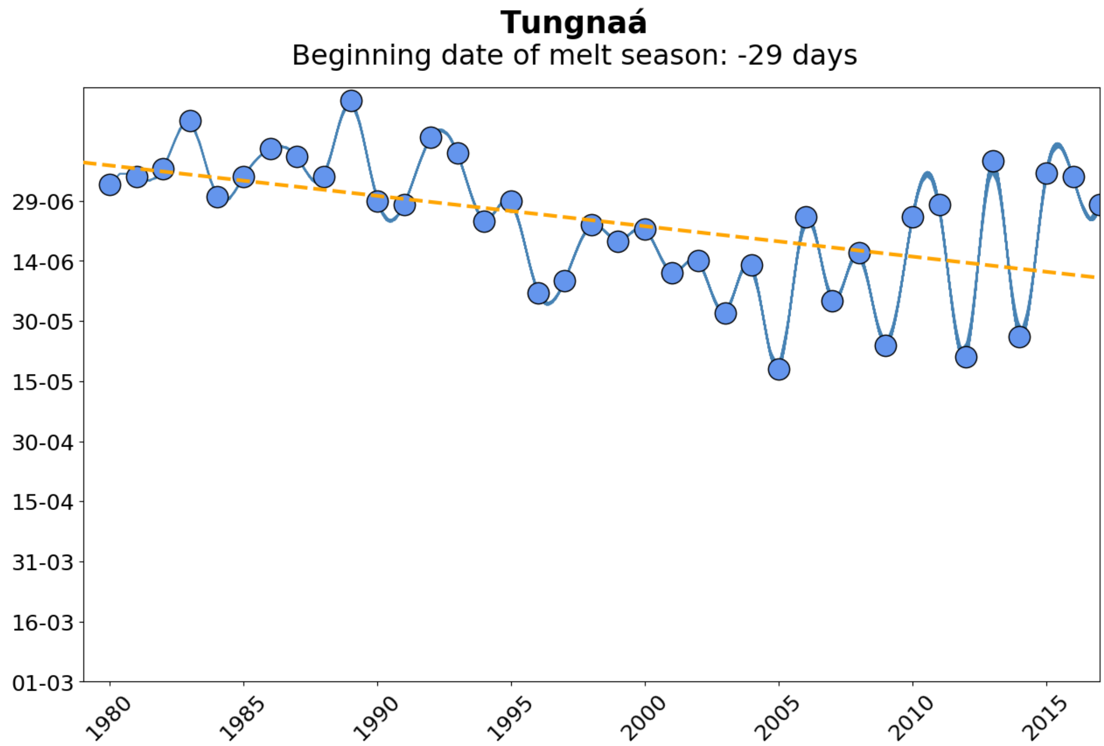

Figure I.10 – Evolution of the beginning date of the melt season for catchment Tungnaá for the period 1979 – 2017. Results were obtained using an automatic filter on the snowpack, temperature and melting timeseries extracted from the ICRA.

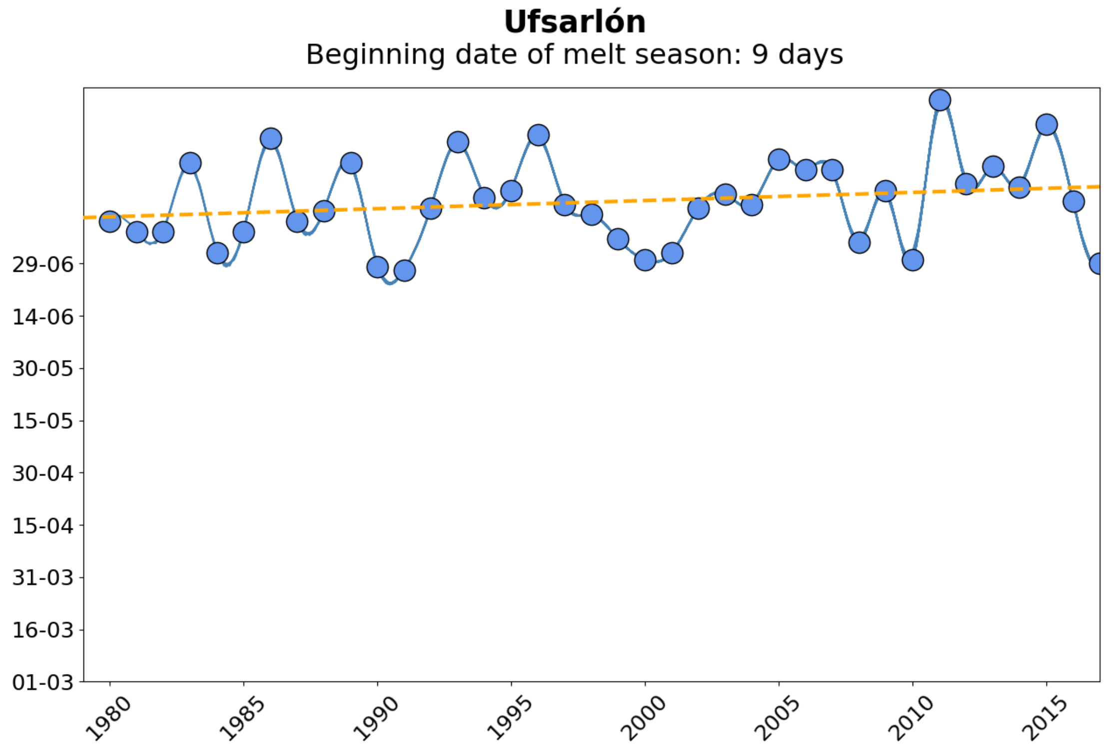

Figure I.11 – Evolution of the beginning date of the melt season for catchment Ufsarlón for the period 1979 – 2017. Results were obtained using an automatic filter on the snowpack, temperature and melting timeseries extracted from the ICRA.

Appendix II. Temporal changes in snow-fraction

In this appendix, figures similar to Figure 9 and 11 from Section 4.2 are presented.

In Figures II.1 – II.11, the solid blue lines show the evolution of the total snow-fraction over the time-period, while the dashed blue lines show the linear regression lines. At the top of each plot, a percentage change over the 39 years is given, calculated as the difference between the snow-fraction of the first and last year of reanalysis based on the regression line.

In Figures II.12 – II.22, the solid blue lines show the monthly snow-fraction evolutions over the years as calculated from the ICRA dataset, while the dashed-blue lines give the regression fit. To complement those results, snow-fractions from the ERA-20c reanalysis are added: the figures show the minimum-maximum snow-fraction intervals (in light orange) from the 10 realizations of the ERA-20c dataset, with the mean values represented by the solid orange line. The dashed red lines indicate the regression fits based on the ERA-20c mean snow-fraction values.

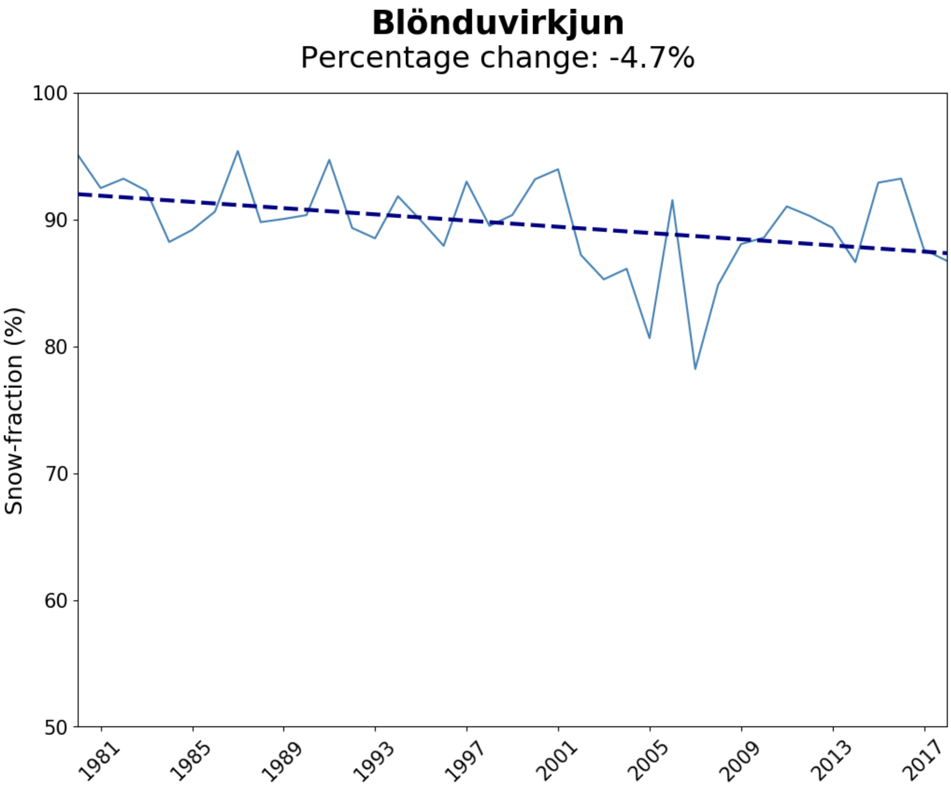

Figure II.1 - Total snow-fraction (%) evolution for catchment Blönduvirkjun, based on the ICRA dataset for the time-period 1979 – 2017.

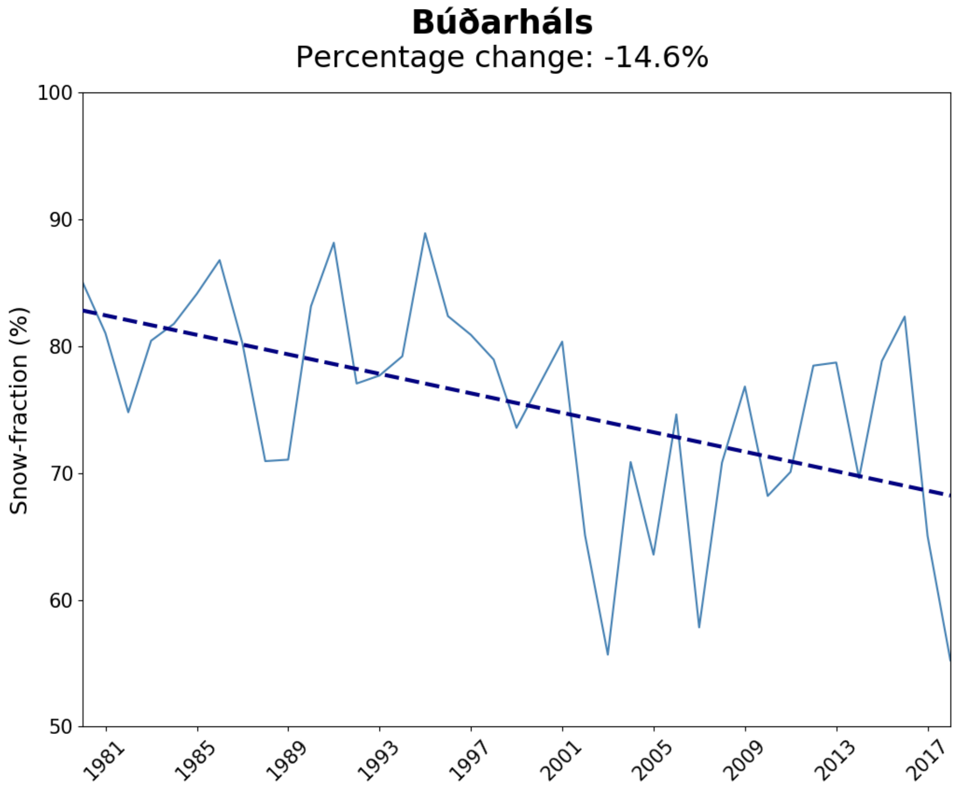

Figure II.2 - Total snow-fraction (%) evolution for catchment Búðarháls, based on the ICRA dataset for the time-period 1979 – 2017.

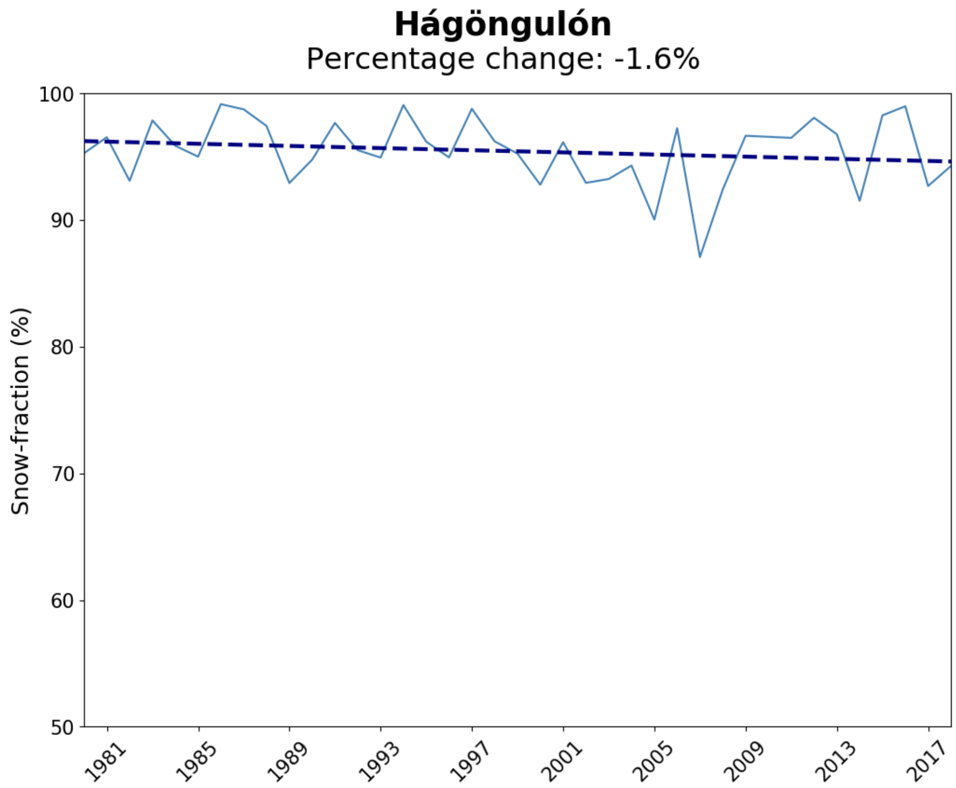

Figure II.3 - Total snow-fraction (%) evolution for catchment Hágöngulón, based on the ICRA dataset for the time-period 1979 – 2017.

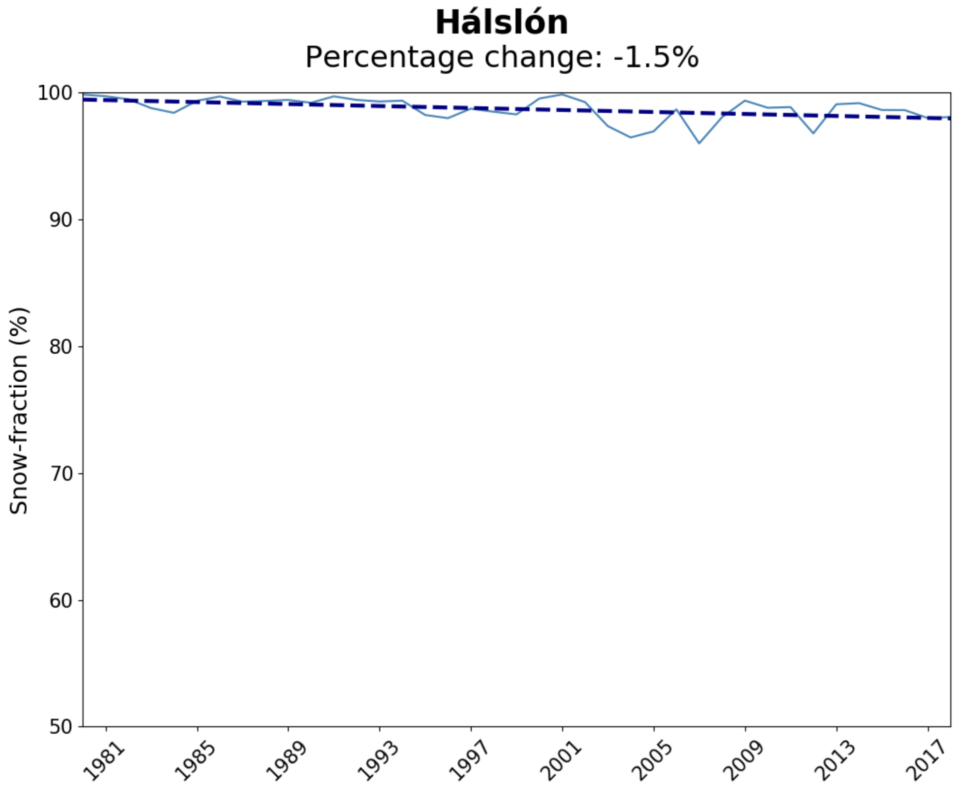

Figure II.4 - Total snow-fraction (%) evolution for catchment Hálslón, based on the ICRA dataset for the time-period 1979 – 2017.

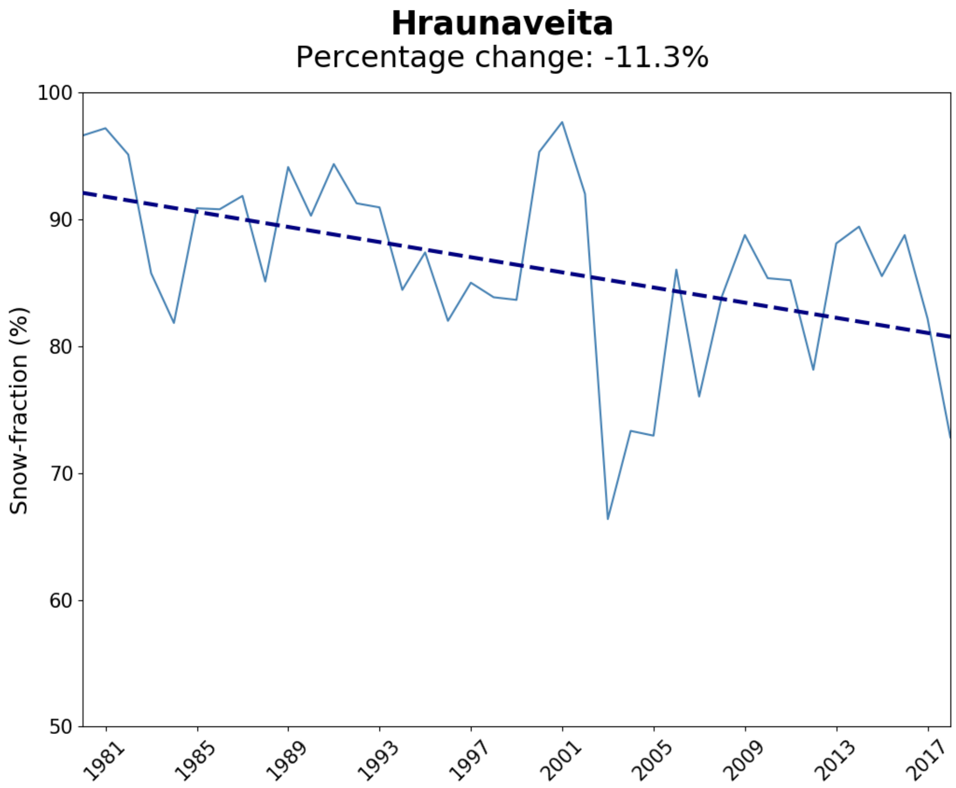

Figure II.5 - Total snow-fraction (%) evolution for catchment Hraunaveita, based on the ICRA dataset for the time-period 1979 – 2017.

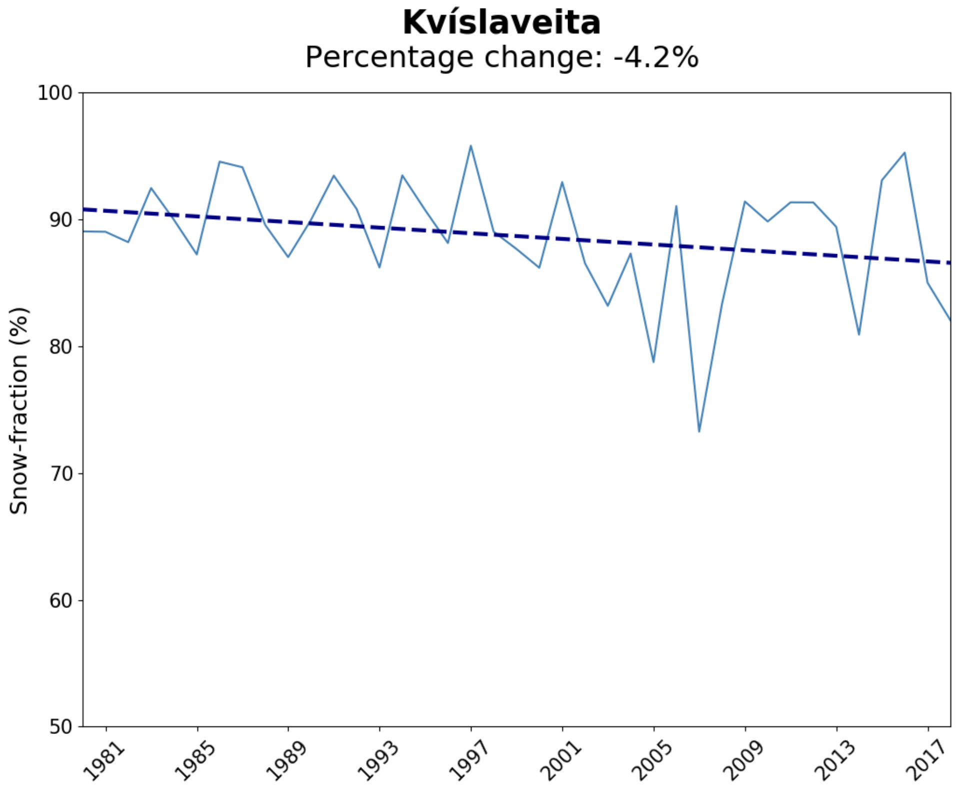

Figure II.6 - Total snow-fraction (%) evolution for catchment Kvíslaveita, based on the ICRA dataset for the time-period 1979 – 2017.

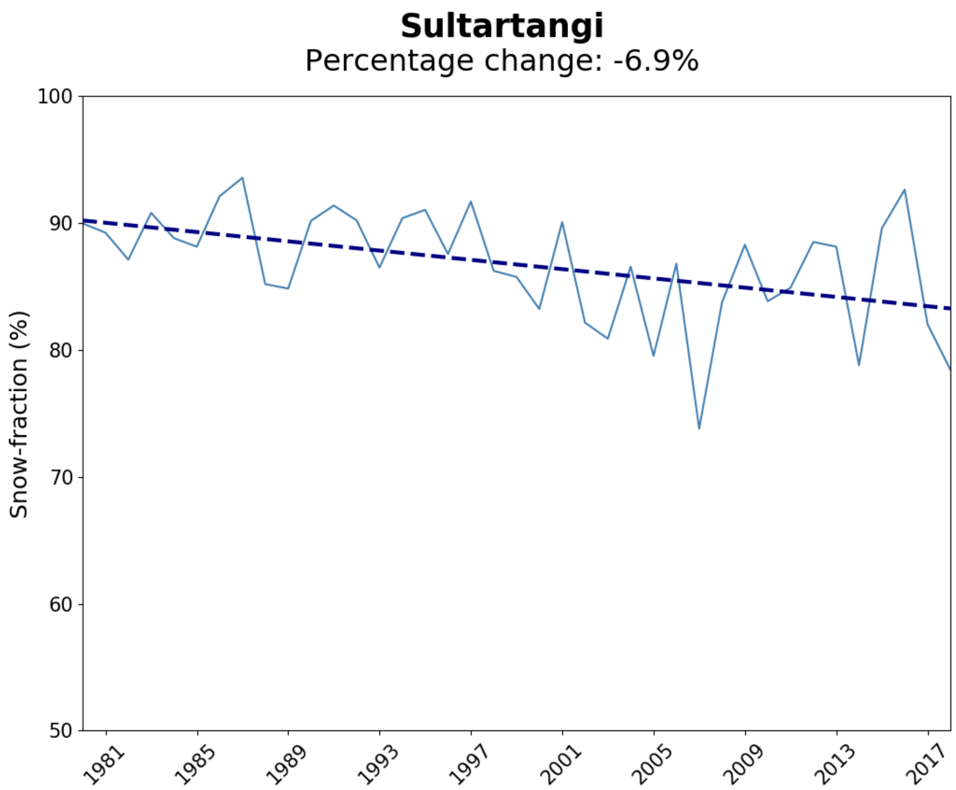

Figure II.7 - Total snow-fraction (%) evolution for catchment Sultartangi, based on the ICRA dataset for the time-period 1979 – 2017.

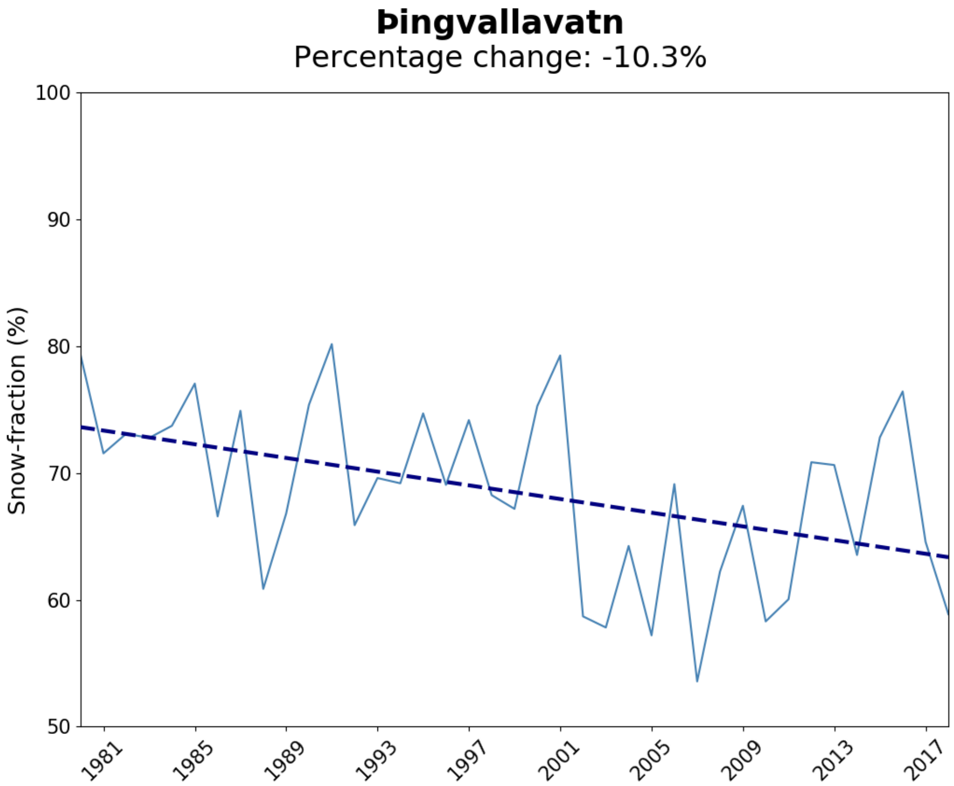

Figure II.8 - Total snow-fraction (%) evolution for catchment Þingvallavatn, based on the ICRA dataset for the time-period 1979 – 2017.

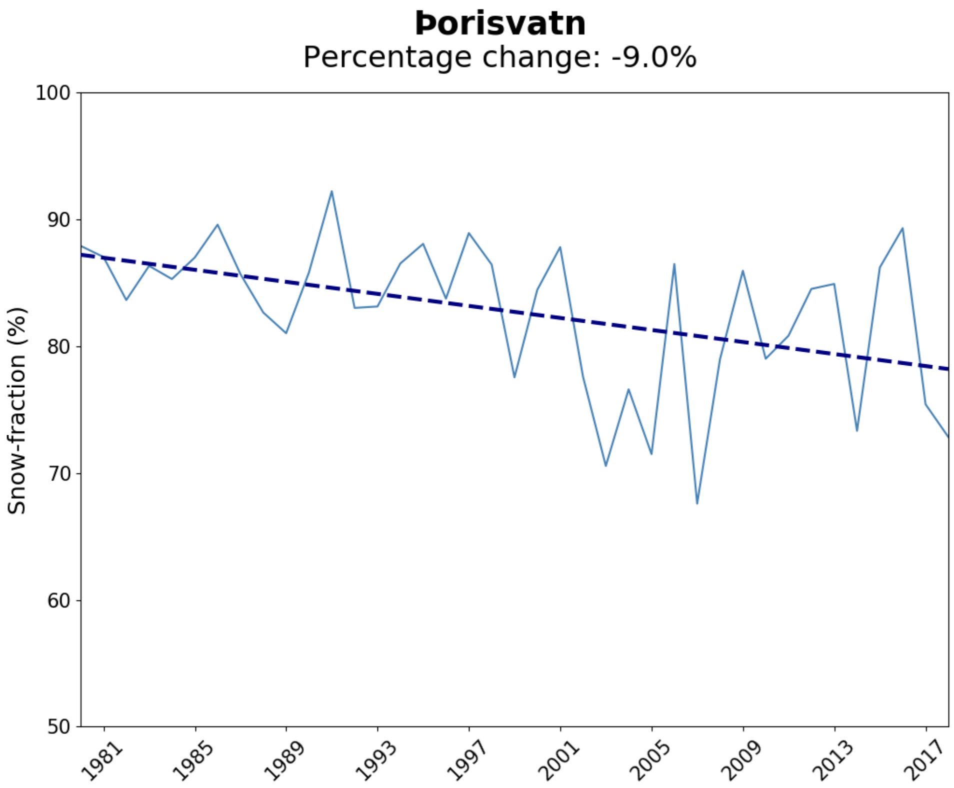

Figure II.9 - Total snow-fraction (%) evolution for catchment Þorisvatn, based on the ICRA dataset for the time-period 1979 – 2017.

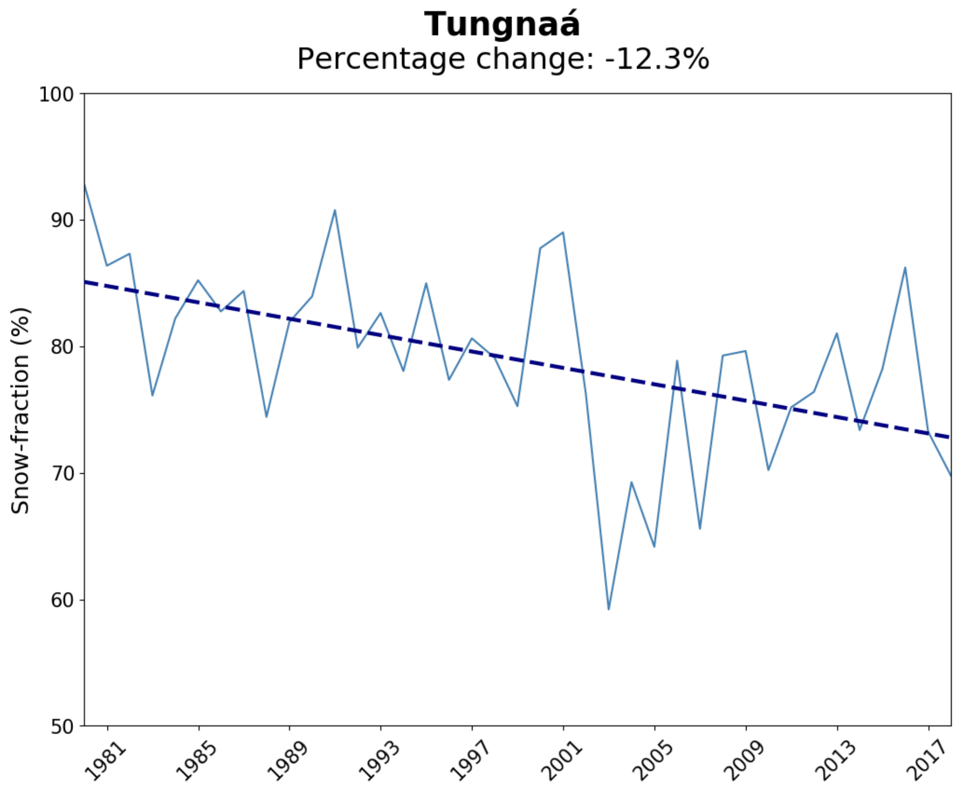

Figure II.10 - Total snow-fraction (%) evolution for catchment Tungnaá, based on the ICRA dataset for the time-period 1979 – 2017.

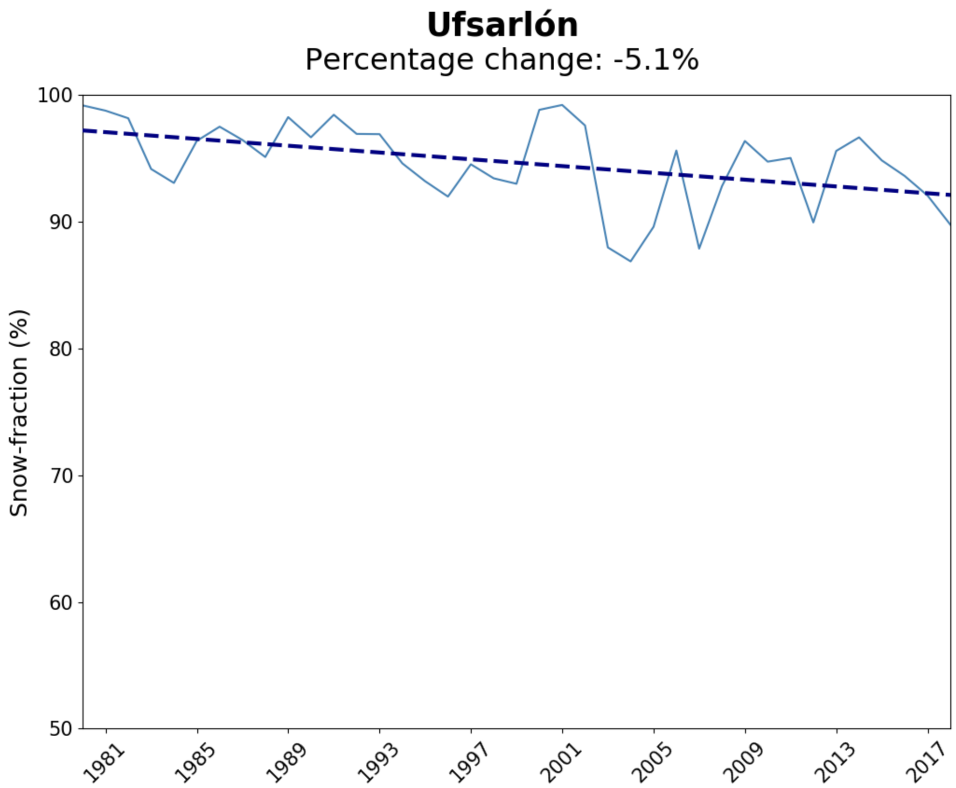

Figure II.11 - Total snow-fraction (%) evolution for catchment Ufsarlón, based on the ICRA dataset for the time-period 1979 – 2017.

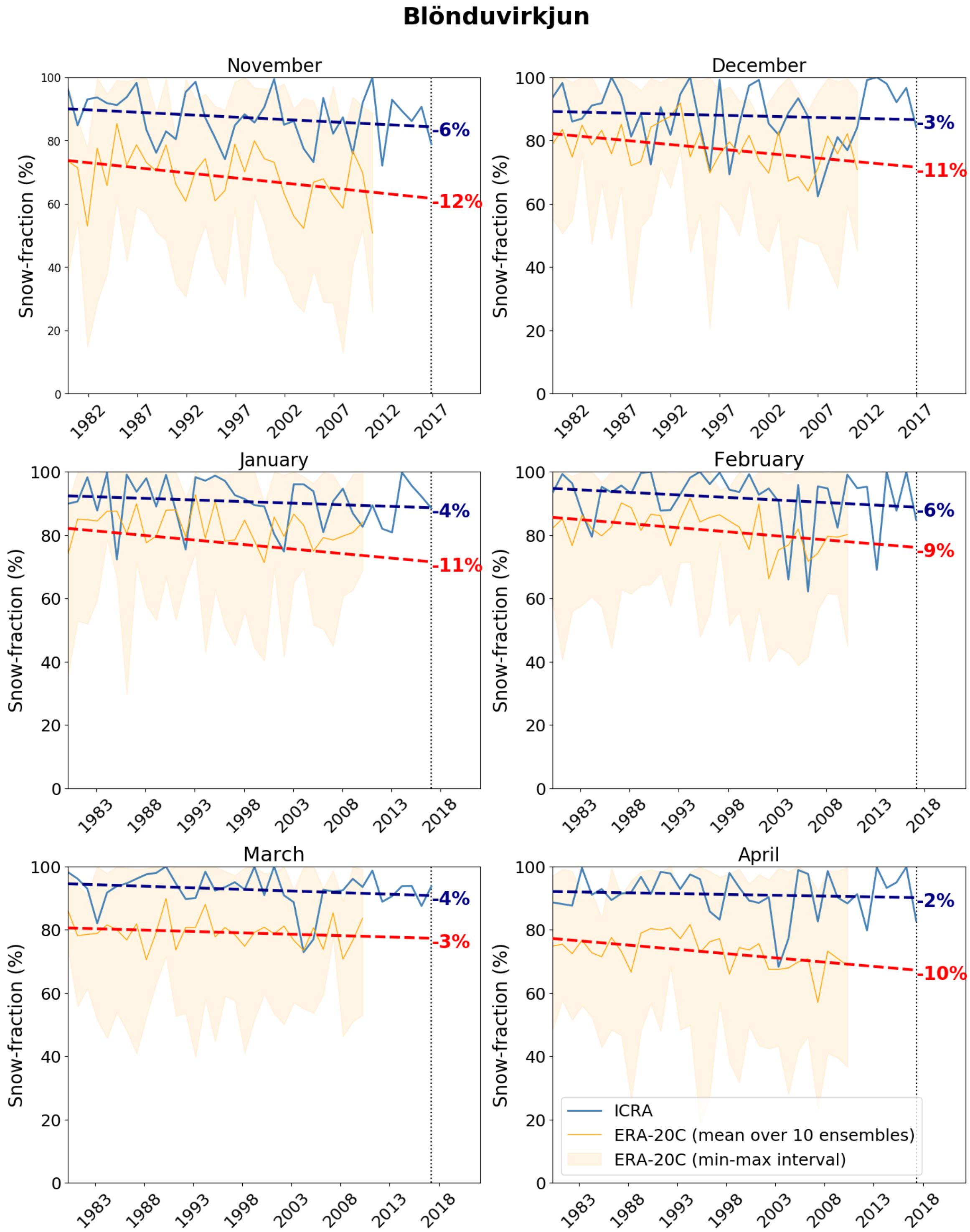

Figure II.12 – Monthly snow-fraction (%) evolution for catchment Blönduvirkjun. Results are based on the ICRA and ERA-20c datasets. Regression lines are shown for both datasets results, along with the percentage changes.

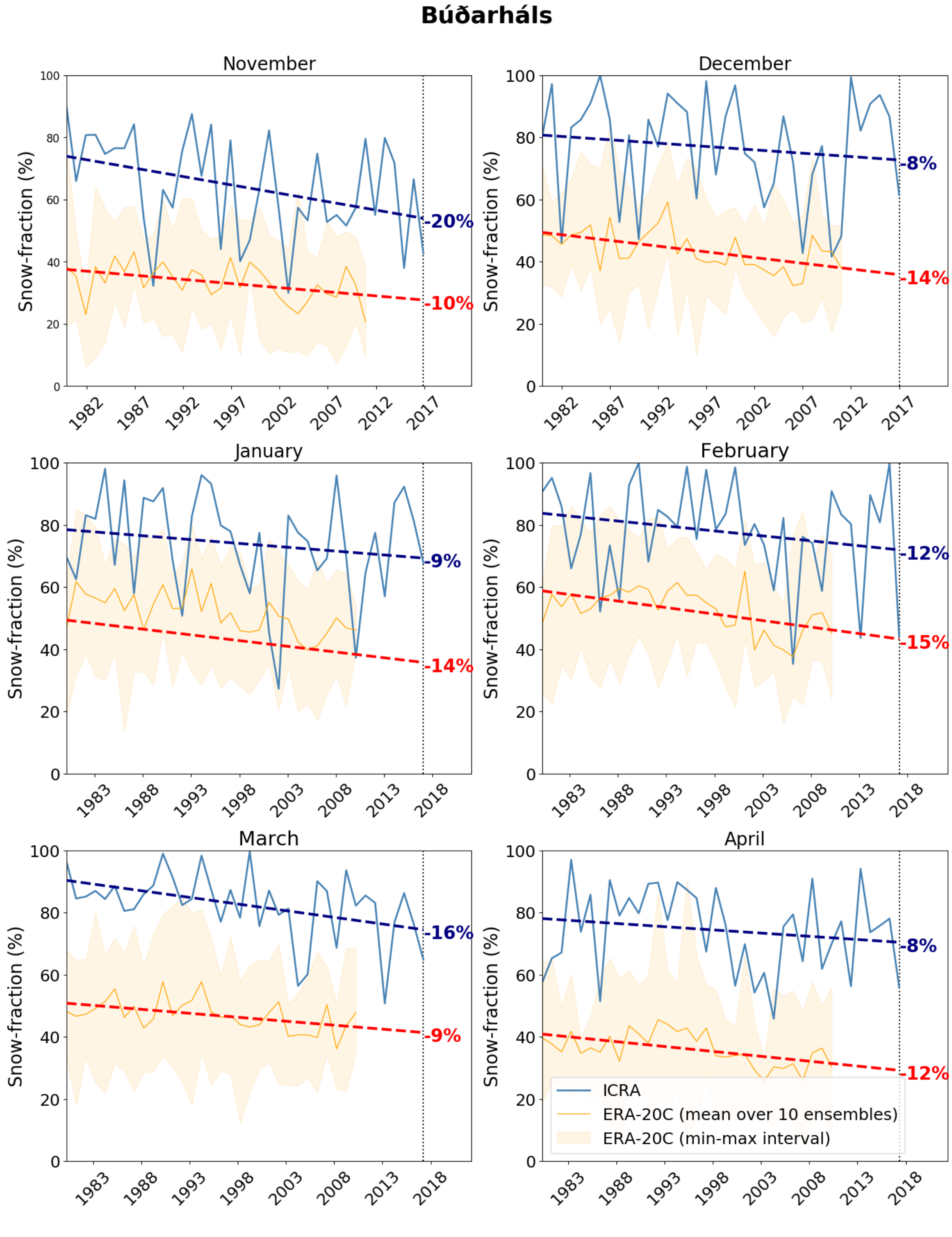

Figure II.13 – Monthly snow-fraction (%) evolution for catchment Búðarháls. Results are based on the ICRA and ERA-20c datasets. Regression lines are shown for both datasets results, along with the percentage changes.

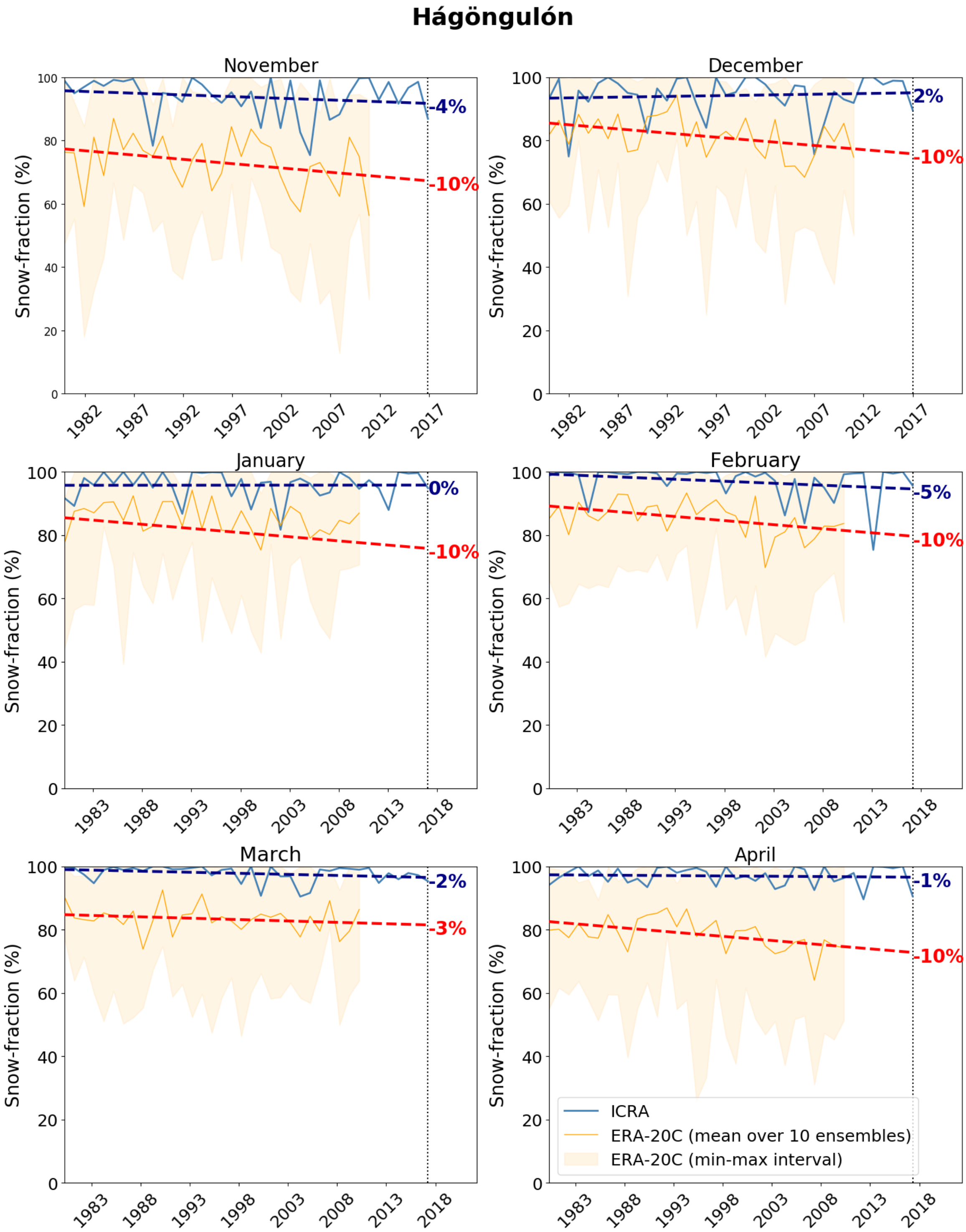

Figure II.14 – Monthly snow-fraction (%) evolution for catchment Hágöngulón. Results are based on the ICRA and ERA-20c datasets. Regression lines are shown for both datasets results, along with the percentage changes.

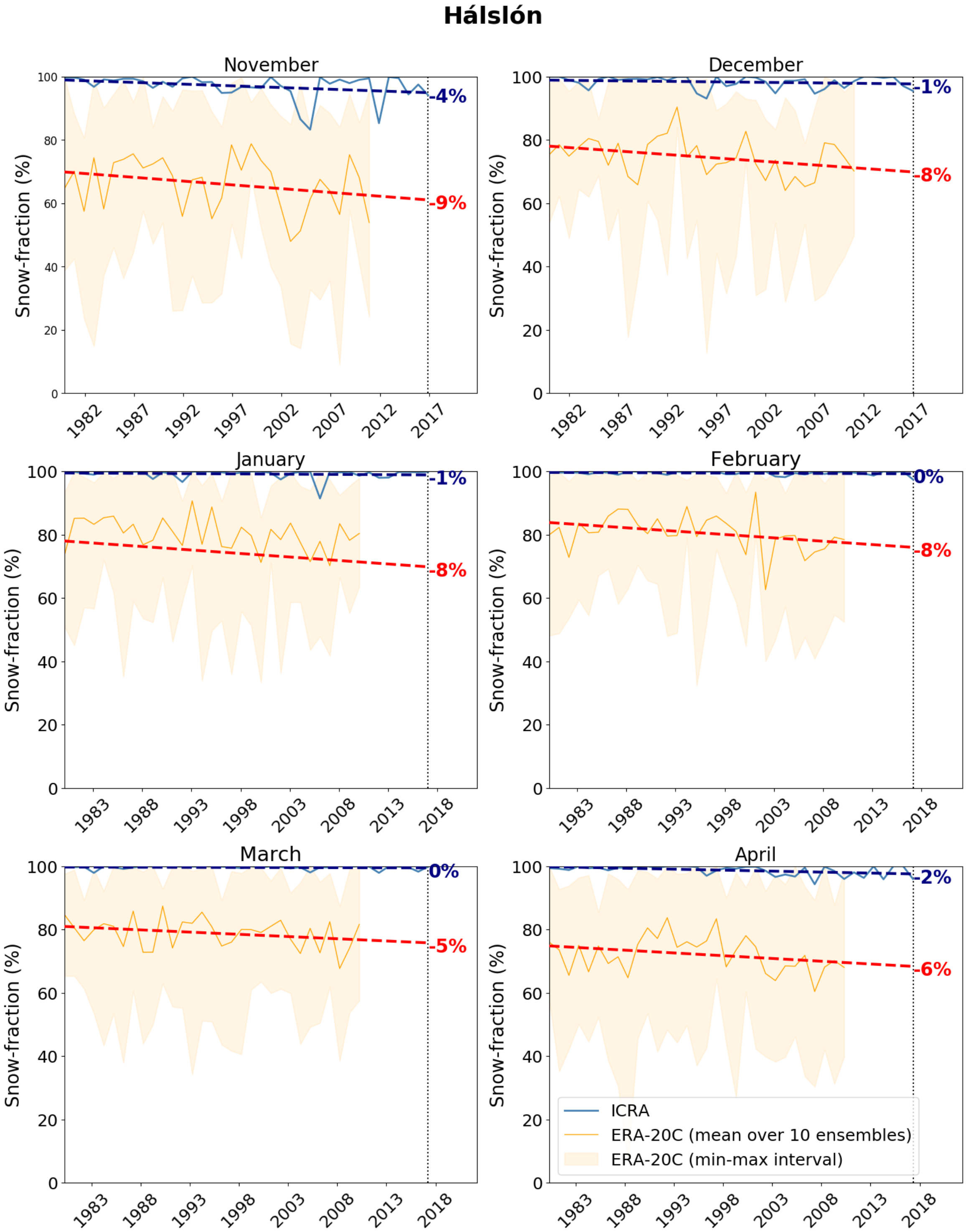

Figure II.15 – Monthly snow-fraction (%) evolution for catchment Hálslón. Results are based on the ICRA and ERA-20c datasets. Regression lines are shown for both datasets results, along with the percentage changes.

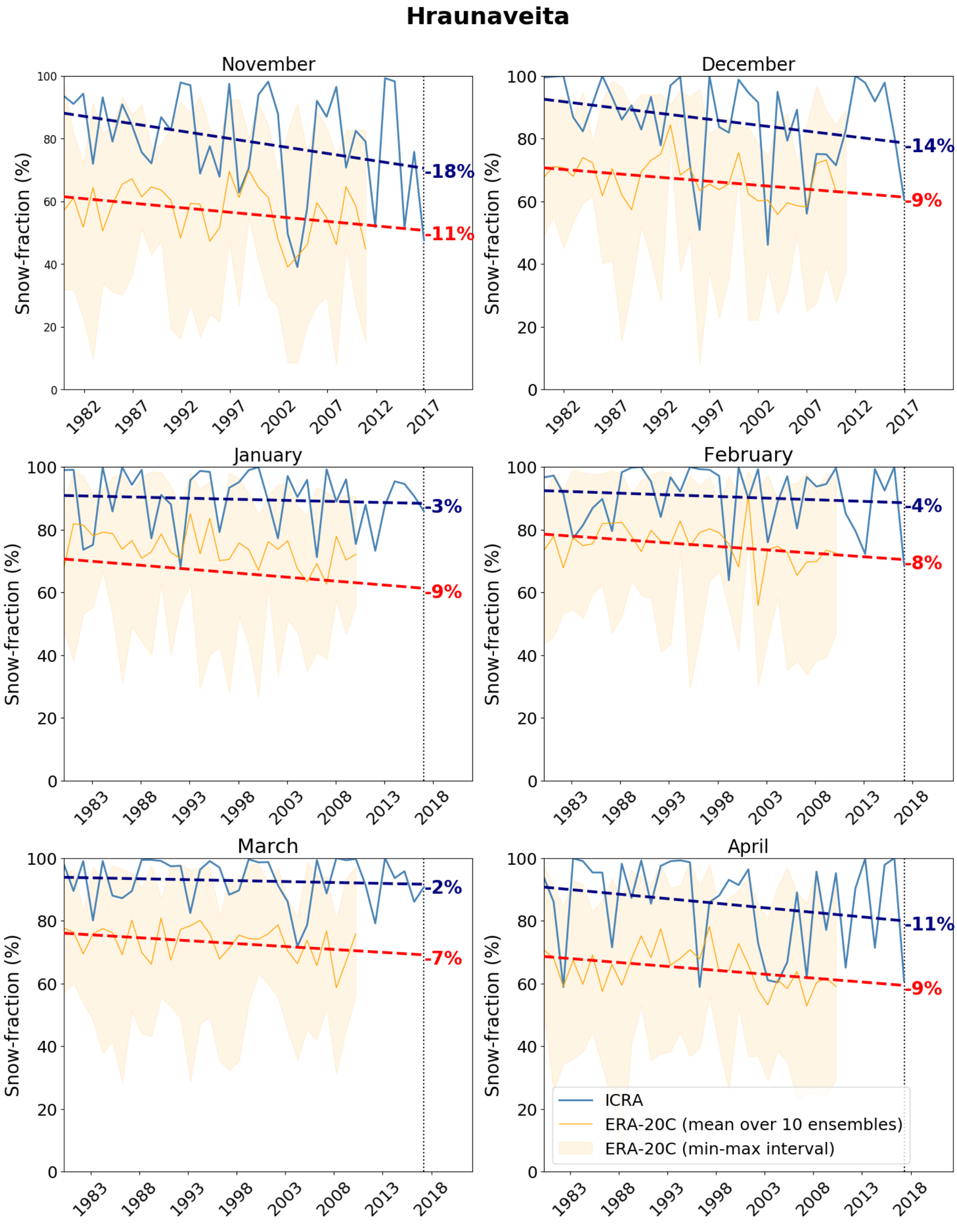

Figure II.16 – Monthly snow-fraction (%) evolution for catchment Hraunaveita. Results are based on the ICRA and ERA-20c datasets. Regression lines are shown for both datasets results, along with the percentage changes.

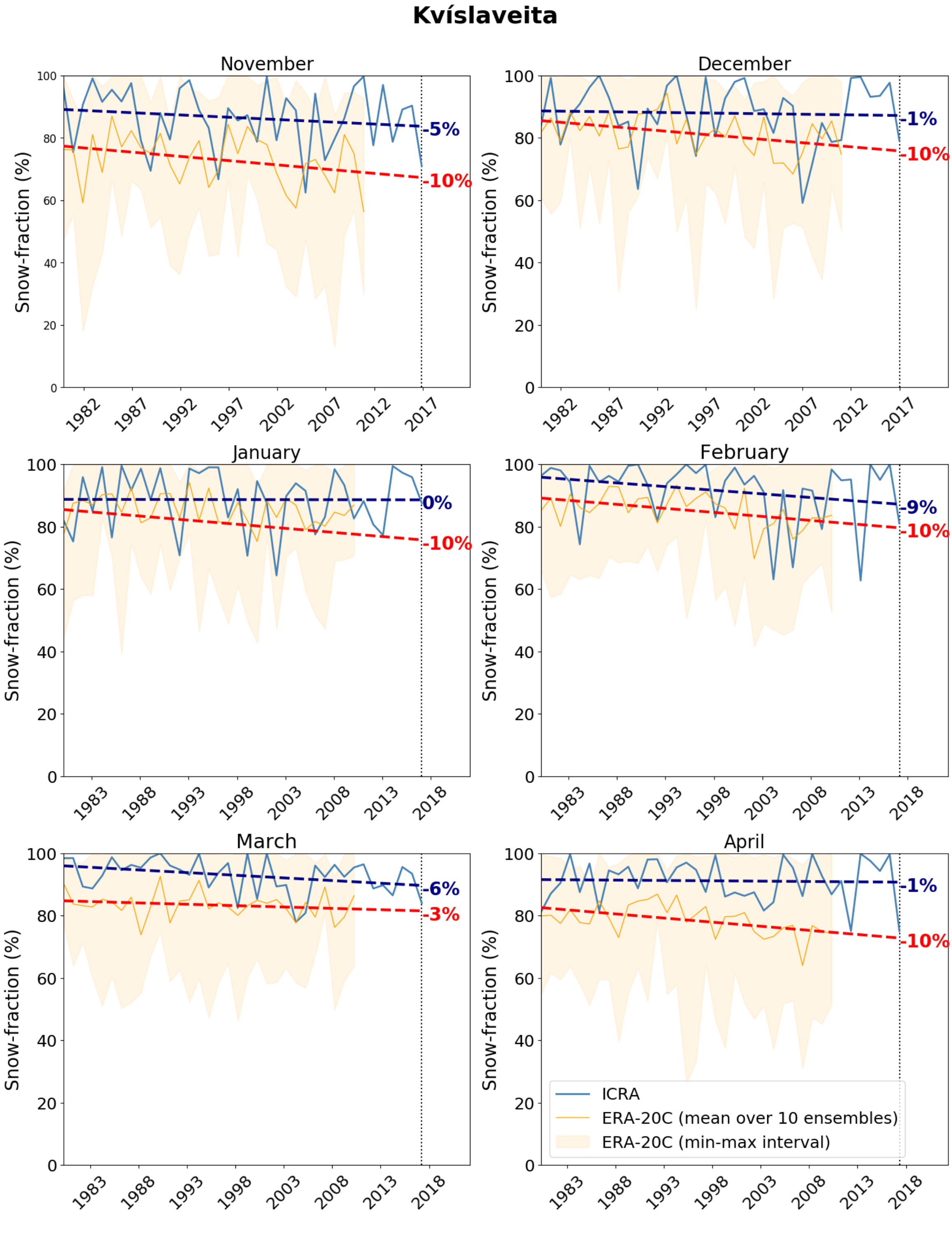

Figure II.17 – Monthly snow-fraction (%) evolution for catchment Kvíslaveita. Results are based on the ICRA and ERA-20c datasets. Regression lines are shown for both datasets results, along with the percentage changes.

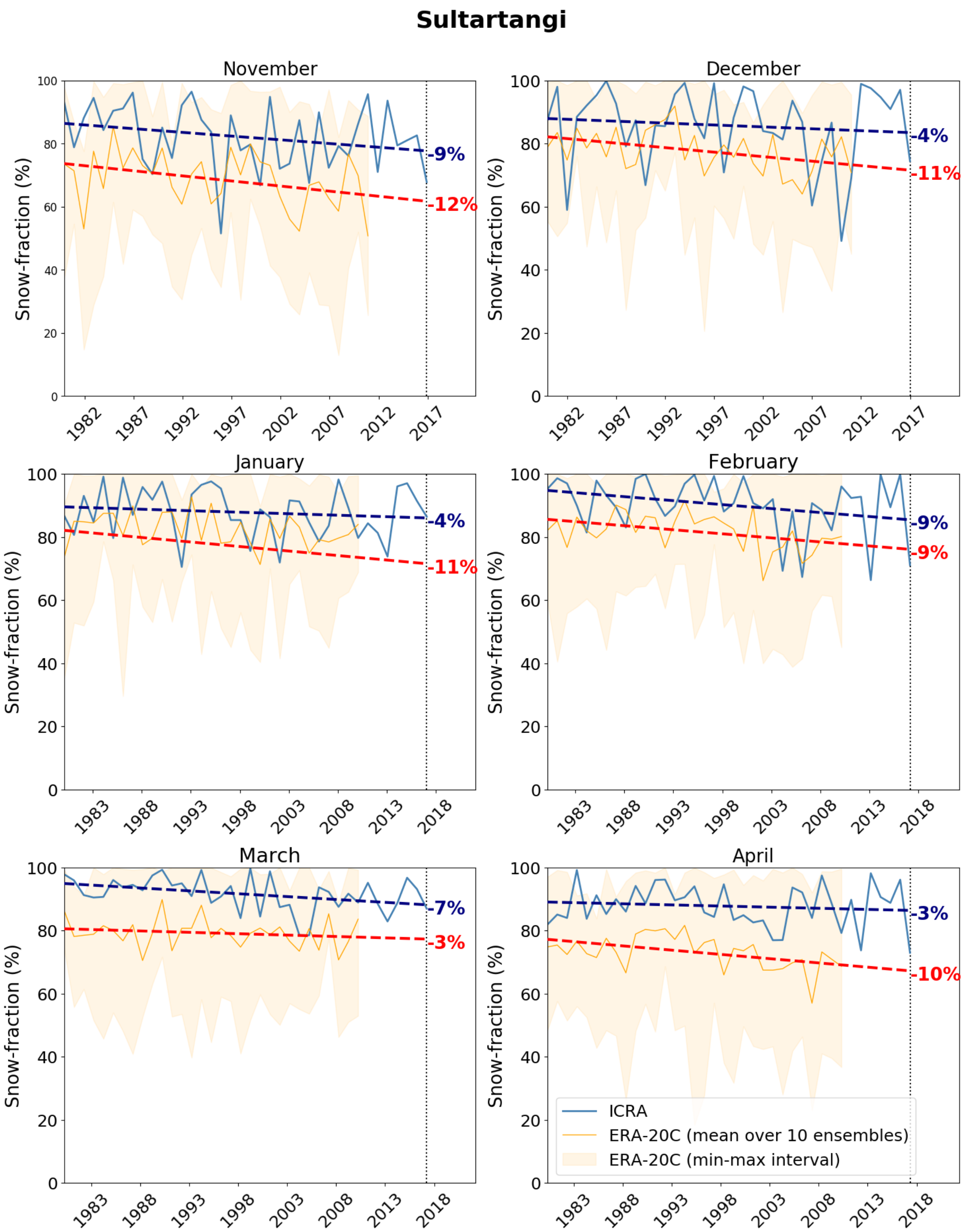

Figure II.18 – Monthly snow-fraction (%) evolution for catchment Sultartangi. Results are based on the ICRA and ERA-20c datasets. Regression lines are shown for both datasets results, along with the percentage changes.

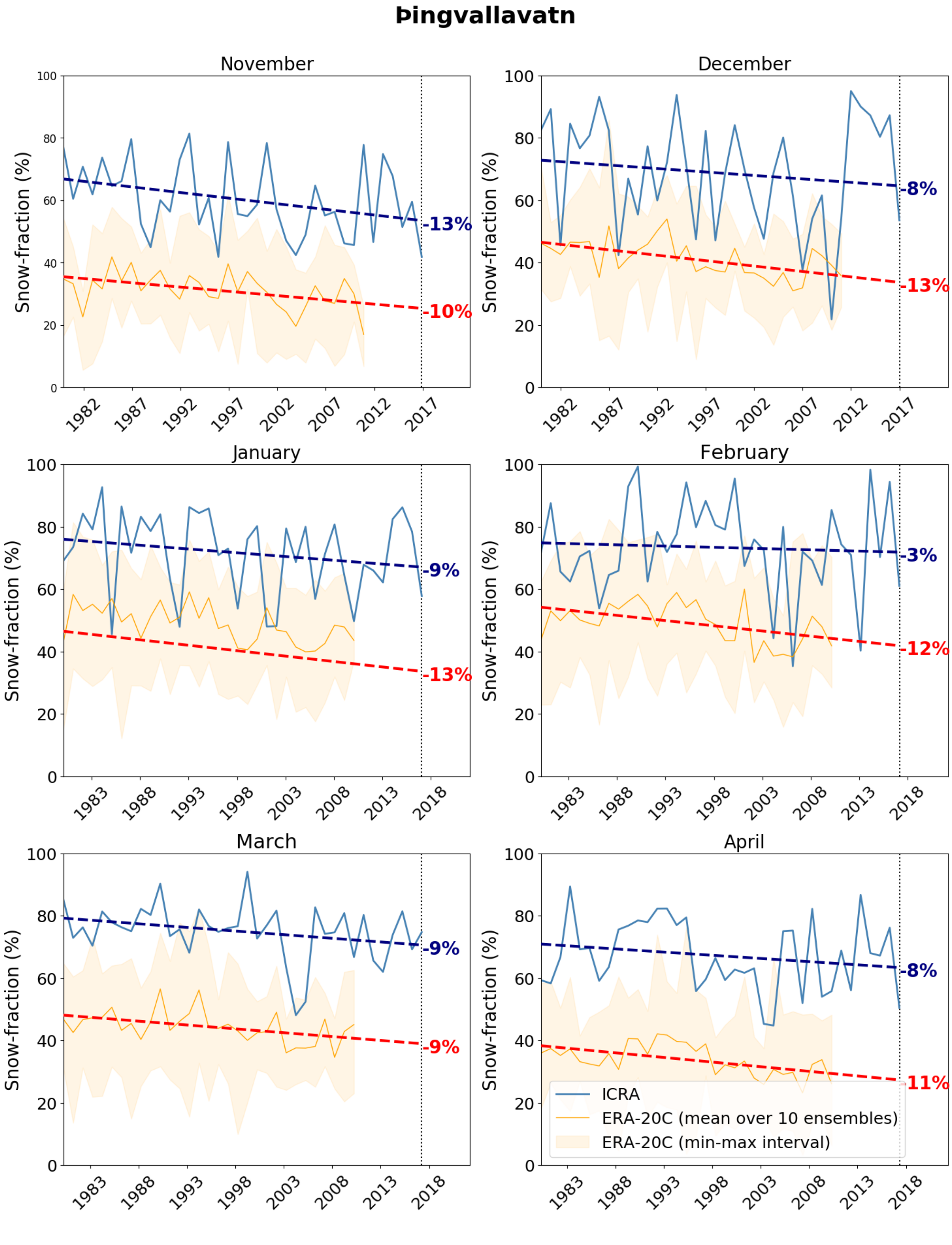

Figure II.19 – Monthly snow-fraction (%) evolution for catchment Þingvallavatn. Results are based on the ICRA and ERA-20c datasets. Regression lines are shown for both datasets results, along with the percentage changes.

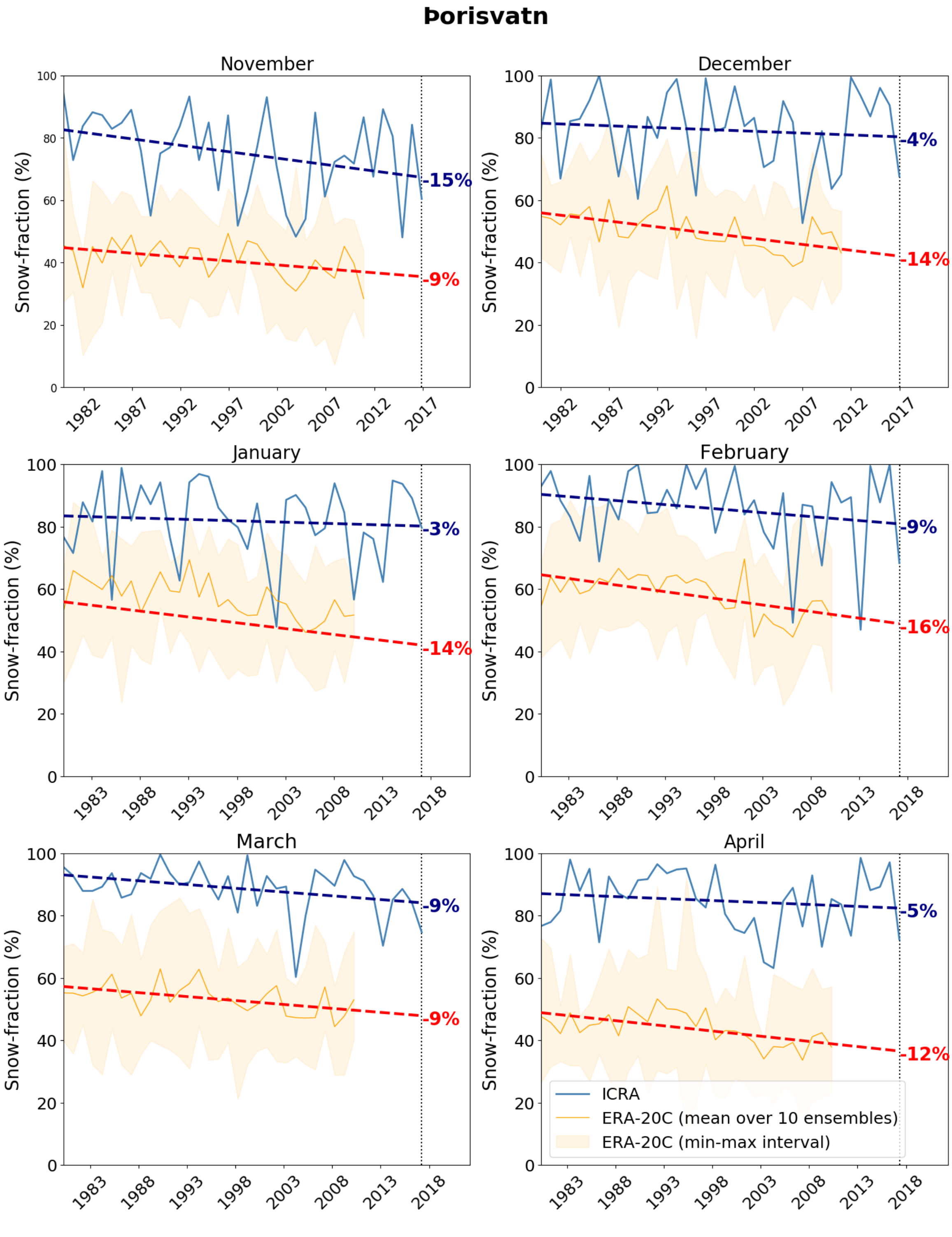

Figure II.20 – Monthly snow-fraction (%) evolution for catchment Þorisvatn. Results are based on the ICRA and ERA-20c datasets. Regression lines are shown for both datasets results, along with the percentage changes.

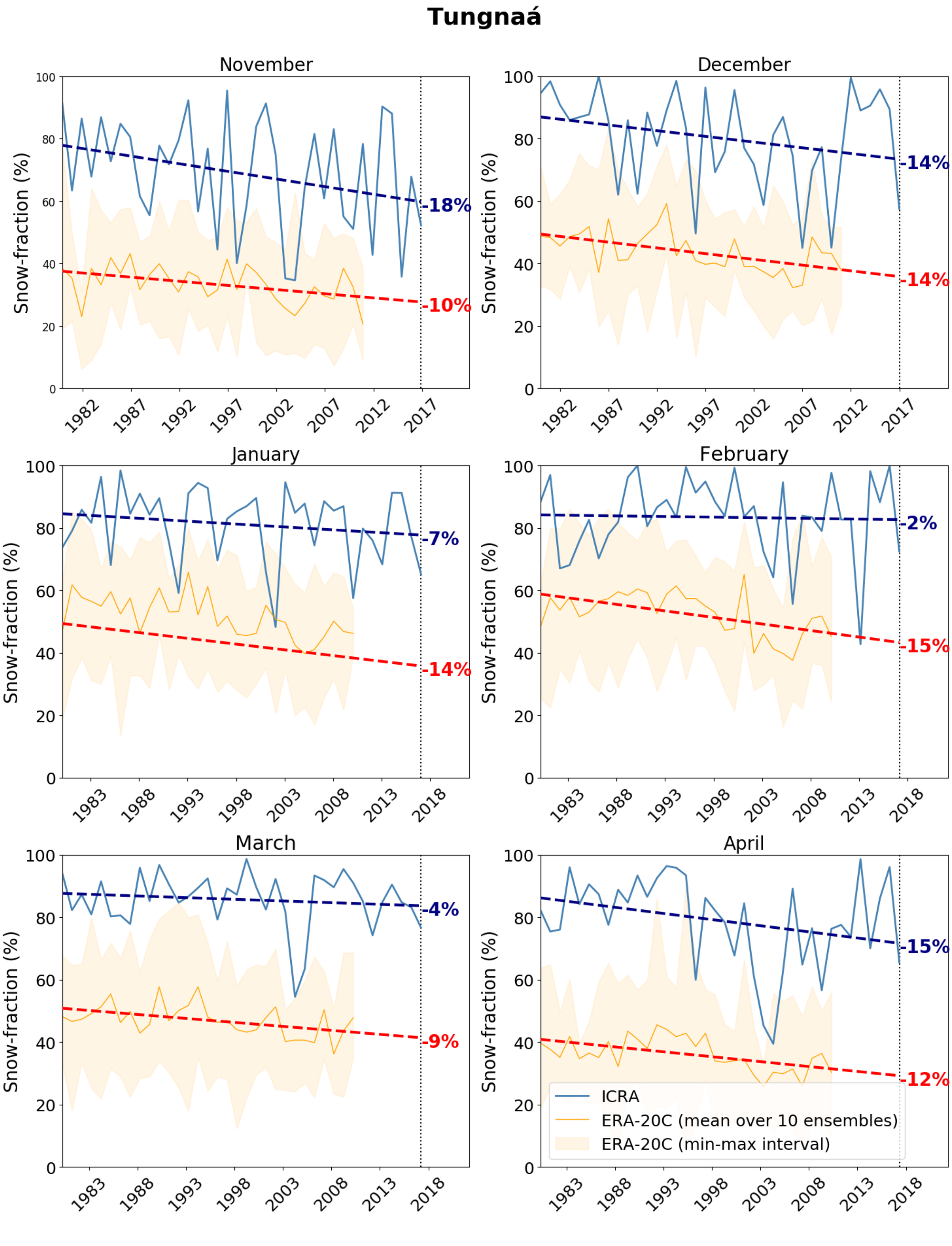

Figure II.21 – Monthly snow-fraction (%) evolution for catchment Tungnaá. Results are based on the ICRA and ERA-20c datasets. Regression lines are shown for both datasets results, along with the percentage changes.

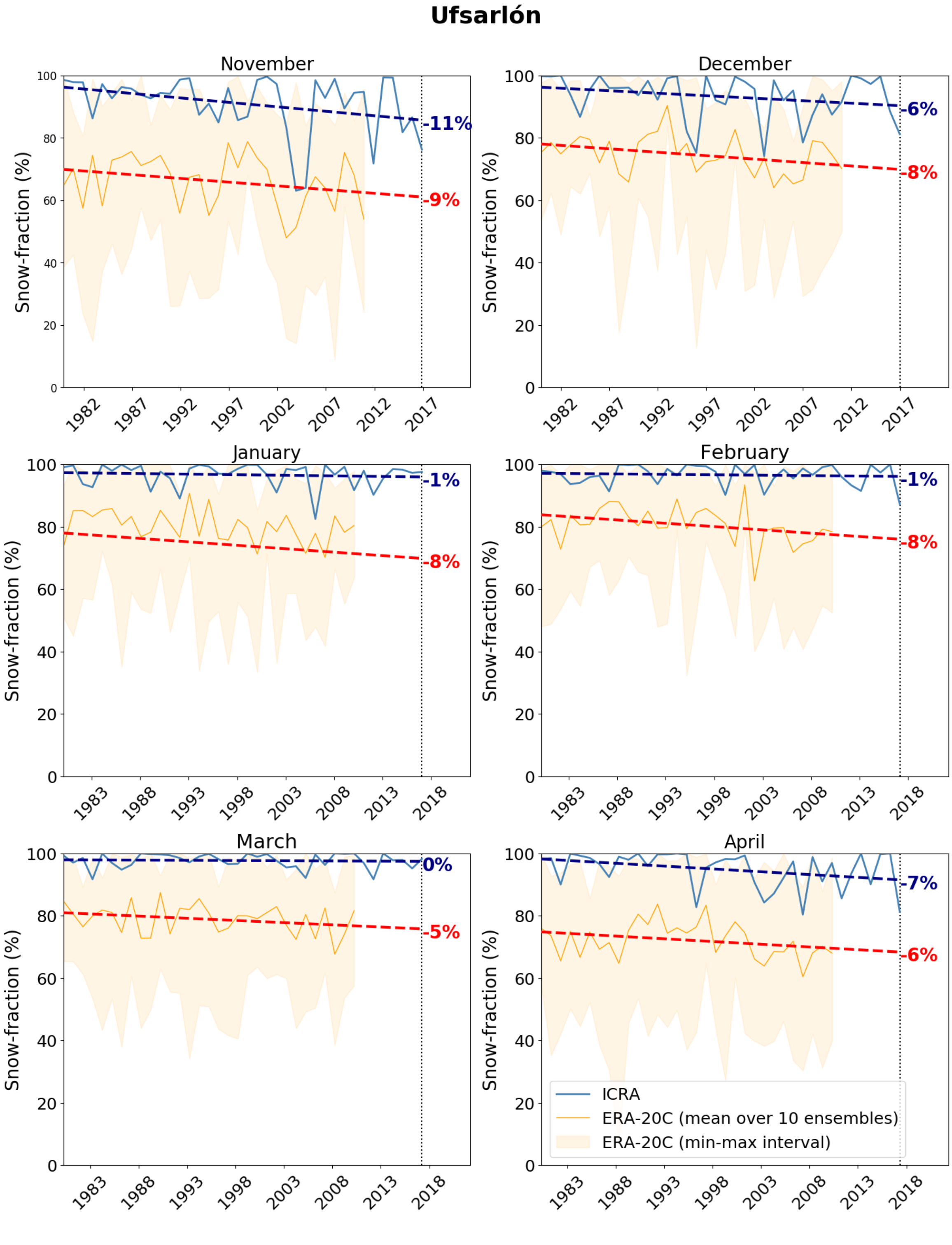

Figure II.22 – Monthly snow-fraction (%) evolution for catchment Ufsarlón. Results are based on the ICRA and ERA-20c datasets. Regression lines are shown for both datasets results, along with the percentage changes.

Appendix III. Precipitation return levels

In this appendix, results from Section 5 are presented.

Figures III.1 – III.11 show individual 1M5 maps for all the catchment, with and without climate projections, similar to Figure 19 in the report.

In Tables III.1 – III.11 and Figures III.12 – 22, precipitation return levels are shown in both table form and on Intensity-Duration-Frequency curves. Values are given for 3-, 6-, 12-, 24- and 48-hour return levels with a 2-, 5-, 10-, 25-, 50- and 100-year return period, based on the complete ICRA dataset, with and without climate projections from the CMIP5. Timeseries were extracted using the average value of all the grid-points within the catchments and resampled for the various durations using a rolling window.

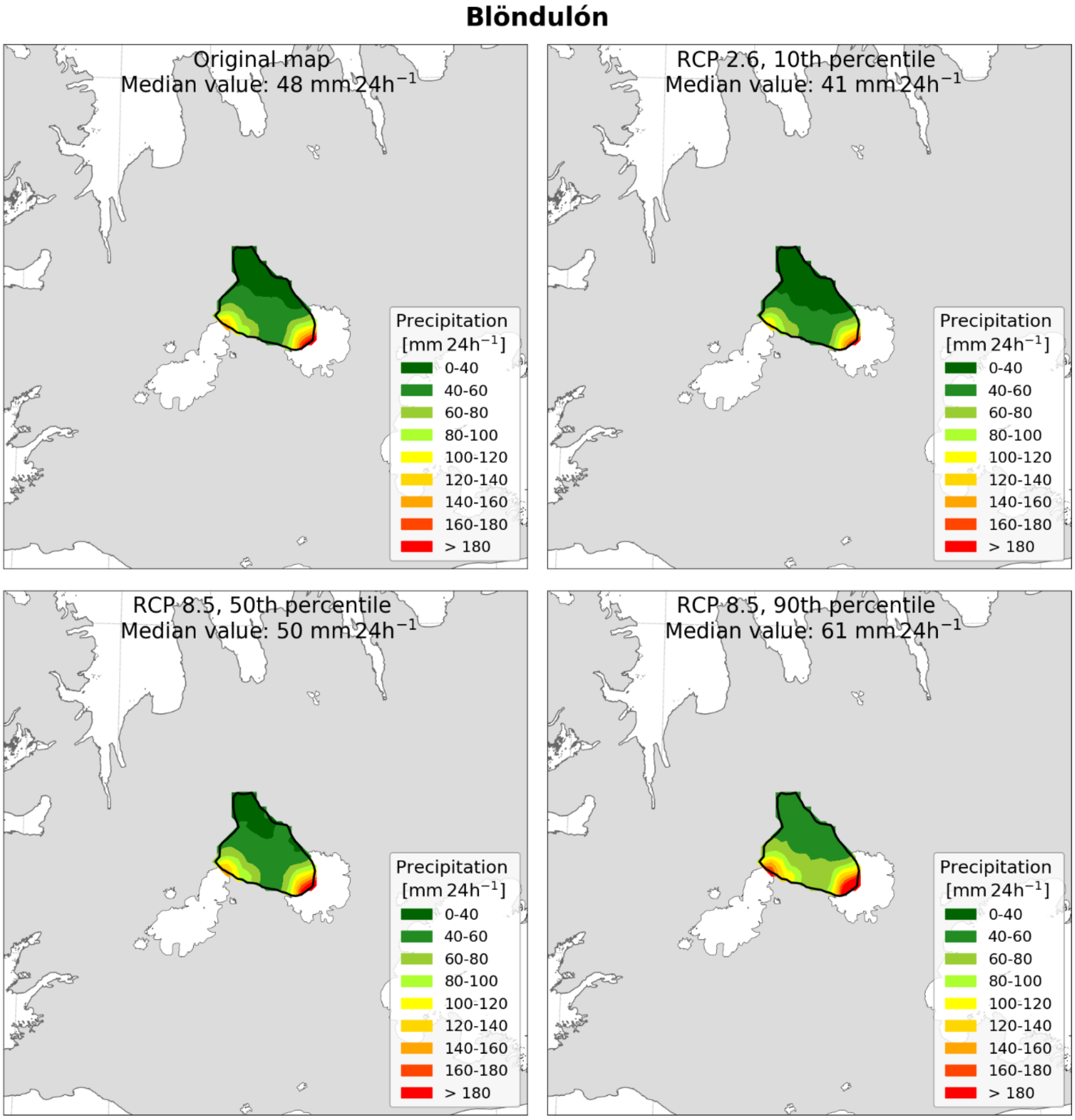

Figure III.1 – 1M5 maps for catchment Blönduvirkjun, based on the ICRA dataset without projection (top left), with RCP 2.6 and 10th percentile percentage changes (top right), with RCP 8.5 and median percentage changes bottom left), and with RCP 8.5 and 90th percentile percentage changes (bottom right). Projections were calculated for the time-period 2080 – 2100 and come from the CMIP5.

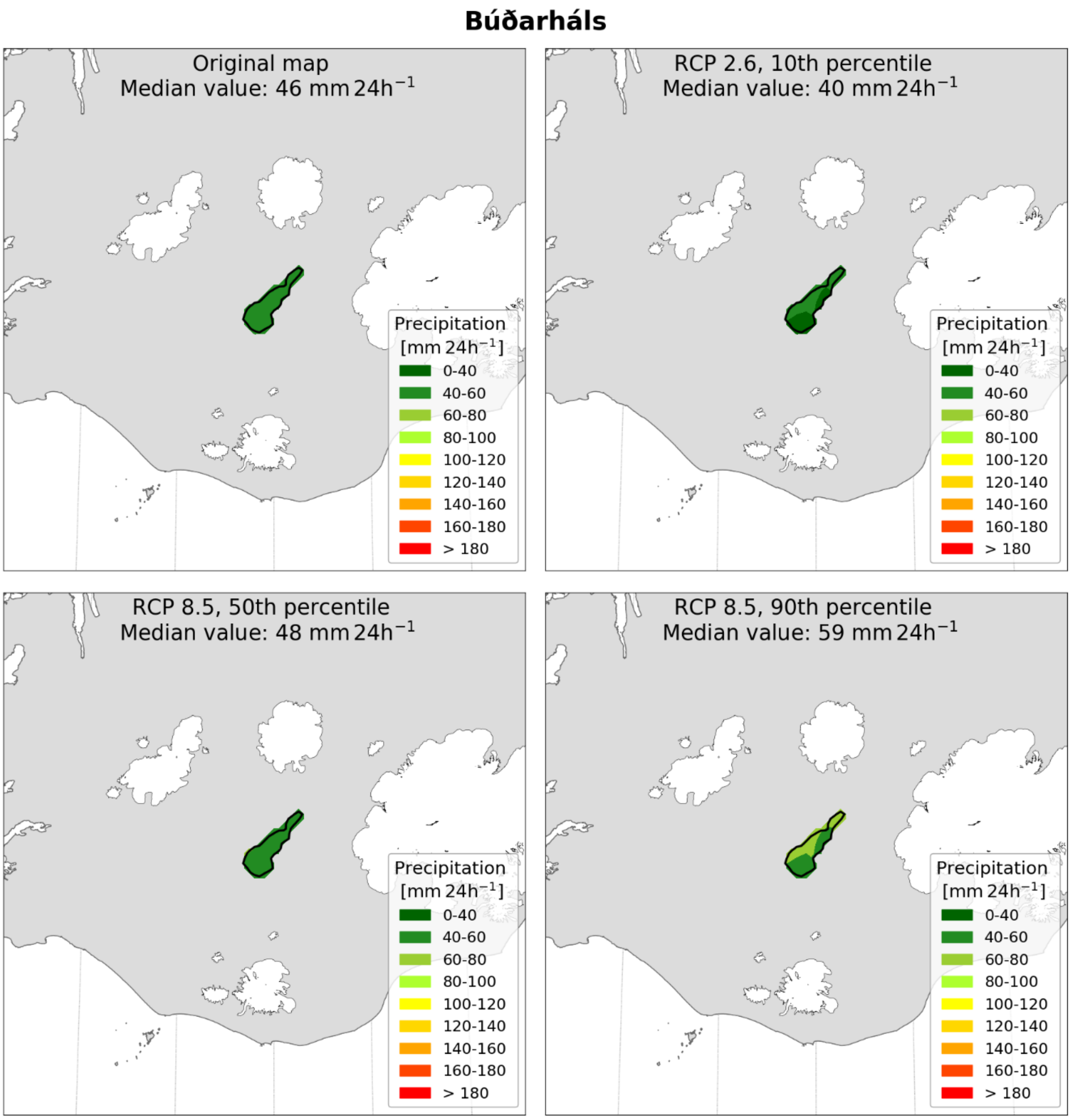

Figure III.2 – 1M5 maps for catchment Búðarháls, based on the ICRA dataset without projection (top left), with RCP 2.6 and 10th percentile percentage changes (top right), with RCP 8.5 and median percentage changes bottom left), and with RCP 8.5 and 90th percentile percentage changes (bottom right). Projections were calculated for the time-period 2080 – 2100 and come from the CMIP5.

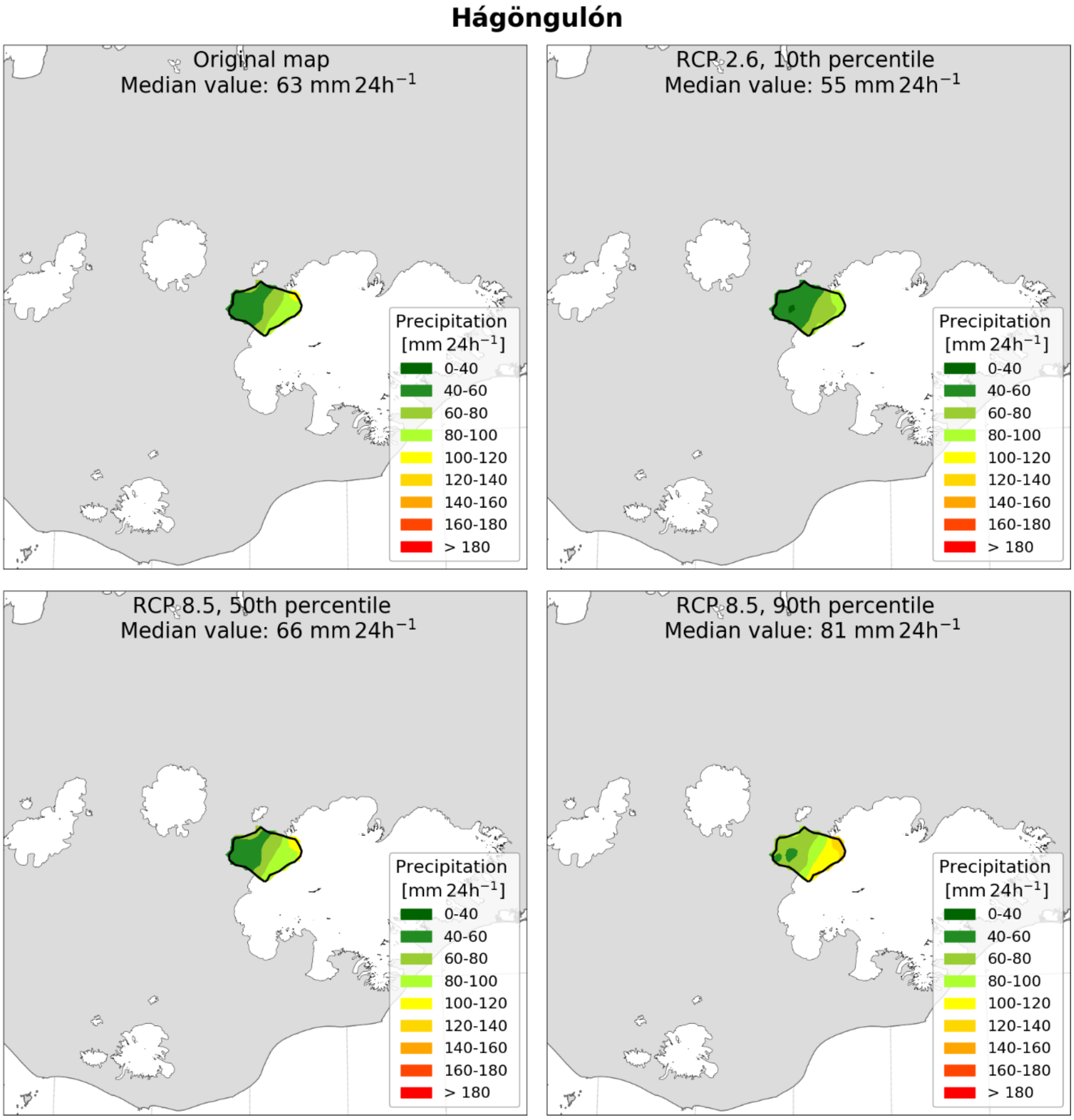

Figure III.3 – 1M5 maps for catchment Hágöngulón, based on the ICRA dataset without projection (top left), with RCP 2.6 and 10th percentile percentage changes (top right), with RCP 8.5 and median percentage changes bottom left), and with RCP 8.5 and 90th percentile percentage changes (bottom right). Projections were calculated for the time-period 2080 – 2100 and come from the CMIP5.

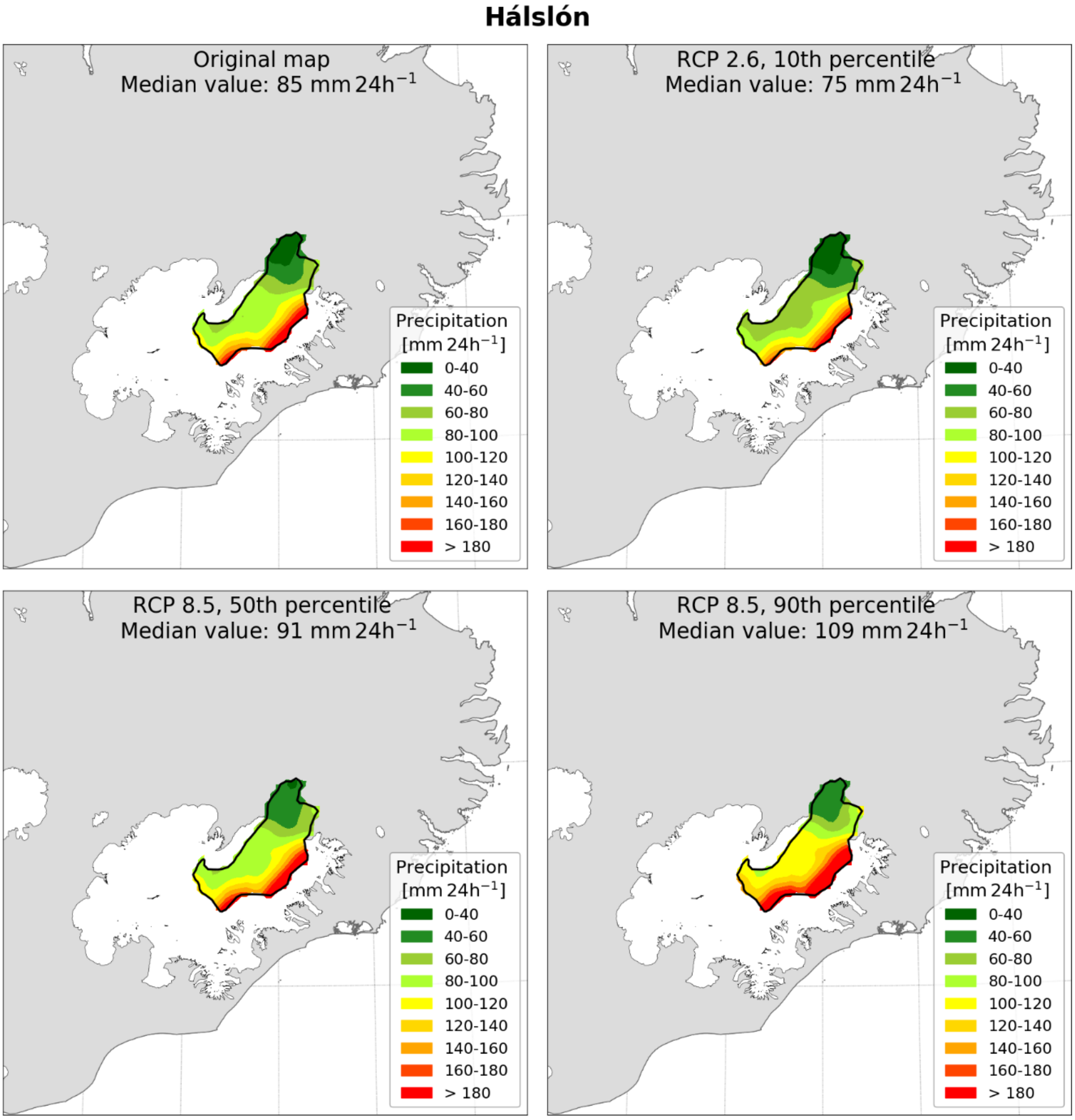

Figure III.4 – 1M5 maps for catchment Hálslón, based on the ICRA dataset without projection (top left), with RCP 2.6 and 10th percentile percentage changes (top right), with RCP 8.5 and median percentage changes bottom left), and with RCP 8.5 and 90th percentile percentage changes (bottom right). Projections were calculated for the time-period 2080 – 2100 and come from the CMIP5.

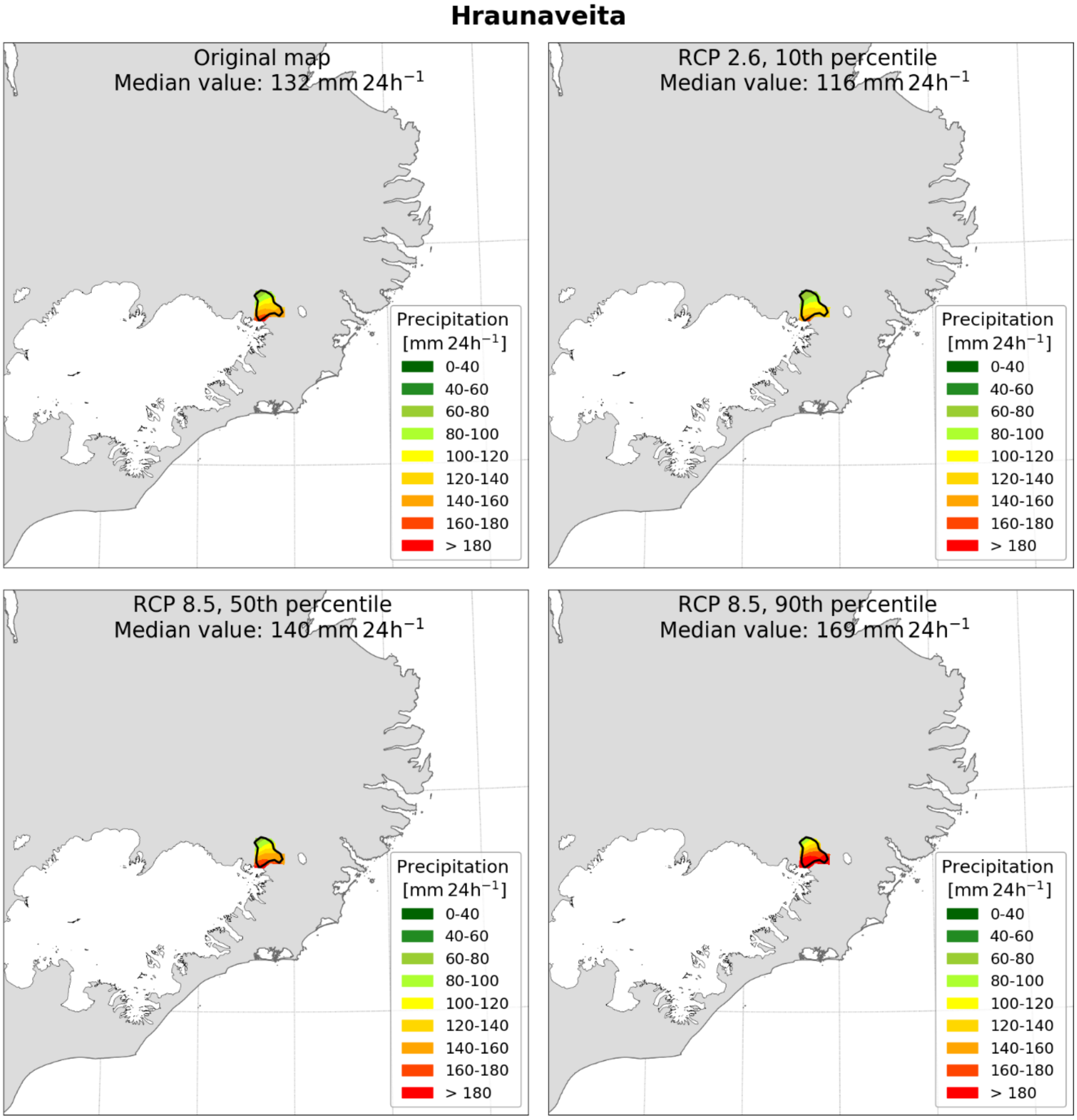

Figure III.5 – 1M5 maps for catchment Hraunaveita, based on the ICRA dataset without projection (top left), with RCP 2.6 and 10th percentile percentage changes (top right), with RCP 8.5 and median percentage changes bottom left), and with RCP 8.5 and 90th percentile percentage changes (bottom right). Projections were calculated for the time-period 2080 – 2100 and come from the CMIP5.

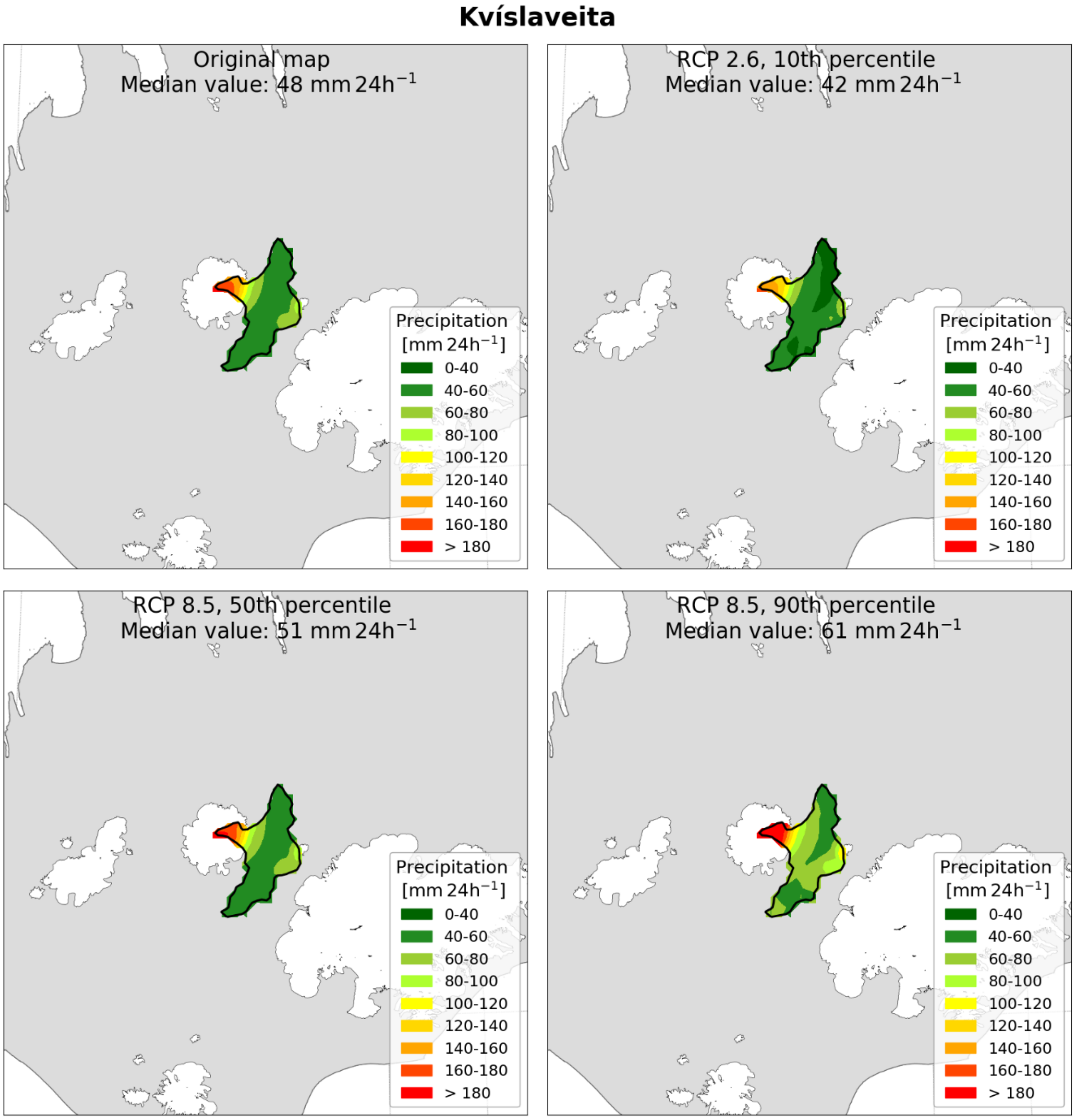

Figure III.6 – 1M5 maps for catchment Kvíslaveita, based on the ICRA dataset without projection (top left), with RCP 2.6 and 10th percentile percentage changes (top right), with RCP 8.5 and median percentage changes bottom left), and with RCP 8.5 and 90th percentile percentage changes (bottom right). Projections were calculated for the time-period 2080 – 2100 and come from the CMIP5.

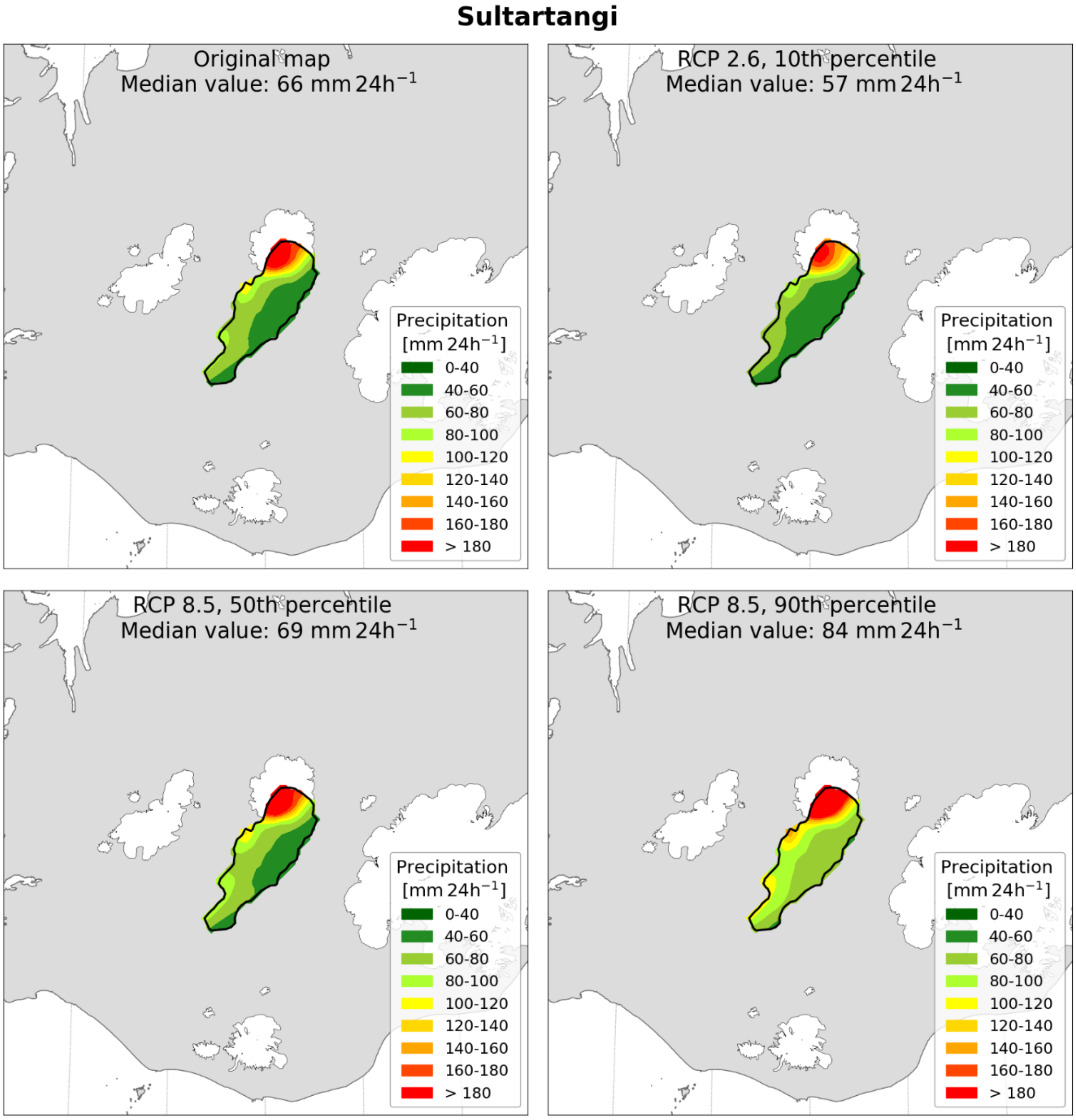

Figure III.7 – 1M5 maps for catchment Sultartangi, based on the ICRA dataset without projection (top left), with RCP 2.6 and 10th percentile percentage changes (top right), with RCP 8.5 and median percentage changes bottom left), and with RCP 8.5 and 90th percentile percentage changes (bottom right). Projections were calculated for the time-period 2080 – 2100 and come from the CMIP5.

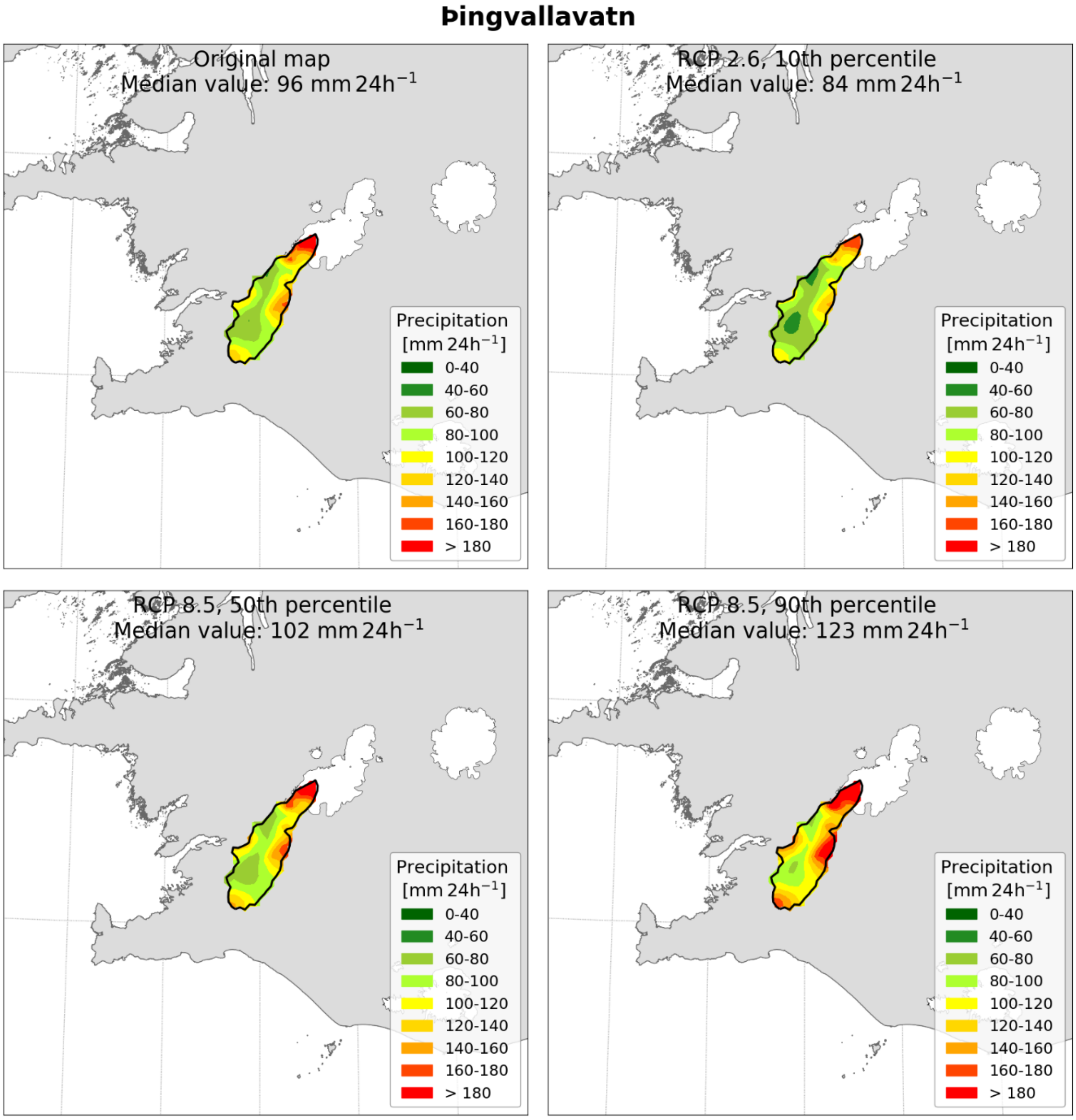

Figure III.8 – 1M5 maps for catchment Þingvallavatn, based on the ICRA dataset without projection (top left), with RCP 2.6 and 10th percentile percentage changes (top right), with RCP 8.5 and median percentage changes bottom left), and with RCP 8.5 and 90th percentile percentage changes (bottom right). Projections were calculated for the time-period 2080 – 2100 and come from the CMIP5.

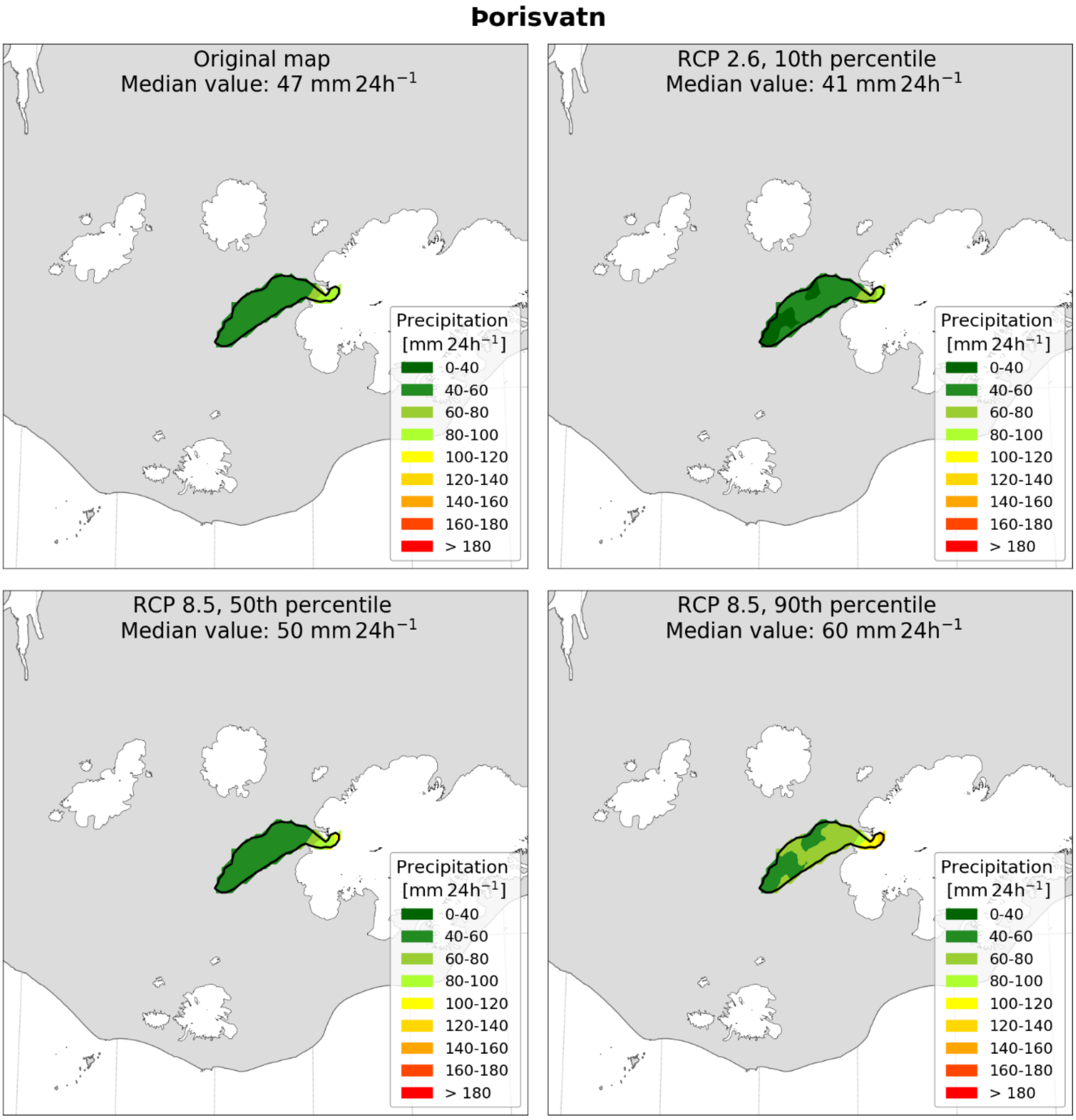

Figure III.9 – 1M5 maps for catchment Þorisvatn, based on the ICRA dataset without projection (top left), with RCP 2.6 and 10th percentile percentage changes (top right), with RCP 8.5 and median percentage changes bottom left), and with RCP 8.5 and 90th percentile percentage changes (bottom right). Projections were calculated for the time-period 2080 – 2100 and come from the CMIP5.

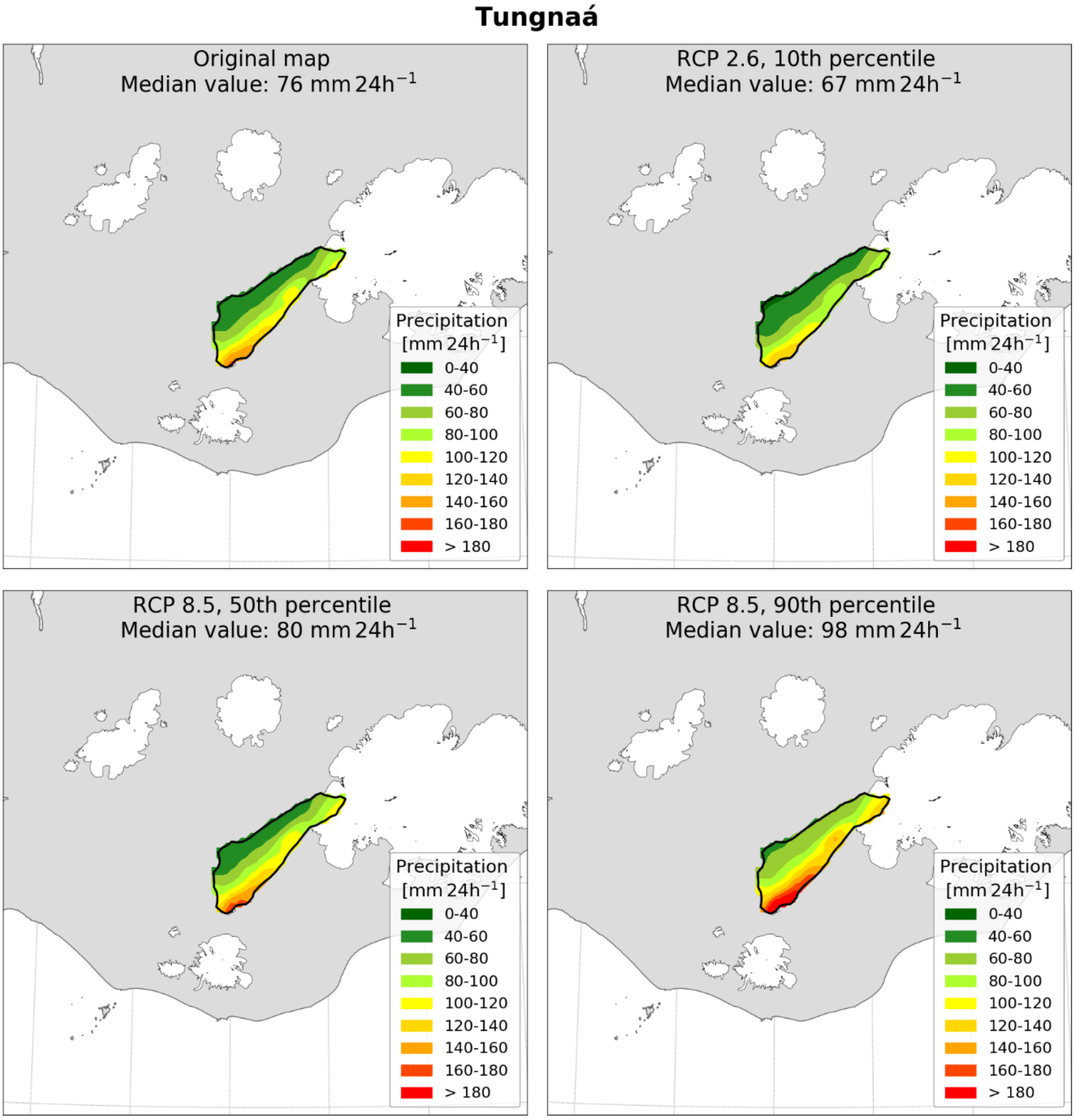

Figure III.10 – 1M5 maps for catchment Tungnaá, based on the ICRA dataset without projection (top left), with RCP 2.6 and 10th percentile percentage changes (top right), with RCP 8.5 and median percentage changes bottom left), and with RCP 8.5 and 90th percentile percentage changes (bottom right). Projections were calculated for the time-period 2080 – 2100 and come from the CMIP5.

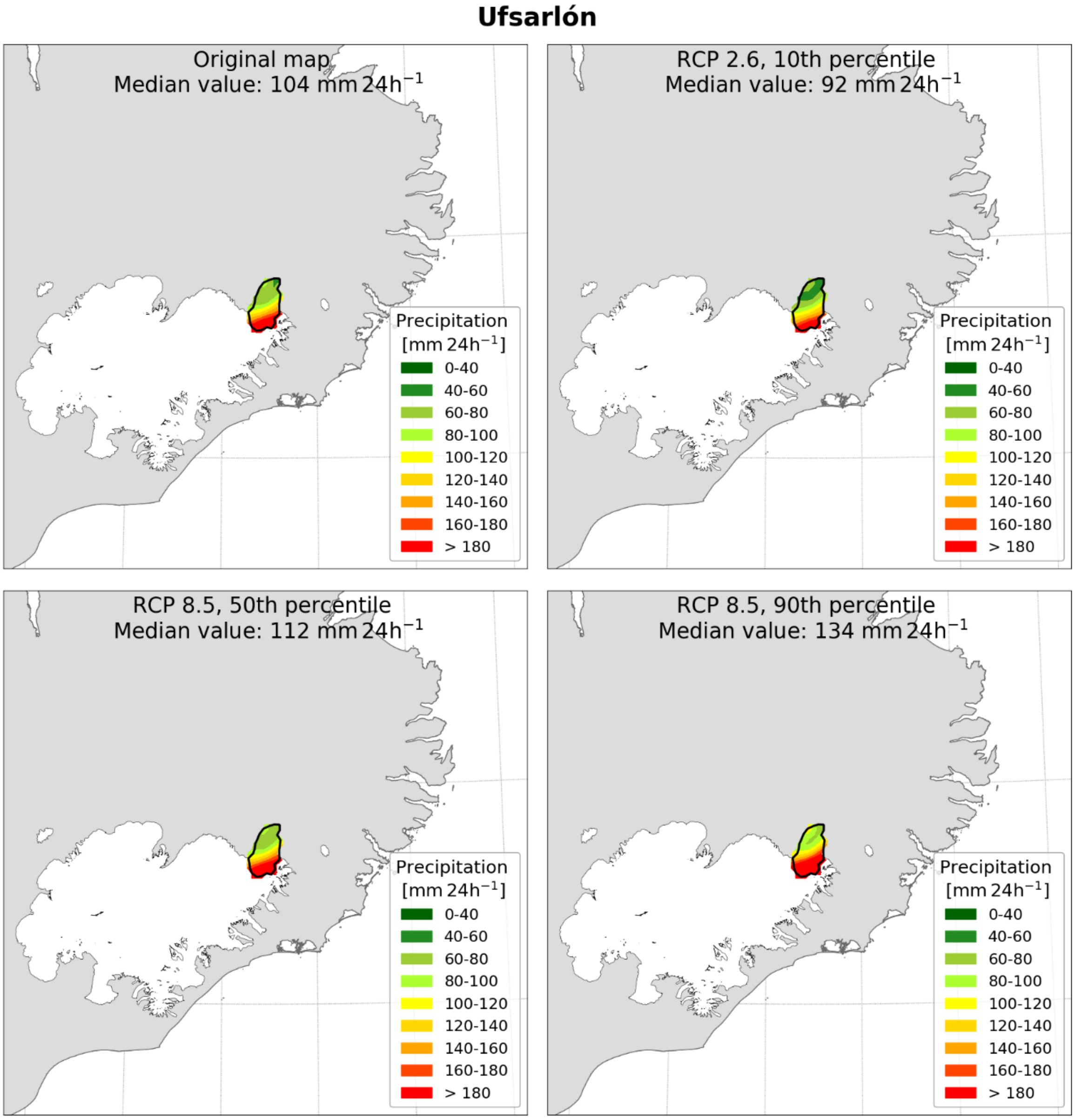

Figure III.11 – 1M5 maps for catchment Ufsarlón, based on the ICRA dataset without projection (top left), with RCP 2.6 and 10th percentile percentage changes (top right), with RCP 8.5 and median percentage changes bottom left), and with RCP 8.5 and 90th percentile percentage changes (bottom right). Projections were calculated for the time-period 2080 – 2100 and come from the CMIP5.

*Table III.1 – **Return levels (mm) for catchment Blönduvirkjun.** Results are based on the ICRA dataset without projections (top), with RCP 2.6 scenario (middle) and with RCP 8.5 scenario (bottom), using the 50th percentile percentage changes. Values are given for 3-, 6-, 12-, 24- and 48-hour return levels with a 2-, 5-, 10-, 25-, 50- and 100-year return period. Timeseries were extracted using the average value of all the grid-points within the catchment. 1M5 value is underlined in red.*

	2 years	**5 years**	**10 years**	**25 years**	**50 years**	**100 years**
3 hours	5	7	8	9	11	12
6 hours	11	14	16	18	20	22
12 hours	21	25	29	32	37	40
24 hours	34	**41**	46	51	59	64
48 hours	53	62	69	76	85	93

	2 years	**5 years**	**10 years**	**25 years**	**50 years**	**100 years**
3 hours	6	7	9	10	11	12
6 hours	12	15	17	19	21	23
12 hours	21	26	30	33	38	42
24 hours	35	**42**	47	53	60	66
48 hours	55	64	71	78	88	96

	2 years	**5 years**	**10 years**	**25 years**	**50 years**	**100 years**
3 hours	6	8	9	10	11	12
6 hours	12	15	17	19	22	23
12 hours	22	27	30	34	39	42
24 hours	36	**43**	48	54	61	67
48 hours	56	65	73	80	90	98

*Table III.2 – **Return levels (mm) for catchment Búðarháls.** Results are based on the ICRA dataset without projections (top), with RCP 2.6 scenario (middle) and with RCP 8.5 scenario (bottom), using the 50th percentile percentage changes. Values are given for 3-, 6-, 12-, 24- and 48-hour return levels with a 2-, 5-, 10-, 25-, 50- and 100-year return period. Timeseries were extracted using the average value of all the grid-points within the catchment. 1M5 value is underlined in red.*

	2 years	**5 years**	**10 years**	**25 years**	**50 years**	**100 years**
3 hours	8	10	11	13	14	15
6 hours	14	18	20	22	24	25
12 hours	24	28	31	33	36	39
24 hours	35	**39**	42	44	47	49
48 hours	48	52	54	56	58	60

	2 years	**5 years**	**10 years**	**25 years**	**50 years**	**100 years**
3 hours	8	10	12	13	15	15
6 hours	15	18	20	22	24	26
12 hours	24	29	32	35	38	40
24 hours	36	**40**	43	46	49	51
48 hours	50	53	56	58	60	61

	2 years	**5 years**	**10 years**	**25 years**	**50 years**	**100 years**
3 hours	8	11	12	13	15	16
6 hours	15	19	21	23	25	26
12 hours	25	30	33	36	39	42
24 hours	37	**41**	45	47	50	52
48 hours	51	55	57	59	61	63

*Table III.3 – **Return levels (mm) for catchment Hágöngulón.** Results are based on the ICRA dataset without projections (top), with RCP 2.6 scenario (middle) and with RCP 8.5 scenario (bottom), using the 50th percentile percentage changes. Values are given for 3-, 6-, 12-, 24- and 48-hour return levels with a 2-, 5-, 10-, 25-, 50- and 100-year return period. Timeseries were extracted using the average value of all the grid-points within the catchment. 1M5 value is underlined in red.*

	2 years	**5 years**	**10 years**	**25 years**	**50 years**	**100 years**
3 hours	7	9	11	13	14	15
6 hours	15	19	21	24	27	29
12 hours	29	35	39	43	47	50
24 hours	51	**59**	65	71	79	84
48 hours	79	91	101	111	123	133

	2 years	**5 years**	**10 years**	**25 years**	**50 years**	**100 years**
3 hours	7	19	11	13	15	16
6 hours	16	19	22	25	28	30
12 hours	30	36	40	44	48	51
24 hours	52	**61**	67	73	80	86
48 hours	81	94	104	114	127	136

	2 years	**5 years**	**10 years**	**25 years**	**50 years**	**100 years**
3 hours	8	10	12	13	15	16
6 hours	16	20	23	25	28	31
12 hours	31	37	41	45	49	53
24 hours	53	**62**	69	75	82	87
48 hours	84	96	104	112	122	129

Table III.4 – Return levels (mm) for catchment Hálslón. Results are based on the ICRA dataset without projections (top), with RCP 2.6 scenario (middle) and with RCP 8.5 scenario (bottom), using the 50th percentile percentage changes. Values are given for 3-, 6-, 12-, 24- and 48-hour return levels with a 2-, 5-, 10-, 25-, 50- and 100-year return period. Timeseries were extracted using the average value of all the grid-points within the catchment. 1M5 value is underlined in red.

	2 years	**5 years**	**10 years**	**25 years**	**50 years**	**100 years**
3 hours	8	11	13	15	18	20
6 hours	18	23	27	31	36	39
12 hours	35	43	49	54	62	67
24 hours	60	**70**	78	85	94	101
48 hours	91	105	115	125	137	147

	2 years	**5 years**	**10 years**	**25 years**	**50 years**	**100 years**
3 hours	8	11	13	16	19	21
6 hours	18	24	28	32	37	41
12 hours	36	44	50	56	64	69
24 hours	62	**72**	80	88	97	104
48 hours	94	108	119	129	142	152

	2 years	**5 years**	**10 years**	**25 years**	**50 years**	**100 years**
3 hours	8	11	14	16	19	22
6 hours	19	24	29	33	38	42
12 hours	37	46	52	58	65	71
24 hours	63	**74**	82	90	100	107
48 hours	97	111	121	131	143	152

*Table III.5 – **Return levels (mm) for catchment Hraunaveita.** Results are based on the ICRA dataset without projections (top), with RCP 2.6 scenario (middle) and with RCP 8.5 scenario (bottom), using the 50th percentile percentage changes. Values are given for 3-, 6-, 12-, 24- and 48-hour return levels with a 2-, 5-, 10-, 25-, 50- and 100-year return period. Timeseries were extracted using the average value of all the grid-points within the catchment. 1M5 value is underlined in red.*

	2 years	**5 years**	**10 years**	**25 years**	**50 years**	**100 years**
3 hours	11	17	22	27	34	40
6 hours	27	37	46	55	67	78
12 hours	53	70	84	99	121	139
24 hours	89	**114**	135	157	191	219
48 hours	141	177	208	243	294	339

	2 years	**5 years**	**10 years**	**25 years**	**50 years**	**100 years**
3 hours	12	18	23	28	35	42
6 hours	28	38	47	56	69	80
12 hours	55	72	87	102	124	143
24 hours	92	**117**	139	162	196	225
48 hours	145	182	213	248	299	343

	2 years	**5 years**	**10 years**	**25 years**	**50 years**	**100 years**
3 hours	12	18	23	29	36	43
6 hours	29	39	48	57	71	82
12 hours	57	74	89	104	127	146
24 hours	94	**120**	142	165	199	228
48 hours	149	185	216	250	300	342

*Table III.6 – **Return levels (mm) for catchment Kvíslaveita.** Results are based on the ICRA dataset without projections (top), with RCP 2.6 scenario (middle) and with RCP 8.5 scenario (bottom), using the 50th percentile percentage changes. Values are given for 3-, 6-, 12-, 24- and 48-hour return levels with a 2-, 5-, 10-, 25-, 50- and 100-year return period. Timeseries were extracted using the average value of all the grid-points within the catchment. 1M5 value is underlined in red.*

	2 years	**5 years**	**10 years**	**25 years**	**50 years**	**100 years**
3 hours	6	9	10	11	13	14
6 hours	13	17	19	21	23	25
12 hours	24	29	33	36	40	43
24 hours	40	**48**	54	59	67	73
48 hours	61	72	81	90	103	113

	2 years	**5 years**	**10 years**	**25 years**	**50 years**	**100 years**
3 hours	7	9	11	12	13	14
6 hours	14	17	20	22	24	26
12 hours	25	30	34	37	41	44
24 hours	41	**49**	55	61	68	74
48 hours	63	75	84	93	106	116

	2 years	**5 years**	**10 years**	**25 years**	**50 years**	**100 years**
3 hours	7	9	11	12	14	15
6 hours	14	18	20	22	25	27
12 hours	26	31	35	38	42	45
24 hours	42	**50**	56	62	69	75
48 hours	65	76	85	95	108	118

*Table III.7 – **Return levels (mm) for catchment Sultartangi.** Results are based on the ICRA dataset without projections (top), with RCP 2.6 scenario (middle) and with RCP 8.5 scenario (bottom), using the 50th percentile percentage changes. Values are given for 3-, 6-, 12-, 24- and 48-hour return levels with a 2-, 5-, 10-, 25-, 50- and 100-year return period. Timeseries were extracted using the average value of all the grid-points within the catchment. 1M5 value is underlined in red.*

	2 years	**5 years**	**10 years**	**25 years**	**50 years**	**100 years**
3 hours	9	12	13	15	17	18
6 hours	19	23	26	28	31	33
12 hours	34	40	44	47	51	54
24 hours	56	**64**	70	75	81	86
48 hours	84	95	103	111	120	127

	2 years	**5 years**	**10 years**	**25 years**	**50 years**	**100 years**
3 hours	9	12	14	16	17	18
6 hours	19	24	27	29	32	34
12 hours	36	41	45	49	53	56
24 hours	58	**66**	72	77	84	88
48 hours	87	98	106	114	124	131

	2 years	**5 years**	**10 years**	**25 years**	**50 years**	**100 years**
3 hours	9	12	14	16	18	19
6 hours	20	24	27	30	33	35
12 hours	37	43	47	51	55	58
24 hours	59	**68**	74	79	86	91
48 hours	89	100	108	116	126	134

*Table III.8 – **Return levels (mm) for catchment Þingvallavatn.** Results are based on the ICRA dataset without projections (top), with RCP 2.6 scenario (middle) and with RCP 8.5 scenario (bottom), using the 50th percentile percentage changes. Values are given for 3-, 6-, 12-, 24- and 48-hour return levels with a 2-, 5-, 10-, 25-, 50- and 100-year return period. Timeseries were extracted using the average value of all the grid-points within the catchment. 1M5 value is underlined in red.*

	2 years	**5 years**	**10 years**	**25 years**	**50 years**	**100 years**
3 hours	12	15	18	19	21	23
6 hours	26	31	35	38	41	44
12 hours	48	56	62	67	73	77
24 hours	78	**90**	99	107	117	124
48 hours	113	128	138	148	159	168

	2 years	**5 years**	**10 years**	**25 years**	**50 years**	**100 years**
3 hours	12	16	18	20	22	23
6 hours	26	32	36	39	43	45
12 hours	49	58	64	69	76	80
24 hours	80	**93**	102	110	120	128
48 hours	117	132	142	151	163	172

	2 years	**5 years**	**10 years**	**25 years**	**50 years**	**100 years**
3 hours	13	16	19	21	23	24
6 hours	27	33	37	40	44	46
12 hours	50	59	66	71	78	83
24 hours	82	**95**	104	112	123	130
48 hours	120	135	146	156	168	177

*Table III.9 – **Return levels (mm) for catchment Þorisvatn.** Results are based on the ICRA dataset without projections (top), with RCP 2.6 scenario (middle) and with RCP 8.5 scenario (bottom), using the 50th percentile percentage changes. Values are given for 3-, 6-, 12-, 24- and 48-hour return levels with a 2-, 5-, 10-, 25-, 50- and 100-year return period. Timeseries were extracted using the average value of all the grid-points within the catchment. 1M5 value is underlined in red.*

	2 years	**5 years**	**10 years**	**25 years**	**50 years**	**100 years**
3 hours	7	9	10	11	12	13
6 hours	13	16	17	19	20	21
12 hours	22	26	29	31	34	36
24 hours	35	**41**	45	48	53	56
48 hours	55	63	69	74	82	88

	2 years	**5 years**	**10 years**	**25 years**	**50 years**	**100 years**
3 hours	7	9	10	11	12	13
6 hours	13	16	18	19	21	22
12 hours	23	27	30	32	35	37
24 hours	36	**42**	46	50	54	57
48 hours	56	64	71	77	86	92

	2 years	**5 years**	**10 years**	**25 years**	**50 years**	**100 years**
3 hours	7	9	10	12	13	14
6 hours	14	17	18	20	22	23
12 hours	24	28	30	33	36	38
24 hours	37	**43**	47	50	55	58
48 hours	57	66	72	78	86	91

*Table III.10 – **Return levels (mm) for catchment Tungnaá.** Results are based on the ICRA dataset without projections (top), with RCP 2.6 scenario (middle) and with RCP 8.5 scenario (bottom), using the 50th percentile percentage changes. Values are given for 3-, 6-, 12-, 24- and 48-hour return levels with a 2-, 5-, 10-, 25-, 50- and 100-year return period. Timeseries were extracted using the average value of all the grid-points within the catchment. 1M5 value is underlined in red.*

	2 years	**5 years**	**10 years**	**25 years**	**50 years**	**100 years**
3 hours	8	11	13	15	18	20
6 hours	17	22	26	31	37	42
12 hours	33	42	49	57	68	78
24 hours	55	**68**	79	90	106	119
48 hours	87	104	117	131	150	165

	2 years	**5 years**	**10 years**	**25 years**	**50 years**	**100 years**
3 hours	8	11	13	15	18	20
6 hours	17	23	27	32	38	43
12 hours	34	43	51	59	71	80
24 hours	57	**71**	82	94	111	125
48 hours	89	107	121	135	155	171

	2 years	**5 years**	**10 years**	**25 years**	**50 years**	**100 years**
3 hours	8	11	14	16	19	21
6 hours	18	23	28	32	39	43
12 hours	35	44	52	61	72	82
24 hours	58	**72**	84	96	113	127
48 hours	92	111	126	142	164	182

Table III.11 – ***Return levels (mm) for catchment Ufsarlón.*** *Results are based on the ICRA dataset without projections (top), with RCP 2.6 scenario (middle) and with RCP 8.5 scenario (bottom), using the 50th percentile percentage changes. Values are given for 3-, 6-, 12-, 24- and 48-hour return levels with a 2-, 5-, 10-, 25-, 50- and 100-year return period. Timeseries were extracted using the average value of all the grid-points within the catchment. 1M5 value is underlined in red.*

	2 years	**5 years**	**10 years**	**25 years**	**50 years**	**100 years**
3 hours	11	16	20	25	30	35
6 hours	27	36	43	50	60	67
12 hours	52	66	76	87	103	114
24 hours	86	**106**	121	137	159	176
48 hours	133	157	176	195	221	241

	2 years	**5 years**	**10 years**	**25 years**	**50 years**	**100 years**
3 hours	12	17	21	25	32	36
6 hours	27	37	44	51	62	69
12 hours	54	68	79	90	106	119
24 hours	89	**109**	125	142	164	182
48 hours	137	162	181	201	227	248

	2 years	**5 years**	**10 years**	**25 years**	**50 years**	**100 years**
3 hours	12	17	22	26	33	38
6 hours	28	38	45	53	63	71
12 hours	55	70	81	93	109	121
24 hours	92	**113**	129	146	170	188
48 hours	141	167	186	206	232	253

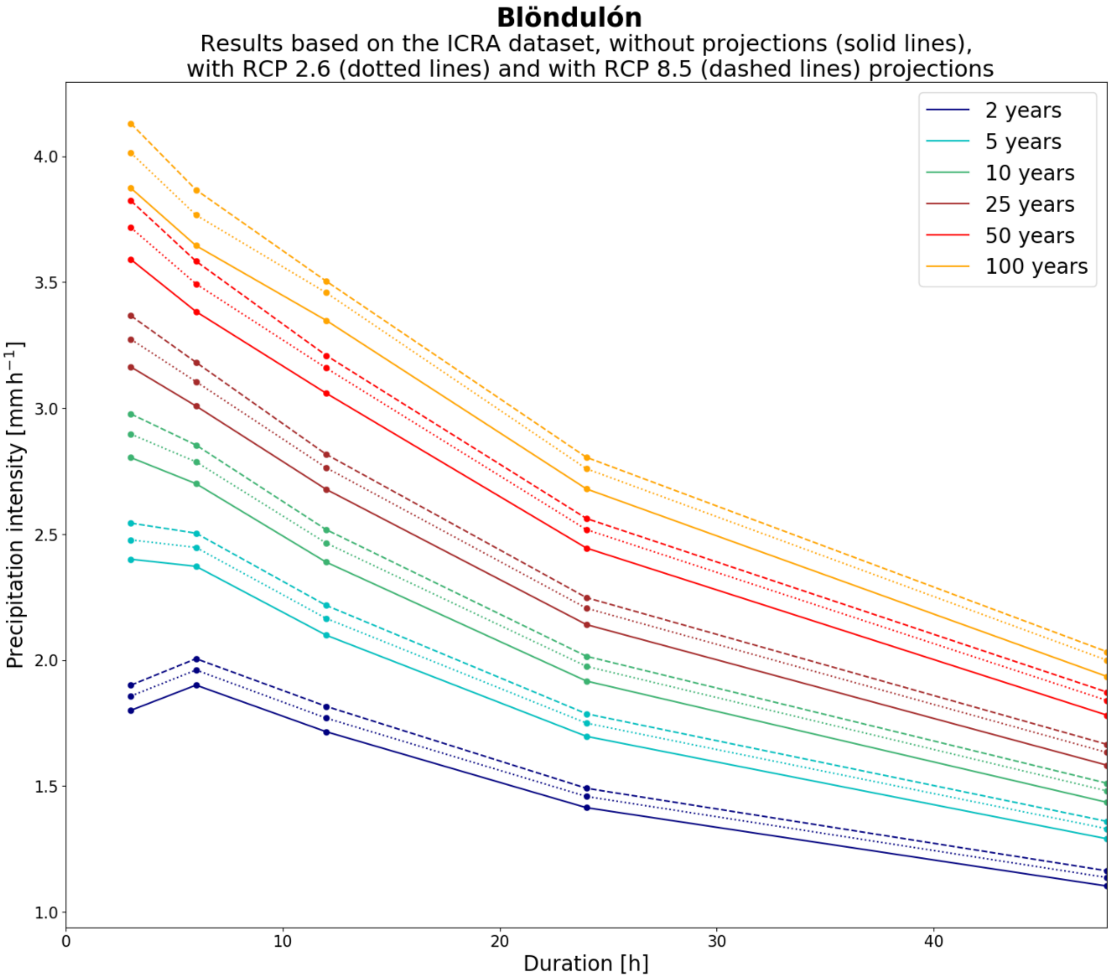

Figure III.12 – IDF curves for catchment Blönduvirkjun based on the ICRA dataset, without projections (solid lines), with RCP 2.6 projections (dotted lines) and with RCP 8.5 projections (dashed lines). Solid points give return levels for 3-, 6-, 12-, 24- and 48-hour duration with a 2-, 5-, 10-, 25-, 50- and 100-year return period. Each coloured line corresponds to a different return period as stated by the legend.

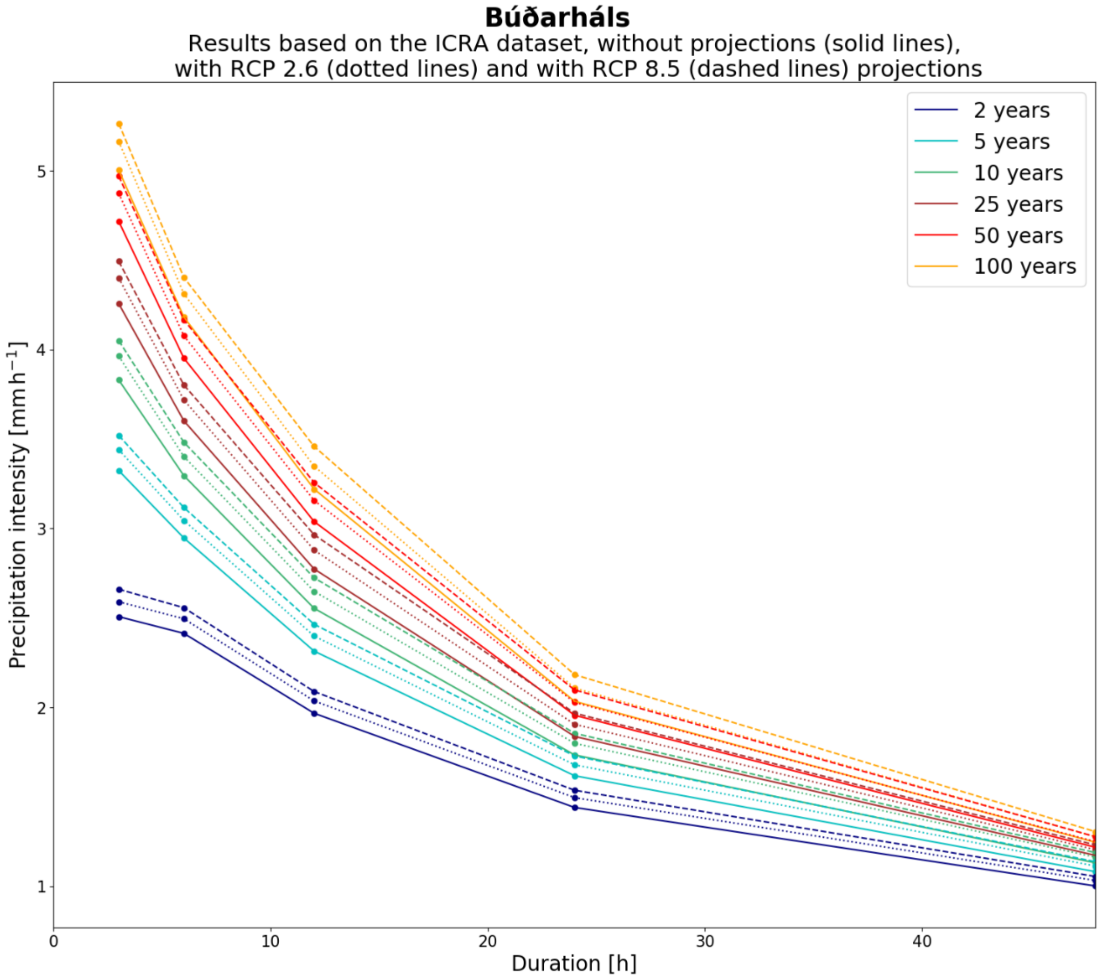

Figure III.13 – IDF curves for catchment Búðarháls based on the ICRA dataset, without projections (solid lines), with RCP 2.6 projections (dotted lines) and with RCP 8.5 projections (dashed lines). Solid points give return levels for 3-, 6-, 12-, 24- and 48-hour duration with a 2-, 5-, 10-, 25-, 50- and 100-year return period. Each coloured line corresponds to a different return period as stated by the legend.

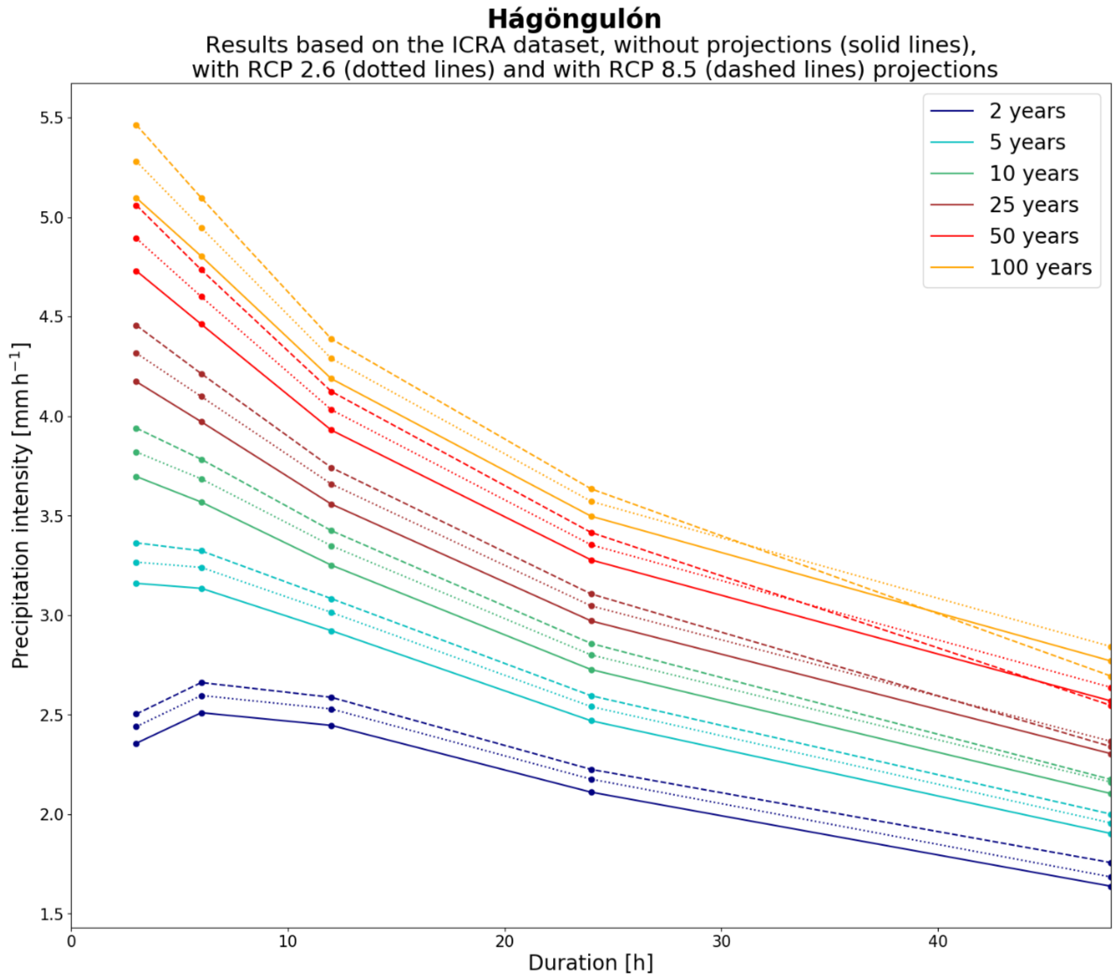

Figure III.14 – IDF curves for catchment Hágöngulón based on the ICRA dataset, without projections (solid lines), with RCP 2.6 projections (dotted lines) and with RCP 8.5 projections (dashed lines). Solid points give return levels for 3-, 6-, 12-, 24- and 48-hour duration with a 2-, 5-, 10-, 25-, 50- and 100-year return period. Each coloured line corresponds to a different return period as stated by the legend.

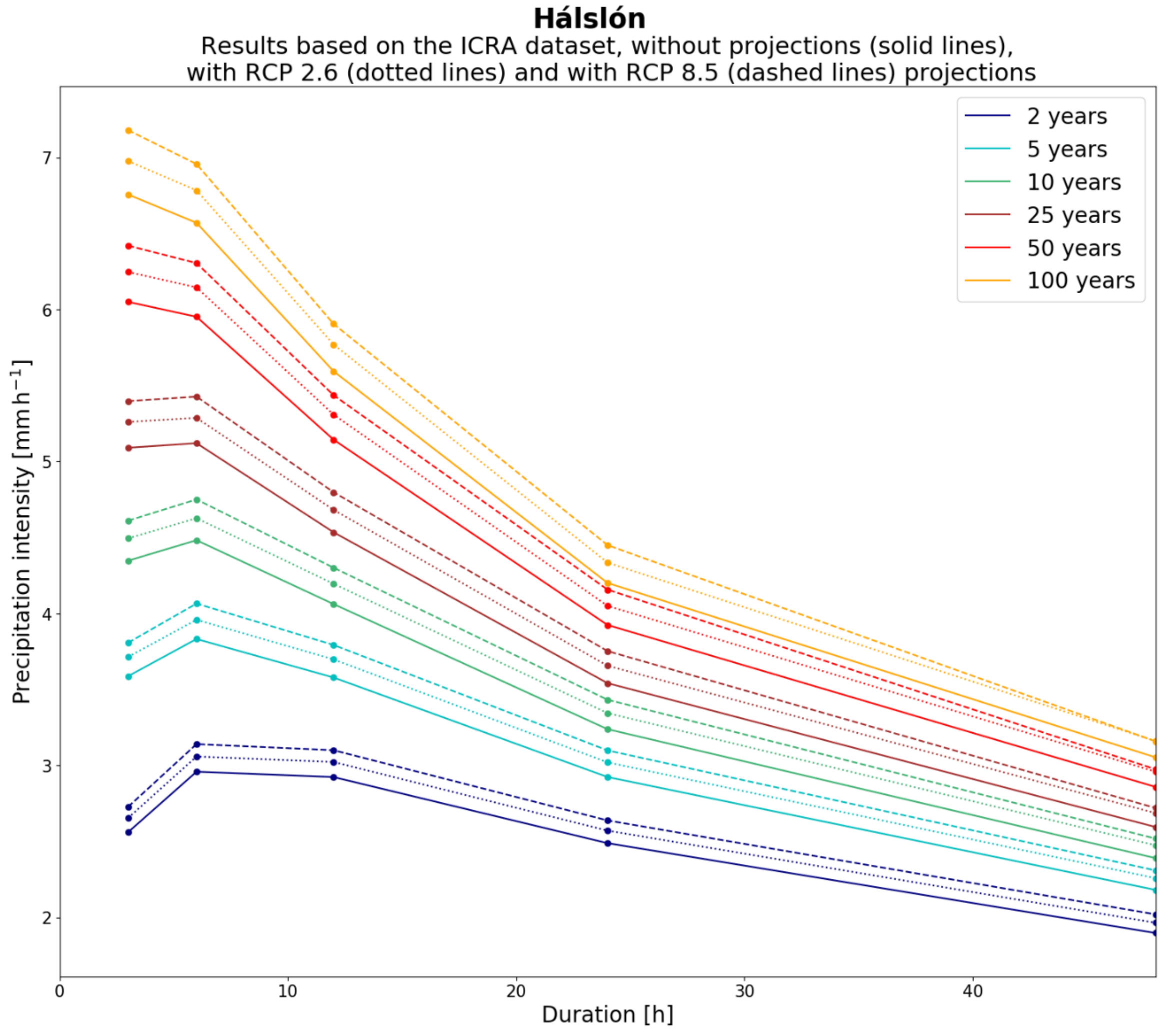

Figure III.15 – IDF curves for catchment Hálslón based on the ICRA dataset, without projections (solid lines), with RCP 2.6 projections (dotted lines) and with RCP 8.5 projections (dashed lines). Solid points give return levels for 3-, 6-, 12-, 24- and 48-hour duration with a 2-, 5-, 10-, 25-, 50- and 100-year return period. Each coloured line corresponds to a different return period as stated by the legend.

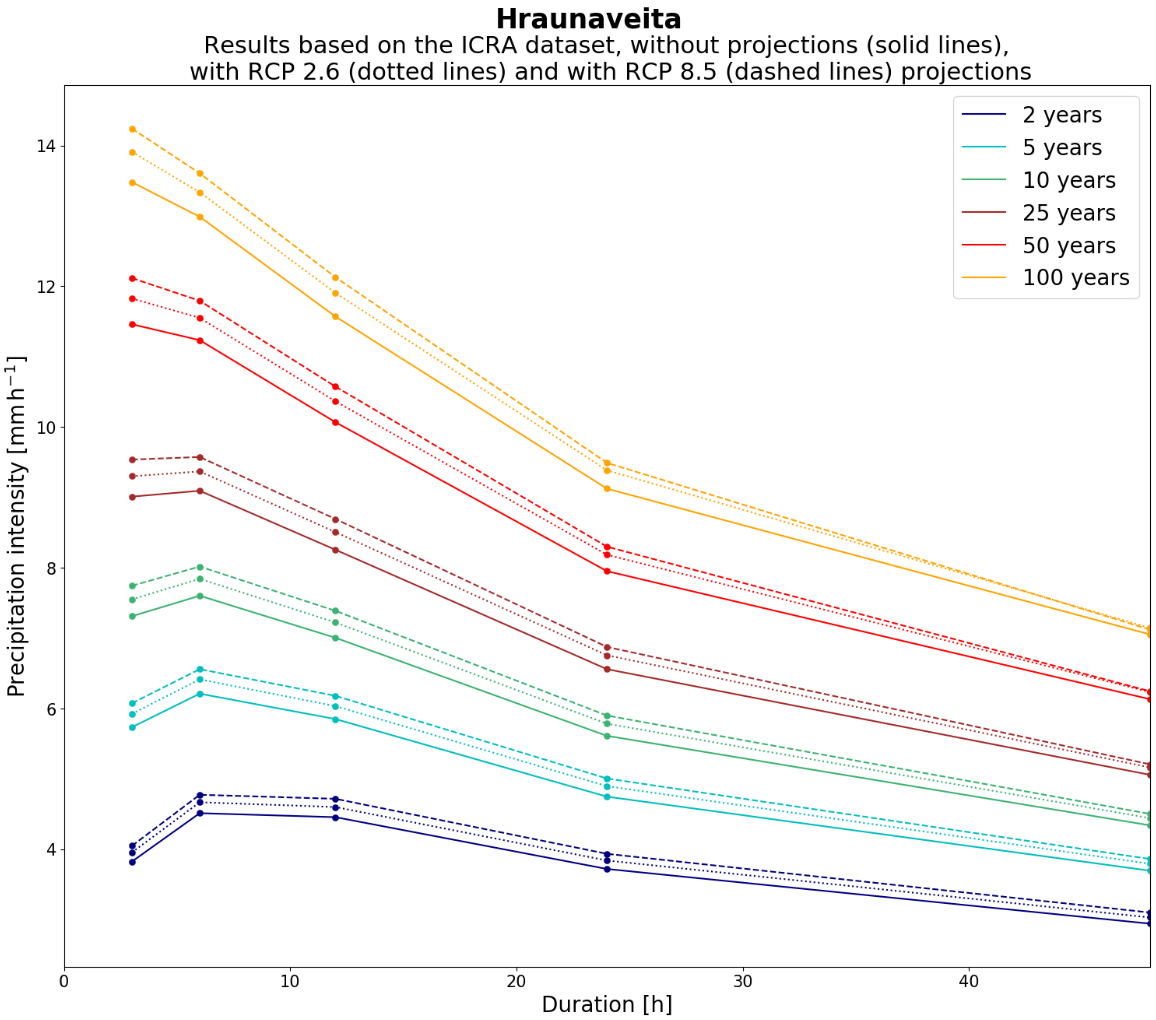

Figure III.16 – IDF curves for catchment Hraunaveita based on the ICRA dataset, without projections (solid lines), with RCP 2.6 projections (dotted lines) and with RCP 8.5 projections (dashed lines). Solid points give return levels for 3-, 6-, 12-, 24- and 48-hour duration with a 2-, 5-, 10-, 25-, 50- and 100-year return period. Each coloured line corresponds to a different return period as stated by the legend.

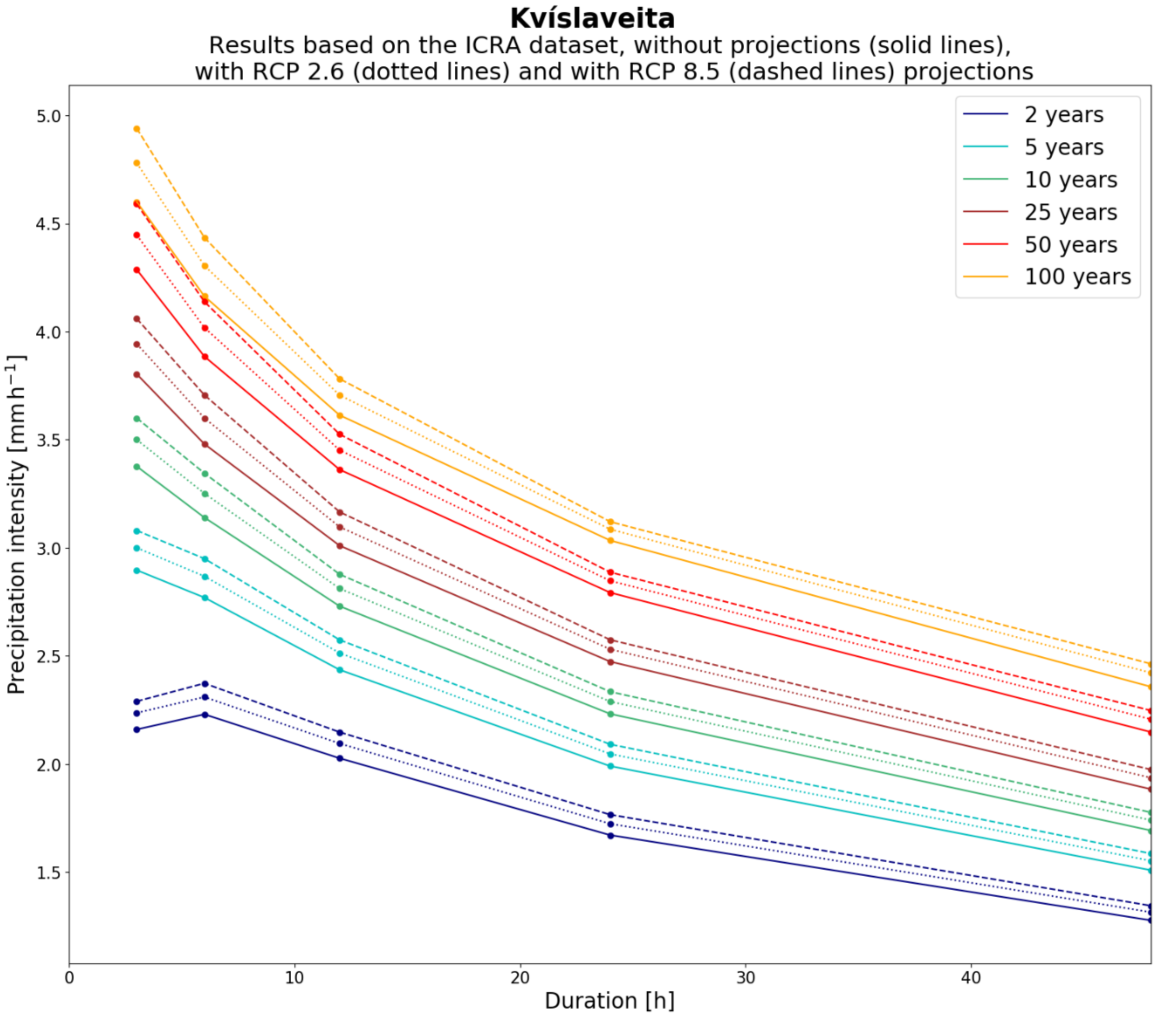

Figure III.17 – IDF curves for catchment Kvíslaveita based on the ICRA dataset, without projections (solid lines), with RCP 2.6 projections (dotted lines) and with RCP 8.5 projections (dashed lines). Solid points give return levels for 3-, 6-, 12-, 24- and 48-hour duration with a 2-, 5-, 10-, 25-, 50- and 100-year return period. Each coloured line corresponds to a different return period as stated by the legend.

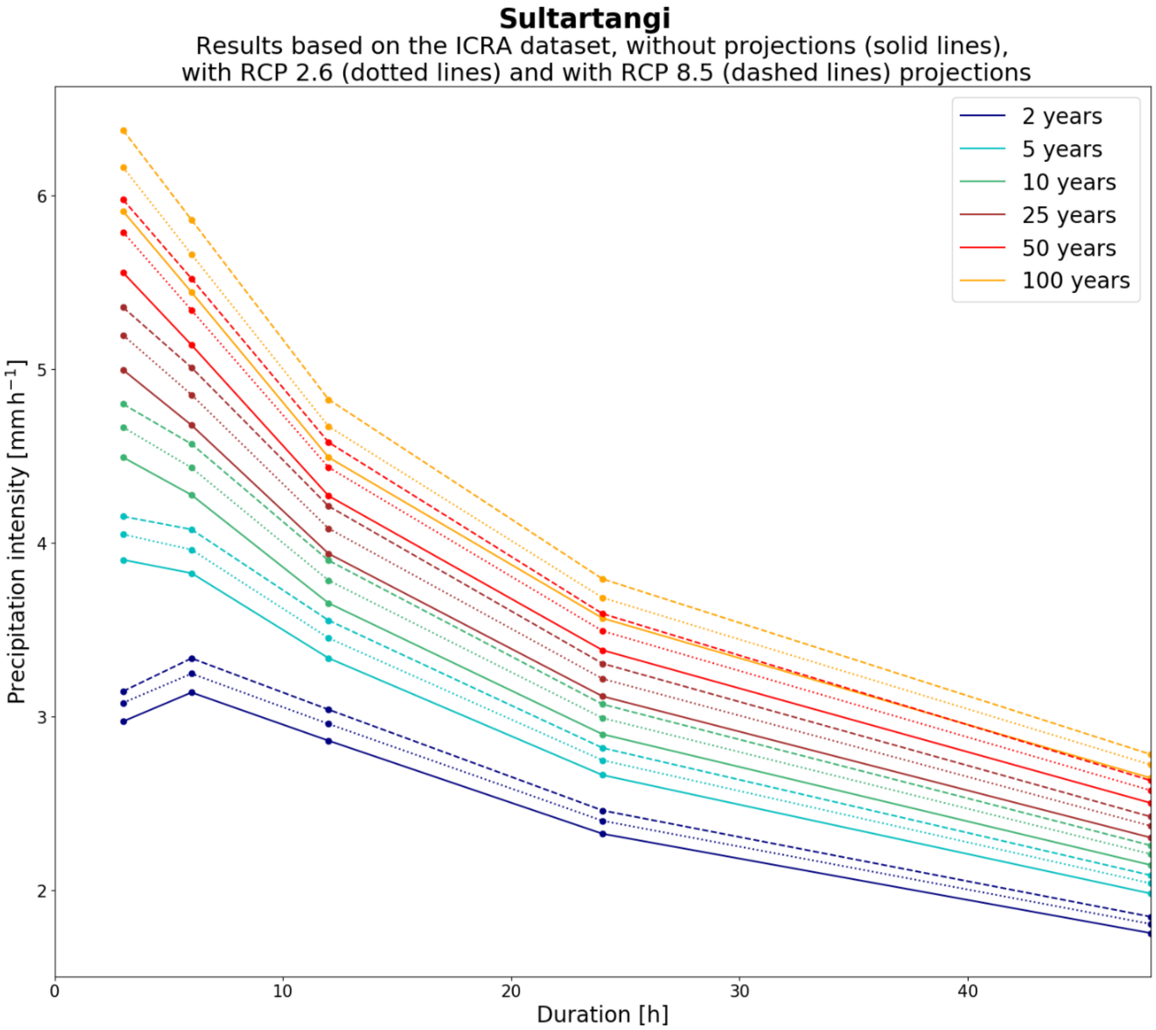

Figure III.18 – IDF curves for catchment Sultartangi based on the ICRA dataset, without projections (solid lines), with RCP 2.6 projections (dotted lines) and with RCP 8.5 projections (dashed lines). Solid points give return levels for 3-, 6-, 12-, 24- and 48-hour duration with a 2-, 5-, 10-, 25-, 50- and 100-year return period. Each coloured line corresponds to a different return period as stated by the legend.

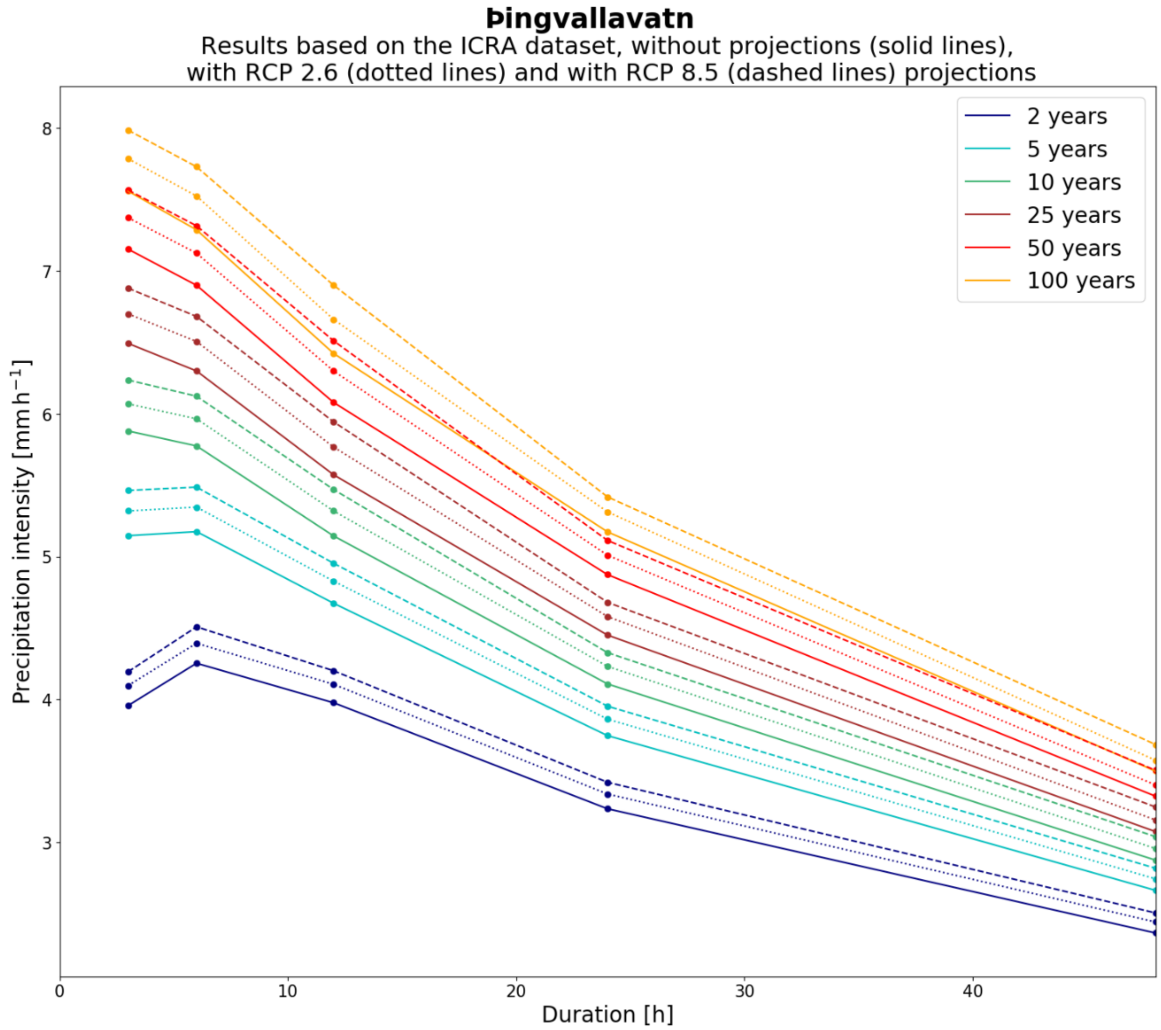

Figure III.19 – IDF curves for catchment Þingvallavatn based on the ICRA dataset, without projections (solid lines), with RCP 2.6 projections (dotted lines) and with RCP 8.5 projections (dashed lines). Solid points give return levels for 3-, 6-, 12-, 24- and 48-hour duration with a 2-, 5-, 10-, 25-, 50- and 100-year return period. Each coloured line corresponds to a different return period as stated by the legend.

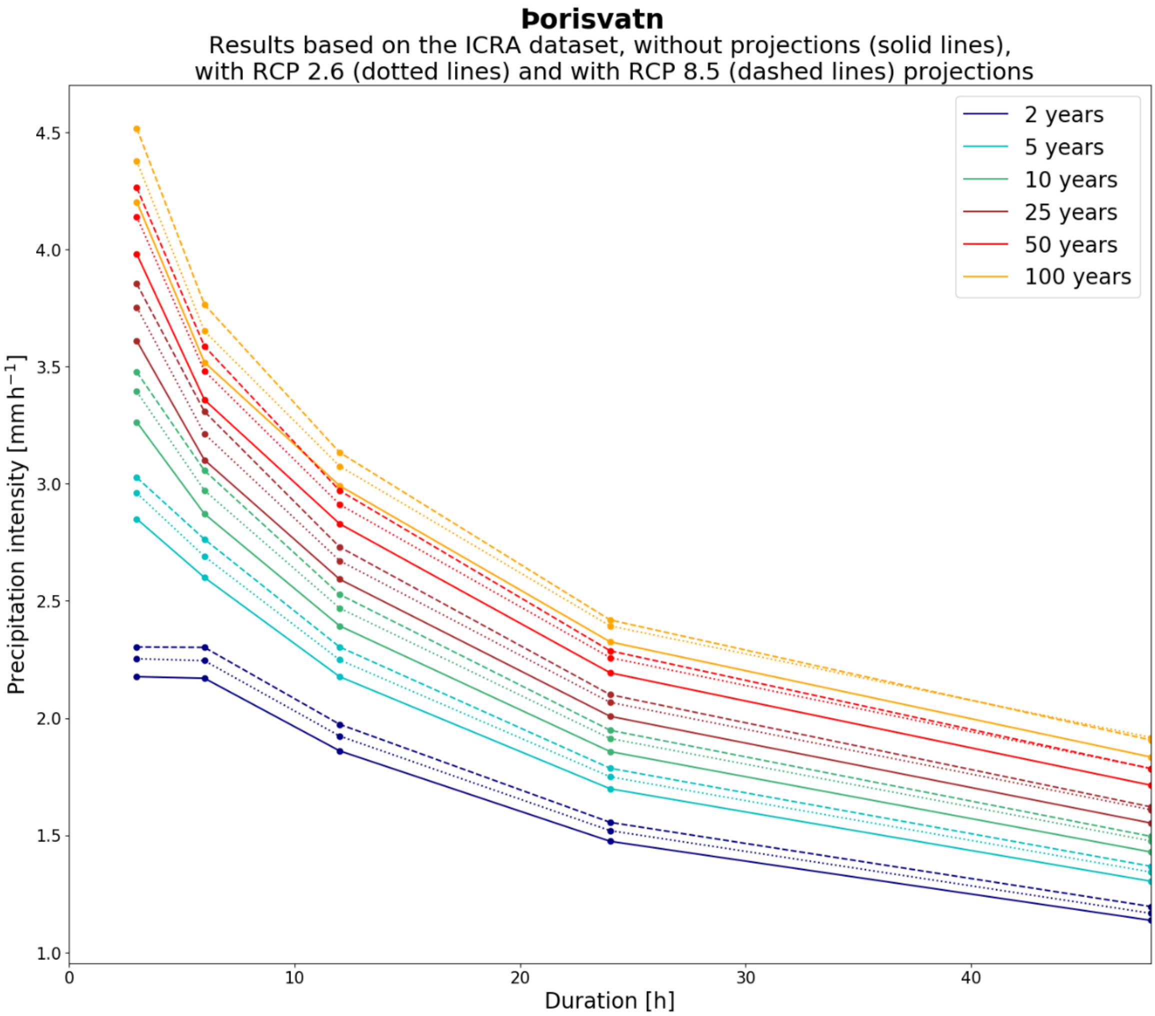

Figure III.20 – IDF curves for catchment Þorisvatn based on the ICRA dataset, without projections (solid lines), with RCP 2.6 projections (dotted lines) and with RCP 8.5 projections (dashed lines). Solid points give return levels for 3-, 6-, 12-, 24- and 48-hour duration with a 2-, 5-, 10-, 25-, 50- and 100-year return period. Each coloured line corresponds to a different return period as stated by the legend.

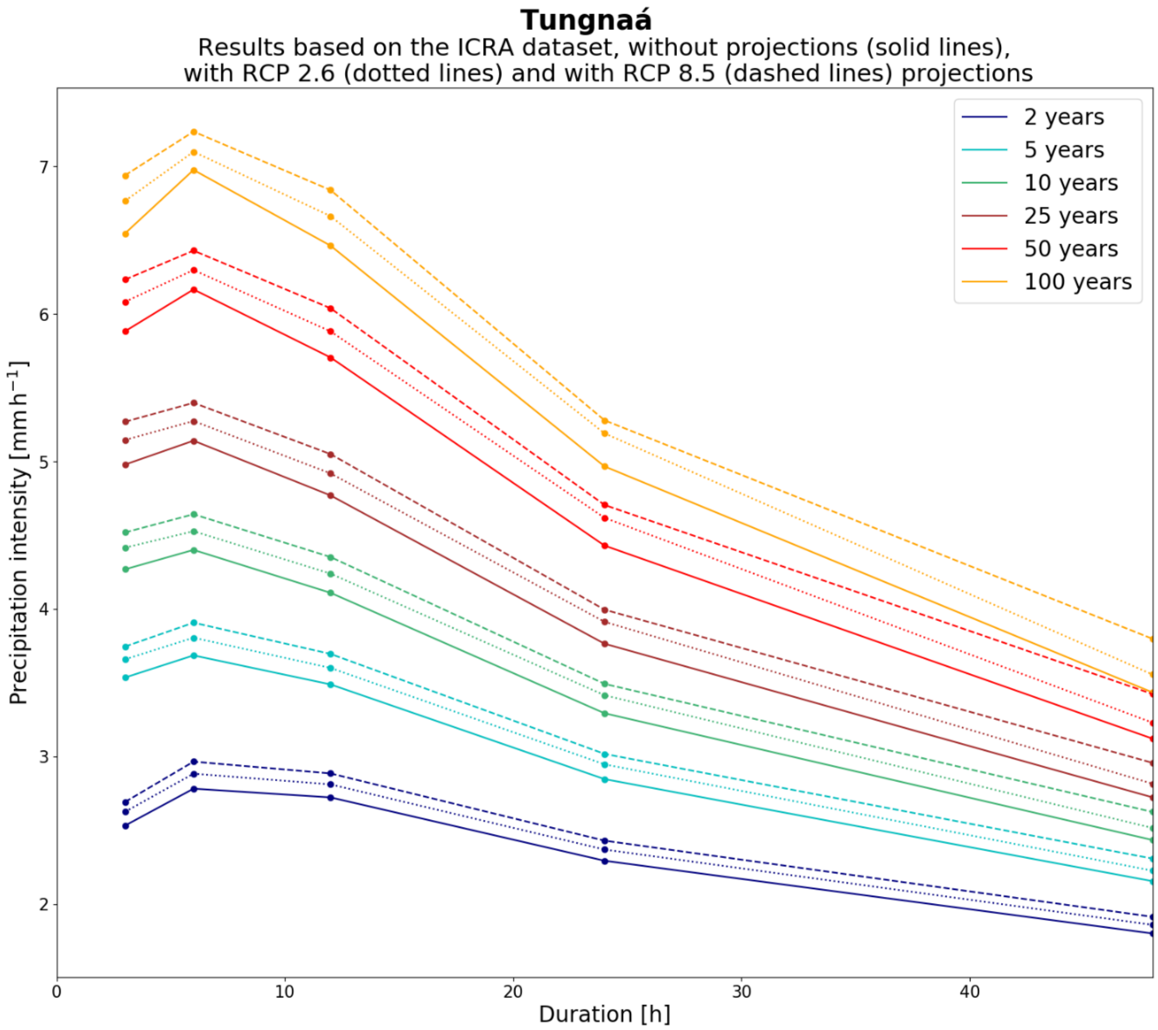

Figure III.21 – IDF curves for catchment Tungnaá based on the ICRA dataset, without projections (solid lines), with RCP 2.6 projections (dotted lines) and with RCP 8.5 projections (dashed lines). Solid points give return levels for 3-, 6-, 12-, 24- and 48-hour duration with a 2-, 5-, 10-, 25-, 50- and 100-year return period. Each coloured line corresponds to a different return period as stated by the legend.

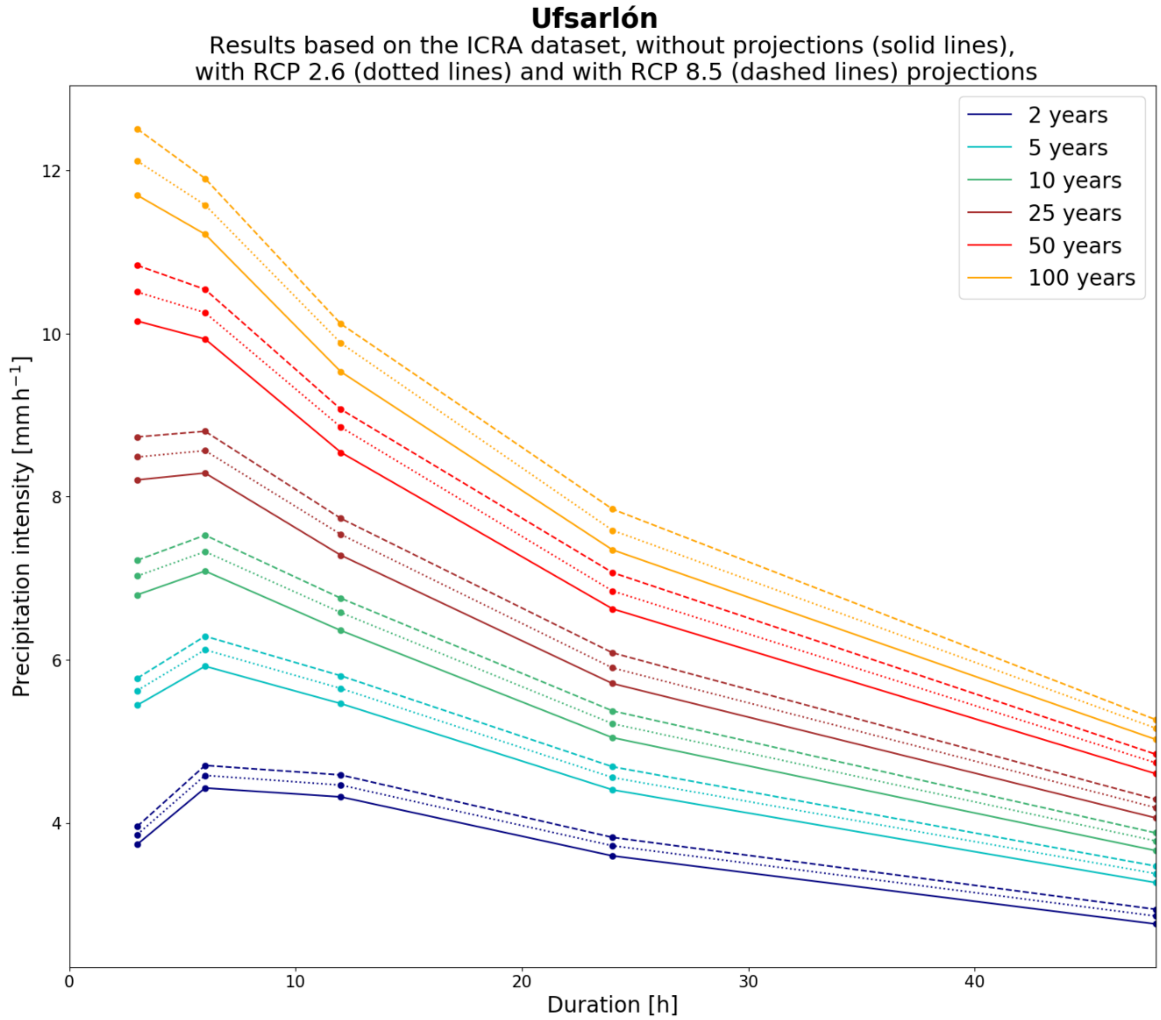

Figure III.22 – IDF curves for catchment Ufsarlón based on the ICRA dataset, without projections (solid lines), with RCP 2.6 projections (dotted lines) and with RCP 8.5 projections (dashed lines). Solid points give return levels for 3-, 6-, 12-, 24- and 48-hour duration with a 2-, 5-, 10-, 25-, 50- and 100-year return period. Each coloured line corresponds to a different return period as stated by the legend.